Modelling South African traffic for large networks – An extension of the gravity model for traffic demand modelling

Stefanus Jacobus Swarts

The financial assistance of the National Research Foundation (NRF) towards this research is hereby acknowledged. Opinions expressed and conclusions arrived at, are those of the author and are not necessarily to be attributed to the NRF.

Thesis presented in partial fulfilment of the requirements for the degree of
Master of Commerce (Operations Research)
in the Faculty of Economic and Management Sciences at Stellenbosch University

Supervisor: Prof SE Visagie

March 2017

Declaration

By submitting this thesis electronically, I declare that the entirety of the work contained therein is my own, original work, that I am the sole author thereof (save to the extent explicitly otherwise stated), that reproduction and publication thereof by Stellenbosch University will not infringe any third party rights and that I have not previously in its entirety or in part submitted it for obtaining any qualification.

Date: March 2017

Abstract

Traffic congestion is a growing burden on society. Due to the complexity of modelling transportation, many approaches do not scale efficiently. Assumptions are made to estimate the locality and quantity of traffic that passes through, leaves or enters a study area. Infrastructure investment based on inaccurate transportation modelling could potentially increase congestion. Furthermore, the effects of changes in infrastructure outside a study area are also unknown. It is therefore necessary to model transportation networks at a larger scale than required before.

This thesis presents a large scale traffic modelling framework, potentially capable of modelling the impact of public transport and infrastructure investment for the South African context. The framework builds on the basic procedure of the Four-Step Modelling methodology.

To address the shortcomings of static trip distribution models, a proposed, temporally adjusted, doubly constrained gravity model is formulated. Kernel density functions are fitted from survey data to define unique impedance of travel functions for each travel analysis zone. Route selection is determined by a heuristic approach to dynamic traffic assignment which is implemented in a mesoscopic traffic simulator.

The proposed gravity model is iteratively calibrated using the output of the traffic simulator in a positive feedback loop to produce a trip distribution that approaches an equilibrium assignment. The gravity model calibration and validation shows that the proposed gravity model is more accurate than the single impedance of travel gravity model. The framework produces OD trip matrices, inter- and intra-zonal routes, quarter-hourly traffic flows and a measure of congestion, all which can be visualised in a GIS environment.

Opsomming

Verkeersopeenhopings is 'n immertoenemende probleem in Suid-Afrika. Verskeie bestaande tegnieke wat gebruik word om verkeer te modelleer, is ondoeltreffend wanneer dit op 'n groot skaal geïmplementeer word. Aannames word gemaak oor die kwantiteit en lokaliteit van verkeer wat vanuit, na en deur die studie-area vloei. Infrastruktuurontwikkeling gebaseer op onakkurate verkeersmodellering kan die intensiteit van verkeersopeenhopings vererger.

Die impak wat so 'n verandering van infrastruktuur sal hê buite die studie-area kan ook nie geëvalueer word nie. Dit is daarom nodig om vervoerinfrastruktuur op 'n groter skaal as vantevore te modelleer.

Hierdie tesis bied 'n grootskaalse verkeersmodelleringsraamwerk aan wat potensieel die impak van publieke vervoer en infrastruktuurontwikkelings kan modelleer vir die Suid-Afrikaanse konteks. Die raamwerk bou voort op die beginsels van die Vier-Stap Modelleringsmetodologie.

'n Dubbele beperkte gravitasie model wat aangepas is, word voorgestel en geformuleer om die tekortkominge van statiese ritverspreiding modelle aan te spreek.

Kerndigtheidsfunksies word gepas aan opname-data om unieke reisimpedansiefunksies te definieer vir elke verkeersanalisesone. Ritroetes word bepaal deur middel van dinamiese verkeerstoedeling wat geïmplementeer is deur 'n mesoskopiese verkeerssimulasie. Die gravitasiemodel word iteratiewelik gekalibreer deur die uitvoer van die verkeersimulasie te gebruik in 'n positiewe terugvoer lus om konvergerende ritverdelings te produseer.

Die kalibrering en validering van die voorgestelde gravitasiemodel toon aan dat dit meer akkuraat is as die enkele ritimpedansie gravitasiemodel. Die raamwerk produseer oorsprong-bestemming matrikse, inter- en intrasone roetes, kwartuurlikse verkeersvloeie en 'n maatstaf van verkeersopeenhopings wat in 'n GIS omgewing visualiseer kan word.

Acknowledgements

The author wishes to acknowledge the following people for their various contributions towards the completion of this work:

- Herman Franken
- Kevin Durant
- Matthew Guile

Table of Contents

List of Reserved Symbols

Symbol	Meaning
c_i	Count for bin i
c_i^s	Smoothed distribution count for bin i
O_i	Number of trips originating from TAZ i
D_j	Number of trips destined from TAZ j
T_{ij}	Number of trips originating in TAZ i destined for TAZ j
K_i	Gravity model iterative balancing term for TAZ i
C_{ij}	Cost of travelling from TAZ i to TAZ j
O_{itm}	Number of trips originating from TAZ i for mode m and period t
D_{jtm}	Number of trips destined from TAZ j for mode m and period t
T_{ijtm}	Number of trips originating in TAZ i destined for TAZ j for mode m and period t
p_{im}	Proportion of trips originating from TAZ i using mode m
K_{itm}	Gravity model Iterative balancing term for TAZ i for mode m and period t
C_{ijtm}	Cost of travelling from TAZ i to TAZ j for mode m and period t
η_m	First Tanner function parameter for mode m
ζ_m	Second Tanner function parameter for mode m
α_m	Zonal attraction calibration parameter for mode m
τ_m	Temporal adjustment calibration parameter for mode m
μ_{tm}	Average travel time for mode m and period t
σ_{tm}	Standard deviation of travel times for mode m and period t
B_{tm}	Interval of the temporal adjustment band for mode m and period t
S_a	A function of the traffic passing through link a
v_a	Quantification of traffic passing through link a
ϱ_{ij}^{ar}	Activation variable for link a on route r from origin i to destination j
x_{ij}^r	Number of vehicles on route r between origin i and destination j
p_w^{et}	Proportion employment of ward w in TAZ t
p_w^{vt}	Proportion vehicle ownership of ward w in TAZ t
p_w^{ut}	Proportion urban population of ward w in TAZ t
p_w^{Ot}	Probability of selecting ward w as an origin TAZ connector of TAZ t
T_F	Length of simulation time frame
v_f	Free-flow speed
Q	Capacity
k_n	Density at capacity
v_n	Speed at capacity
t_f	Free-flow travel time
t_n	Travel time at capacity

d_n	Traffic delay at capacity
h_n	Average headway at capacity
L_n	Average spacing at capacity
q_o	Flow limit for free-flow speed
x_o	Saturation below which speed equals free-flow speed
q_a	Number of traffic arrivals
v_a^t	Number of trips that have traversed edge a during iteration t
M_β^ρ	Modelled proportion of arrival time for bin β
M_β^δ	Modelled proportion of departure time for bin β
U_β^ρ	Observed proportion of arrival time for bin β
U_β^δ	Observed proportion of departure time for bin β
σ_β^ρ	Deviation of modelled arrival time distribution β
σ_β^δ	Deviation of modelled departure time distribution β
RMSE_h^x	The trip table RMSE between iteration h and $h-1$
RMSE_h^c	The cost matrix RMSE between iteration h and $h-1$
a_{kh}^o	Observed traffic flow through network segment a during period h
a_{kh}^s	Simulated traffic flow through network segment a during period h

List of Acronyms

ABA: Activity-based approaches
CATS: Chicago area transportation study
CPM: Computational process model
DTA: Dynamic traffic assignment
EVA: Erzeugung verteilung auteilung (Production Distribution Mode choice)
FSM: Four-step models
GAP: Geo-spatial analysis platform
NHTS: National household travel survey
NRMSE: Normalised root mean square error
OTLD: Observed trip length distribution
PCE: Passenger car equivalents
RMSE: Root mean square error
SUE: Stochastic user equilibrium
TAZ: Travel analysis zone
TLD: Trip length distribution

List of Figures

List of Tables

CHAPTER 1

Introduction

Contents

This chapter serves as an introduction and a guide to the layout of the remainder of the thesis. The next section introduces the concepts of congestion and traffic modelling.

Since 1960, the percentage of people living in urban areas have increased from 34% to 54%. Since agricultural activities require far less labour for the same yield due to technological advancement, ex-farm workers look to urban areas for work. The United Nations estimates that cities will absorb most of the population growth between 2016 and 2030 [49]. As the number of people living and working in urban areas increase, so to does the need for transportation. At some point, more vehicles on the road lead to longer commuting times.

1.1 Traffic congestion

The Centre for Economics and Business Research estimated that the cost of congestion in France, Germany, the UK and the US totalled $200 billion USD in 2013. It found that the average driver in a metropolitan area spent 36 additional hours stuck in gridlock traffic per year, a figure which is forecast to increase to 42.8 hours by 2030 [10].

The 2015 TomTom traffic index identified Cape Town as the most congested city in South Africa. Their data shows that morning and evening commuters experience on average a 72% and 58% respective increase in travel time [48].

It has been shown that increasing road capacity does not necessarily reduce congestion levels [15]. Most commuters choose their mode of transportation and route by considering their opportunity cost, meaning, they evaluate and compare each alternative. Choosing one alternative means losing out on all of the other choices. When a specific route is congested, the time cost associated with using such a route is too high for some individuals and they choose an alternative route – a long cut [10]. This route might have a longer distance, but the travel time might be shorter or the absence of congestion might make the route more attractive.

Theoretically, if traffic was a closed system with a constant demand, increasing the network capacity (supply) to meet this demand would be an effective solution. However, a road network does not fulfil either of these requirements. If the capacity on the previously congested route where to increase, it attracts more traffic to itself away from other congested routes. Individuals can also change their mode of transportation. Someone who is carpooling to reduce their travel costs could now begin driving himself because s/he values his time more than the increase of the cost of fuel of driving to work on his own. This can cause routes where additional capacity has already been added, to once more become congested. It is assumed that all individuals travel on the route that has the lowest cost according to their own criteria. Traffic has been observed to rebalance itself until there is no cheaper alternative route for any individual. John Glen Wardrop formulated two principles for traffic equilibrium which state that: Firstly, *the journey times in all routes actually used are equal and less than those which would be experienced by a single vehicle on any unused route* and secondly, that *at equilibrium the average journey time is minimum* [54].

One method for reducing congestion is to increase the price of travelling on a specific road through toll fares. The demand for the route is then controlled by the cost of the fare. Concessionaires can determine a price structure by requesting stakeholders to participate in a survey. This does not decrease the demand for the total network. The congestion could once again spread to other parts of the network as individuals seek to minimize their travel costs [15].

Congestion can therefore be seen as a function of total demand and supply over all routes with a similar destination or origin. Adding additional capacity to only a portion of the network will more often than not, be insignificant relative to the total demand. Furthermore if only a portion of a route's capacity is upgraded it will temporarily alleviate short term congestion, but only for the part of the route where capacity was added.

Another strategy to reduce congestion is the use of higher density transportation modes, which mostly consist of public transportation. Buses and mini-bus taxis are able to transport more people relative to the space on the road that they use. Buses equate to roughly three passenger car equivalents with regards to congestion and can transport upward of 25 individuals while mini-bus taxis are equivalent to 1.5 passenger cars and can transport up to 16 people.

1.2 Traffic flows in networks

Traffic is comprised of many vehicles that travel through a road network. Each vehicle travels at different and constantly varying speeds. The flow of traffic is determined by the individual behaviour of each vehicle which, is in turn, influenced by the physical characteristics of the network and the level of traffic itself. Each additional entry to a network segment marginally reduces the range of available individual behaviour. When a portion of the network becomes saturated, vehicles travel at speeds much lower than they would in the absence of any congestion.

A network typically consists of a combination of interrupted and uninterrupted facilities. The former refers to segments that contain stop streets, roundabouts, traffic circles and signalised intersections. The latter are road segments that do not contain any of the aforementioned elements and consist of mainly highways or freeways. A network facility can only serve a finite number vehicles within a specific time period. This limit depends on the specification of the facility and is referred to as its capacity, which is defined in terms of a volume per time period.

The flow of traffic traversing a network can be classified into three conditions, namely, free flow, congested flow or a jammed stop-start condition which occurs when traffic flow nears the

capacity of a facility. Once the flow of traffic reaches a congested stage it creates a roll-on effect that affects the conditions in the preceding or upstream facilities [50].

Each vehicle is driven by a unique individual and can be seen as an origin, destination and departure time pairing which is referred to as a trip. Given that there is more than one possible option, the individual is free to decide which route he will take through the network, based upon personal preference. The reasoning behind selecting a specific route will vary from one individual to another. Selection of a route may also depend on the travel time, distance, monetary costs, opportunity cost or other subjective criteria. Individuals might, for example, choose a route simply because they like driving it.

Modelling traffic becomes more arduous as the number of vehicles and the network size increases. As the total number of traversing individuals increases, so too does the complexity of their interaction with the network. The size of the network influences the number of potential different routes an individual could travel on. Larger networks provide individuals with more alternatives that satisfy similar criteria.

Depending on the area being studied, traffic will likely not be confined to originate and reach its destination within the bounds of the network. Traffic traversing the network can originate, or be destined to a place in, or outside the network. The different combinations of origin and destination pairing depending on whether the trips originate, or are destined in, or outside the network, can be classified into three types that: Firstly, intra-regional trips start and end within the network. Secondly, inter-regional trips that are destined for a different area than which it originated in. Lastly, through trips that start and end outside the study area, but pass through it. Therefore modelling traffic within a network requires accounting for all the types of trips in order to accurately determine the traffic levels.

1.3 Problem description & statement

Congestion places a burden on society which could have been avoided with sufficient planning. The most commonly used transportation modelling techniques were shaped by the needs of a post second world war economic expansion in the United States. The answers provided by the current status quo of transportation modelling become more misaligned as the world is becoming more urbanised.

South Africa is a developing economy with an established and growing congestion problem. Ill-informed infrastructure investment could potentially increase congestion in the long run by inducing extra demand due to Braess' paradox [7]. Congestion causes increased mechanical wear on vehicles, more emissions, higher opportunity cost associated with travel as well as psychological impacts such as road rage. It is therefore important to determine the short and long term effects of any potential infrastructure development or changes to policy.

Transportation modelling has traditionally been done on a small scale. Studies are performed analysing congested highway segments or a regional district. As urban areas expand so too does the diversity of behaviour within them as well as the distance over which they attract traffic. It is therefore currently necessary to conduct many studies with different sets of data to inform proposed infrastructure investment that do not fall within the same small area. If these studies are completed they would not be able to incorporate the effect of a different infrastructure development falling outside the study area. In the past this approach to transportation modelling was sufficient. As the traffic density inside sprawling urban areas increase, plugging a proverbial leak might cause another leak somewhere else.

Due to the limited study area, inter-regional traffic entering a TAZ and through traffic is derived mostly as origin and destination blind from traffic counts. It is not important for these studies to know where the trips come from or where they are destined for, but only where they enter and leave the study area and what routes they take. This limits the possibility of forecasting the impacts of infrastructure investment. Thus, in this thesis the problem of simultaneously modelling traffic on a large scale within multiple traffic analysis zones is addressed.

1.4 Thesis objectives

Based on the problem description, it is the aim of this thesis to develop, adapt or use an applicable framework using available traffic data to model morning peak hour commuter traffic at a provincial level in South Africa. In order to reach this goal, the following list of objectives is defined:

- Conduct a literature review on existing transportation modelling methodologies.
- Evaluate available data sources.
- Select and implement a traffic modelling framework.
- Validation of the framework.
- Sensitivity analysis of the framework.
- Conclusions and recommendations.

The framework should take into account the different types of modes used by commuters and should be capable of modelling a shift from private to public transportation.

1.5 Thesis layout

This chapter served as an introduction to the concepts of congestion and traffic modelling. It describes the problem of expanding the scale of traffic modelling to larger areas and objectives set out to solve this problem. Chapter 2 reviews possible methods to accomplish the goals set out in this chapter. The data discussed in Chapter 3 is used to construct the framework described in Chapter 4. The models defined in Chapter 4 are calibrated and validated in Chapter 5. Chapter 6 consists of a sensitivity analysis on the simulation parameters used in the framework. The framework outputs in Chapter 7, which presents outputs from the framework. The thesis concludes with a discussion of the key findings and recommendations in Chapter 8.

CHAPTER 2

Literature Review

Contents

Chapter 1 introduced the problem description and sets out the goals that this thesis aims to achieve. This chapter contains a review of the methods with which traffic can be modelled.

Transport modelling with the focus on urban and highway development dates back to the early 1950s. Post-World War II America experienced a surge in vehicle and home ownership. A combination of rapid urban expansion and deteriorating road conditions, led to wide scale congestion on the USA's highways. At the time only crude linear forecasting of traffic counts and very basic applications of gravity models existed [56]. The first comprehensive studies to link land use and travel were the Detroit Metropolitan Area Traffic Study, conducted from 1953 to 1955, and the Chicago Area Transportation Study (CATS) [41].

Currently, the two main methods for modelling transport are the Four-Stage Modelling (FSM) and Activity-Based Approaches (ABA) [40]. FSMs are of a aggregate nature and consist of four stages namely, trip generation, trip distribution, modal choice and route assignment. ABAs simulate all transport activity for individuals from a synthesised population. A literature review on the different steps of FSMs is presented in Section 2.1 and an overview of ABAs is given in Section 2.2.

2.1 Four-stage modelling

Despite strong criticism [14, 8], institutional inertia has caused the field of transportation modelling to be dominated by the FSM approach [40]. Trip generation is the first step of the FSM and it is used to forecast trips based on future land use. FSMs divide the area being modelled into smaller areas referred to as Travel Analysis Zones (TAZ).

2.1.1 Trip generation

Trip generation is a practise of estimating how many trips will travel to and from an area of specific land use zone. Trip generation rates are estimated through finding relationships between the characteristics of and the number of trips observed coming to or leaving from the area. It is assumed that, during the morning peak hours, trips start at residential areas and are typically destined for non residential areas. Therefore residential characteristics of a zone are evaluated when modelling trips leaving an area and non-residential attributes are used when modelling trips entering an area [12].

The results of surveys are used to estimate a relationship between a unit of measure, such as number of employees or gross leasable area, and the number of trips generated from the land use. The relationships are traditionally linear or logarithmic and estimated through regression [34, 32]. Artificial Neural Networks [20] have been used to fit more accurate relationships between land use and trip generation and logistic regression models [33] have proven to improve the temporal stability of trip generation rates.

After trips have been generated, they need to be distributed between the different zones.

2.1.2 Trip distribution

Early research on trip distribution models [17, 37] and their calibration techniques [18, 57] still form the basis for more recent research [9], [1]. The most predominant model for trip distribution is the doubly constrained gravity model [40] which is usually solved through an iterative process [19].

The doubly constrained gravity model can be defined as follows. Given that O_i is the total number of trips originating at TAZ i, D_i is the total number of jobs in TAZ j, and C_{ij} is the cost of travelling from TAZ i to TAZ j, the number of trips originating from i, destined for j, T_{ij} can be expressed as

$$T_{ij} = K_i K_j O_i D_j f(C_{ij}), \tag{2.1}$$

with

$$K_i = \frac{1}{\sum_j K_j D_j f(C_{ij})}, \tag{2.2}$$

$$K_j = \frac{1}{\sum_i K_i O_i f(C_{ij})} \tag{2.3}$$

and f an impedance of travel function of cost C_{ij}. The column and row totals are preserved through iteratively calculating K_i and K_j until the number for trips from all the origins sum up to the number of jobs at the destinations.

The impedance of travel functions that are predominantly used are the power function $C_{ij}^{-\eta}$, an exponential function $e^{-\zeta C_{ij}}$ or a Tanner function, which is the product of the aforementioned power and exponential function $C_{ij}^{-\eta}e^{-\zeta C_{ij}}$. Parameters η and ζ are calibrated so that the differences between the observed trip length distribution (OTLD) and the modelled trip length distribution (TLD) is minimized. This distribution produces trip tables which are used as the basis for the modal choice and route assignments. These will be discussed seperately below.

2.1.3 Modal choice

Trip tables for each of the distinct modes of transportation are created by assigning portions of the initial trip table for each mode. The CATS study had a modal split between public transportation and private auto mobile use [41]. After the modal split has been decided, the trips need to be assigned to the transportation network under evaluation.

2.1.4 Route assignment

Route assignment is the last step of the traditional FSM. There are several different methods available in literature. Early techniques, such as all or nothing assignment, assign all trips for a unique TAZ pairing via the shortest route. Stochastic assignment assigns different portions of origin-destination flows to different routes depending on a predetermined vector of probabilities. Equilibrium assignment is based on the idea that travellers will choose a route which minimizes the cost of their travel, whatever it may be. If a traveller chose a specific route, it would mean that the cost of that route is less than or equal to all the other options s/he could choose from. This is referred to as Wardrop's equilibrium [54].

The equilibrium assignment problem can be solved with the following nonlinear programming problem. Given the set of all links, A, routes, R, TAZ origins, O, TAZ destinations D, S_a is a function of the volume of traffic v_a for a link a which determines the average travel time for a vehicle on a,

$$\text{minimise} \sum_{a \in A} \int_0^{v_a} S_a(x)\mathrm{d}x \tag{2.4}$$

subject to

$$v_a = \sum_{i \in O} \sum_{j \in D} \sum_{r \in R} \varrho_{ij}^{ar} x_{ij}^r \qquad a \in A \tag{2.5}$$

$$\sum_{r \in R} x_{ij}^r = T_{ij} \qquad i \in O, j \in D \tag{2.6}$$

$$v_a \geq 0 \qquad a \in A \tag{2.7}$$

$$x_{ij}^r \geq 0 \qquad r \in R, i \in O, j \in D \tag{2.8}$$

ϱ_{ij}^{ar} is an activation variable which is 1 if link a is on the route r from origin i to destination j or zero otherwise. x_{ij}^r represents the number of vehicles on route r between origin i and destination j. By minimising the sum of the average travel times for all the links in a network, Wardrop's equilibrium is achieved.

A critique to the equilibrium assignment model is that it is insufficient from a infrastructure planning perspective due to possible variation in future traffic demand or supply. Stochastic

User Equilibrium (SUE) assignment seeks evaluate how robust a solution is in response to such variation. Different distributions and methods have been used to model stochastic demand [55, 46, 60], supply [36] and a combination of both [61].

The SUE is, in general, computationally expensive to solve for very large networks using conventional solution algorithms [58]. Some approximations to the SUE, like the incremental stochastic model [3], require the existence of a unique solution. Even though there are improvements to SUE assignments with regard to computation time [59] and uniqueness [28], they still only provide a static solution to an otherwise dynamic problem.

EVA models, whose name is derived from the German terms Erzeugung, Verteilung and Auteilung (production, distribution and mode choice) seek to incorporate trip distribution, modal choice and route assignment into one solution. EVA models are usually based on but not limited to stated preference of travel mode surveys which are modelled with a logit structure. Vrtic et al. [53] states that *the EVA approach is flexible enough to accommodate any problem, which can be formulated in its terms.* Large problems can thus be solved relatively quickly when formulated within the EVA framework, due to the proven convergence of the algorithm that it is based upon.

Dynamic Traffic Assignment (DTA) improves on the static models through the use of time-varying networks. However, this complicates finding a solution because the network is affected by the traffic. Each entry to the network increases congestion which in turn affects the most cost effective path of the next entry. Thus the traffic affects the network and the network affects the traffic. The implication is that the length of an individual trip can only be determined after its completion. For this reason iterative methods need to be used when finding a solution. Chiu et al. [11] notes that in most DTA cases true equilibrium is not found, but rather, approximations which are sufficiently close enough to the true equilibrium are found fall within reasonable time constraints. DTA has been modelled with mathematical programmes [5], optimal control theory [24] and variational inequality [23] formulations.

2.2 Activity-based approaches

The FSM approach to modelling transport was conceived during a post-war period, and is defined by fast economic and urban expansion. The framework was initially developed to decide how large sums of capital, earmarked for building highways, should be spent. Because of the aggregate nature of the FSM approach, it is oblivious to the underlying individual behaviour. Equilibrium-derived travel modelling is ignorant to the complexities of decision making related to participation in activities, household dynamics and habitual driving behaviour [47]. Therefore, an understanding of activity-based behaviour will give insight into travel behaviour [38].

2.2.1 Simulation-based applications

Simulation-based ABA is an operational application to the field of time geography, where individuals are tracked through time and space [38]. The range of possible travel is constructed as a prism in three-dimensional space where the third dimension is time [31]. An individual can only visit points within the prism, but is not able to visit all of them.

Simulation-based ABA models generally function according to three steps. They create individual activity programs (constructing a prism of possible movement) from which activity patterns are developed (enumerating possible routes through the prism). The patterns are then selected

through a pattern choice model, modelling individual travel behaviour. McNally et al. comment on the significance of simulation based ABA models like STARCHILD [42] which construct travel patterns tailored to individuals rather than assigning a pattern to an individual based on an observed aggregate behaviour [38].

TRANSIMS [51] is a comprehensive ABA traffic demand model consisting of a population synthesizer, activity generator, route planner and a traffic microsimulation that produces visual output as well as emissions estimates. It is currently maintained through an open source platform [25]. As powerful as it is, it has extensive data requirements for the area under study and as such has seen very limited application.

2.2.2 Computational process models

Computational Process Models (CPM) are modelled on the basis of a reductionist view. It states that the complexity of travel behaviour can be de constructed as a combination of interdependent individual decisions [27]. CPMs are designed to model travel behaviour through deconstructing the choices individuals make when they tend to their daily activities.

Garling et al. [26] published a paper on SCHEDULER, a CPM that produced short term activity chains from long term activity schedules based on the spatial and temporal activity preferences and constraints, of individuals.

SMASH improved on the framework of SCHEDULER by replacing the scheduler with utility based choices of activities which can be be swapped out, inserted or deleted anywhere on the activity schedule. SMASH is conceptually different to STARCHILD. STARCHILD enables individuals to optimize their travel behaviour through allowing a wide range of alternative routes to select from whereas SMASH has a heuristic approach [16].

ALBATROSS [4] is considered to be the current state-of-the-art model for CPM [38]. ALBATROSS takes household dynamics and socio-demographic variables into account when generating an activity program. Scheduling of the activity program is conducted through a set of decisions related through possible locations where activities can be conducted, their proximity to other individuals, modes of travel available and accounting for spatio-temporal travel linkages.

2.2.3 Econometric-based applications

Econometric-based ABA models are theoretically grounded in methodologies that are traditionally used in trip based modelling [38]. Golob et al. [30] modelled activity participation by relating household characteristics to survey data on how household heads participated in three groups, namely *work*, *maintenance* and *discretionary* activities.

2.2.4 Mathematical programming approaches

The household activity pattern (HAPP) is a variation of the pick up and delivery problem with time windows. Activities are modelled as items that need to be picked up in a Mixed Integer Linear Program (MILP) with household utility as the objective function. Recker [43] implemented a genetic algorithm solution approach. Due to HAPP's MILP formulation it can be solved through a wide variety of generic solvers.

2.3 Chapter conclusion

Transportation modelling originated with the FSM approach. Criticism of the approach has shaped its continual development, due to not only institutional inertia, but also the relative ease with which it can be implemented. Exact solutions for most of the equilibrium assignment based trip routing either require the existence of a unique solution or are computationally too complex for large networks. DTA address the critique that the solutions produced by FSMs are too static in nature through using time-varying networks.

Overall, all the methods have specific data requirements. ABA models are capable of more realistic transportation modelling in principle due to their bottom up nature. However, the limited implementation of ABA approaches highlight that up until now, the cost of obtaining the input data have not justified the additional confidence it potentially provides. Due to institutional inertia, most transportation surveys conducted by traffic departments are FSM-centric and do not fulfil the data requirements of the ABAs.

The pitfalls of both approaches are that they do not scale very well considering their shortcomings. Finding a routing equilibrium in FSMs becomes increasingly difficult because the number of possible routes increase with larger or more complex networks. Expanding the study range increases the amount of data required for ABA, which are already practically too expensive to obtain. As such, both approaches have been limited to relatively small study areas as assumptions are made based on the through- and inter-TAZ traffic intensity. It would be necessary to extend the methods currently available in literature in order to model much larger networks or areas.

This chapter gave a brief overview and discussion of the different methods for modelling traffic and transportation. The next chapter discusses what data sources are prepared and used.

CHAPTER 3

Data

Contents

The previous chapter gave an overview on different techniques that have been developed to model traffic. This chapter discusses data that are available within the South African context to determine the methods that will be used in achieving the objectives set out in Section 1.3.

3.1 CSIR Geo-spatial analysis platform

The Geo-spatial Analysis Platform (GAP) is a *common, mesoscale geo-spatial platform for the assembly, analysis and sharing of economic, development and demand information* [39]. It divides the country into twenty-five thousand distinct zones of approximately 50 square kilometres each. The GAP zones for the Western Cape can be seen in Figure 3.1.

The employment dataset of the GAP is based on where economic activity takes place and not the place of residence of the employed. For use in this study the GAP employment data for base year 2009 is adjusted on the assumption that the locality of employment did not shift over the course of two years to match the 2011 census data. The data are uniformly adjusted to fit the census employment statistics.

3.2 2011 National census

The 2011 National census conducted by Statistics South Africa is available at a census ward level of detail. Household vehicle ownership and employment statistics per ward is used. The

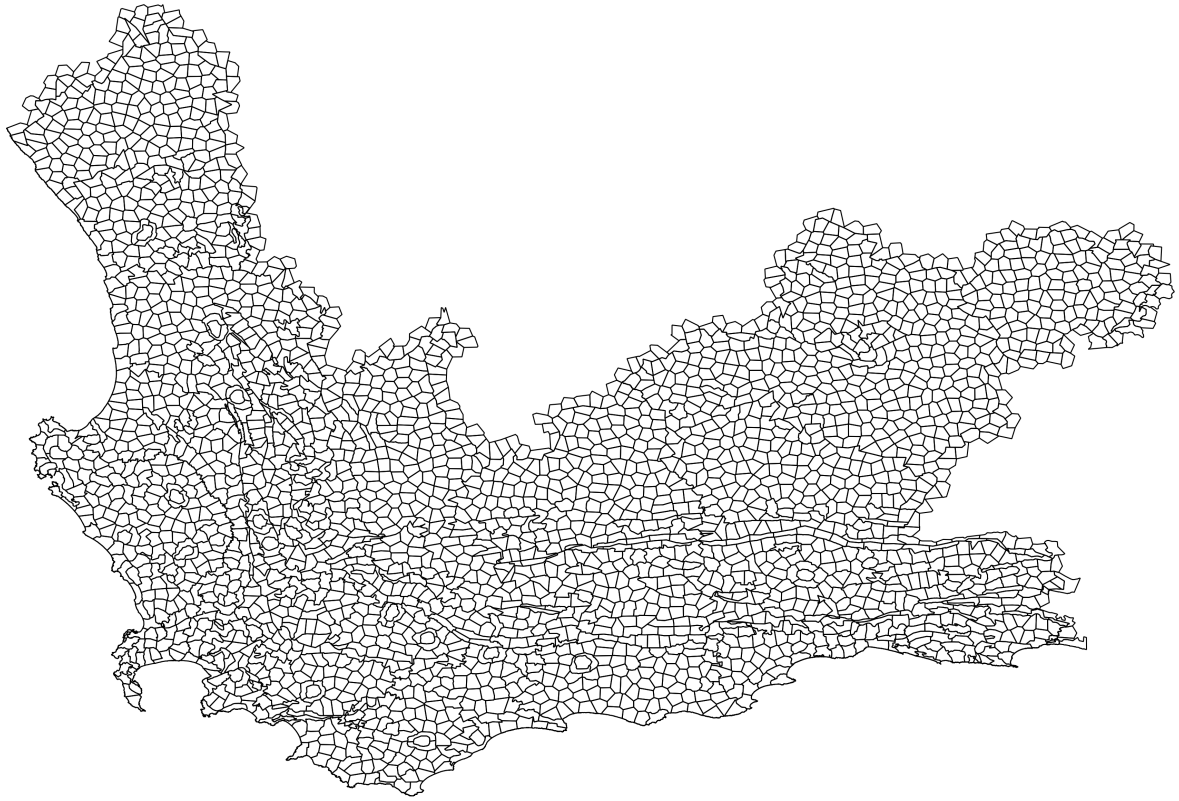

FIGURE 3.1: *A map of the GAP zones for the Western Cape in the CSIR GAP.*

wards, as shown in Figure 3.2, are further divided into enumeration areas as in Table A.2, and classified by geography type (gtype) as in Table A.3. (Appendix A).

3.3 2013 National household travel survey

The 2013 National household Travel Survey (NHTS) [45] is based on a random stratified sampling of South Africa's households and is stated to be sufficient for analysis at a provincial and TAZ (Travel Analysis Zone) level (Figure 3.3). The household dataset is accompanied by person data per household. The survey questionnaire is constructed to give insight into travel patterns within the country. The section that is used for this study is Section 4: Work related travel patterns. In particular questions 4.9, 4.10, 4.13, 4.14 and 4.21 are used which gave information on when people left for work, when they arrived at their place of work and which mode of travel they used in doing so.

From all respondents who indicated that they drove to work on their own, 9145 gave their arrival and departure times. Similar responses for those who indicated they used buses and taxis (options 3 and 5 for question 4.21) were 2503 and 8243 respectively.

Only data points of those who indicated that their journey to work started between 05:00 (denoted further in the format 300, relating to minutes after 00:00) and 09:00 (540) and had a travel time of less than 150 minutes are used. Of these, 1393, 252 and 611 usable data points are available for the Western Cape.

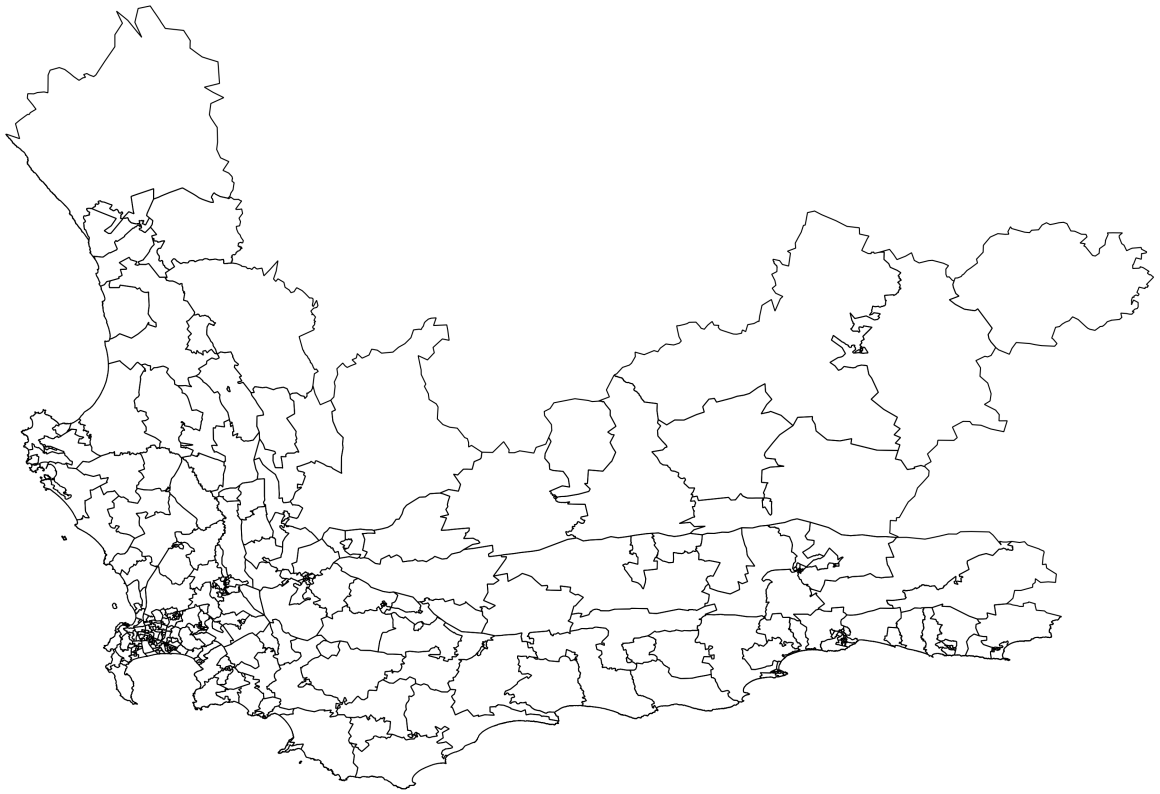

FIGURE 3.2: *A map of the census wards for the Western Cape in the 2011 census.*

The OTLD for each mode is constructed by binning the survey travel times into 5 minute intervals $[0, 5), [5, 10), \ldots, [145, 150]$. The OTLD for the modes *drive*, *bus* and *taxi*, Figures 3.4, 3.5 and 3.6, respectively, illustrate that people tend to approximate their travel and departure times to the nearest multiple of fifteen minutes.

A smoothed OTLD is obtained by averaging the period before and after a bin. Given that the count in bin i, c_i, the count c_i^s in the smoothed distribution for bin i is

$$c_i^s = \begin{cases} \dfrac{c_{i-1} + c_i + c_{i+1}}{3} & \text{for } 1 < i < 30 \quad (3.1) \\ \dfrac{c_i + c_{i+1}}{2} & \text{for } i = 0 \quad (3.2) \\ \dfrac{c_{i-1} + c_i}{2} & \text{for } i = 30. \quad (3.3) \end{cases}$$

The smoothed and original distributions of the binned data used to calibrate the gravity model, can be seen in Figures 3.4, 3.5 and 3.6. Of the 1393, 252 and 611 data points that are usable to construct trip length distributions, only 960, 175 and 397 data points indicated in what TAZ the place of employment is. This smaller, but complete subset is used to calculate the root mean square error (RMSE) of each zones' trip distribution.

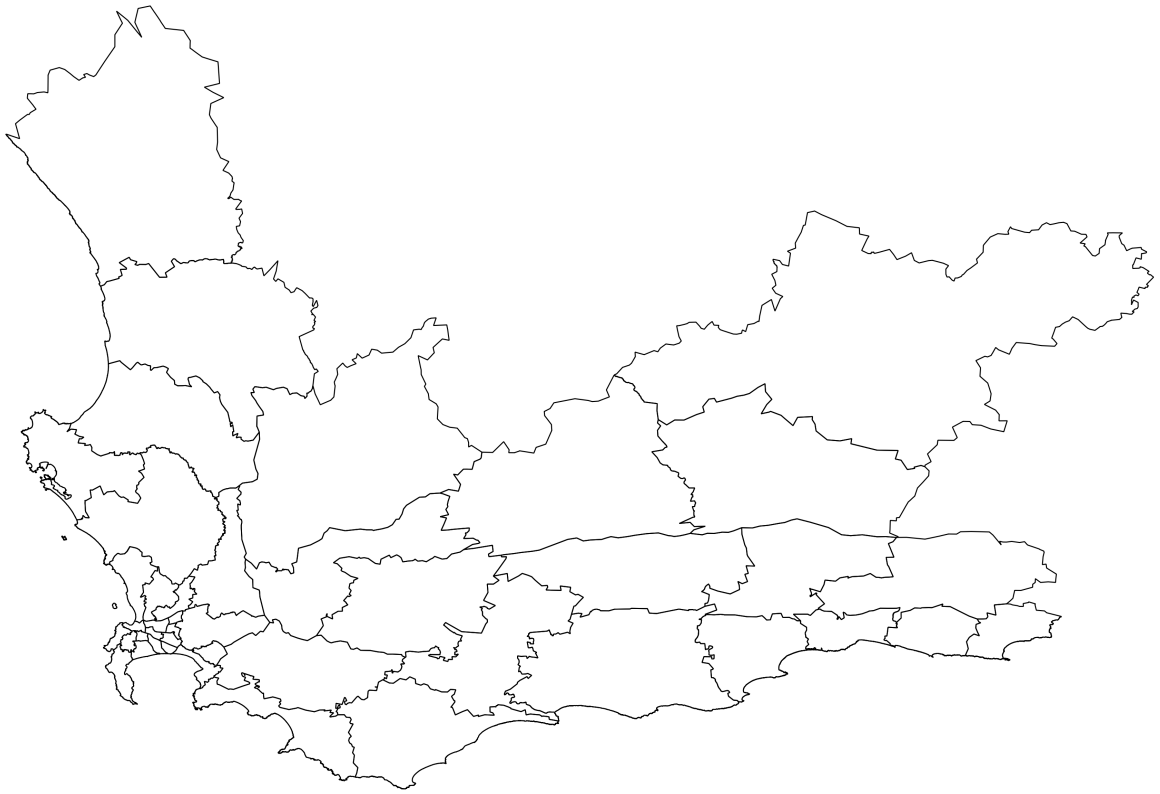

FIGURE 3.3: *The Travel Analysis Zones for the Western Cape*

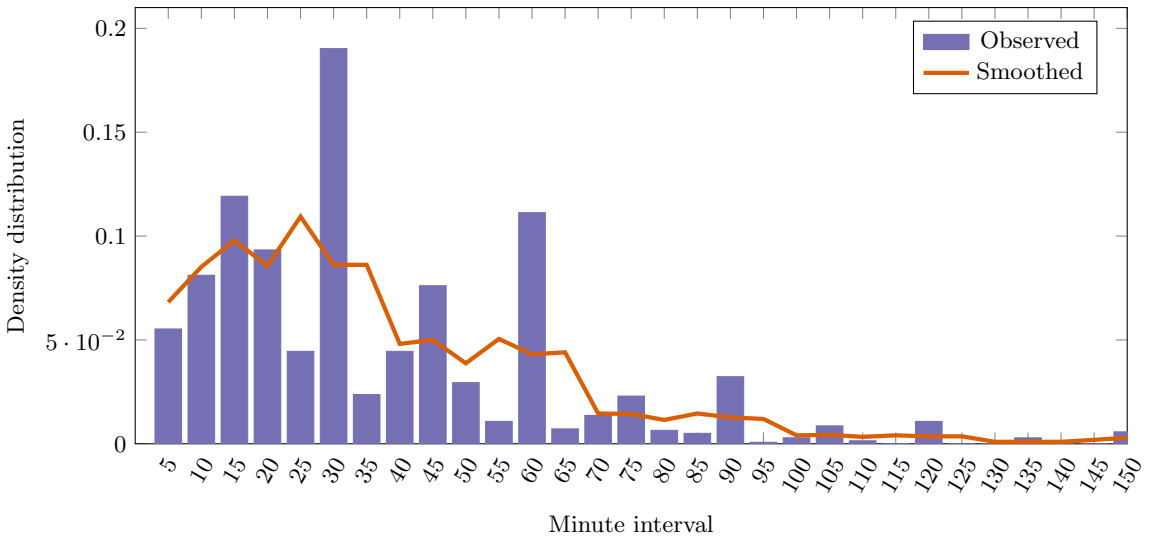

FIGURE 3.4: *Binned and smoothed OTLD for the Western Cape for mode* drive

3.4 Road network

The network through which the trips of the framework has to be flown is developed from an Open Street Map extract from the website `www.Geofabrik.de` [29]. Intersecting segments are cut at their intersection if they are not bridges or on- or off-ramps. Each edge in the network

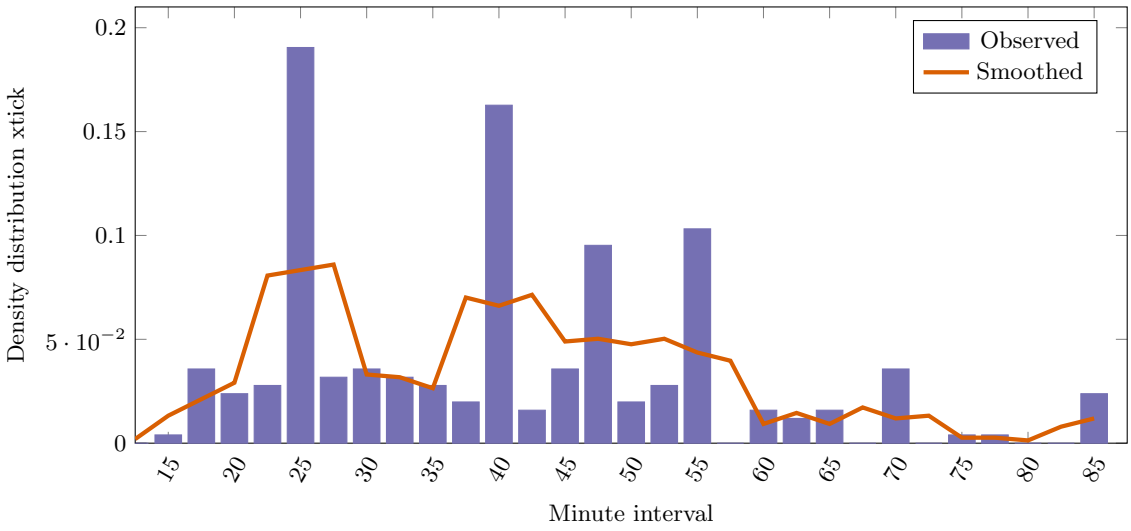

FIGURE 3.5: *Binned and smoothed OTLD for the Western Cape for mode* bus

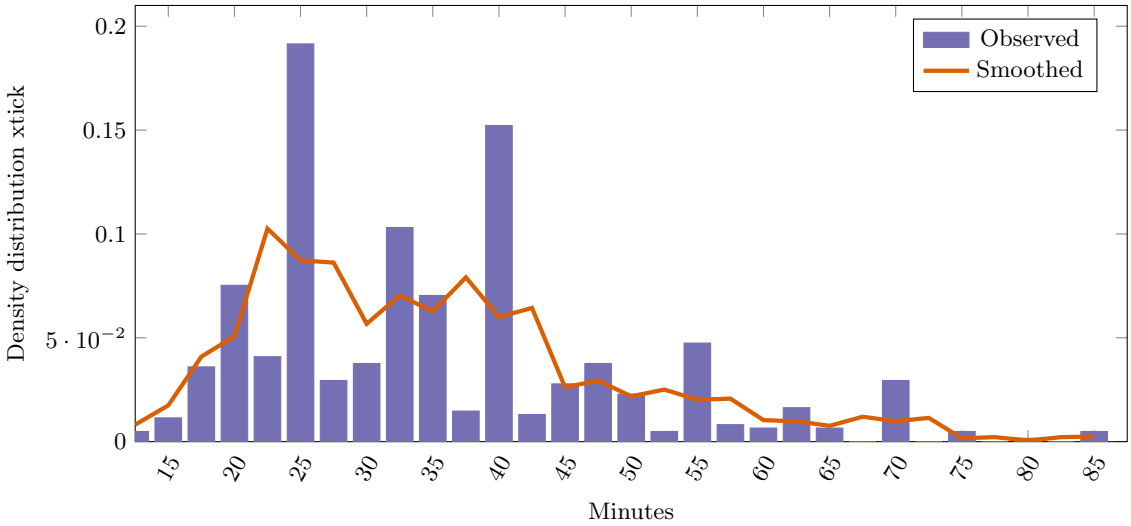

FIGURE 3.6: *Binned and smoothed OTLD for the Western Cape for mode* taxi

is assigned a unique start vertex, end vertex, and geometry ID. The length of each edge is calculated and stored in kilometres.

Segments without a speed limit entry are assigned speed limits through a process of classifying and matching them with segments that do have a speed limit entry. Every segment is classified according to what type of census enumeration area it intersected the most with. Segments without speed limits are then matched to the closest similar segment that had a speed limit based on the enumeration area type, length of the segment and the type of road.

None of the segments had any information regarding the number of lanes. The assumptions that are made for the number of lanes per segment can be seen in Table A.4 (Appendix A). The number of lanes on the national roads and the motorways in the Western Cape are manually updated from satellite imagery available from Google Maps. The fully saturated physical capacity of a segment of road is calculated at 15 m per passenger car equivalent per lane. The network shape file, Figure 3.7 for the Western Cape consists of 174 371 edges and 129 241 vertices. The directed graph of the shape file, in which an additional edge is added for every two way street

FIGURE 3.7: *The road network for the Western Cape*

had 328 628 edges.

The theoretical capacity for each segment, in Table A.5, is estimated based on the parametrisation in Akcelik [2] and adjusted based on observed maximum flow rates from the 2011 SANRAL yearbook [6]. The adjustment factors in Table A.6 are derived as the ratio between observed maximum flow rate per lane for each speed limit and the theoretical capacities. The network edges are stored in a database with the following headings:

- GID,
- start_id,
- end_id,
- lanes,
- speed limit,
- length,
- one-way and
- lanes.

For each census ward, every vertex within its boundaries is assigned a proportion of households who own vehicles. The network vertices are used as TAZ connectors. Origin TAZ connectors are those vertices in the network that fall within the boundaries of a residential area within a TAZ. Destination TAZ connectors are vertices within a farmland, commercial or industrial area. The vertices of the network are stored in a database with the headings

- taz_id,
- point_id,
- cratio,
- uratio,
- eratio.

Given the set of wards W_t in TAZ t, the entry in the ratio columns are

$$\text{cratio} = \frac{p_w^{vt}}{\sum_{j \in W_t} p_j^{vt}}, \tag{3.4}$$

$$\text{uratio} = \frac{p_w^{ut}}{\sum_{j \in W_t} p_j^{ut}}, \tag{3.5}$$

$$\text{eratio} = \frac{p_w^{et}}{\sum_{j \in W_t} p_j^{et}}, \tag{3.6}$$

with p_w^{et} the proportion employment in ward w, p_w^{vt} the proportion vehicle ownership in ward w and p_w^{ut}, the proportion of population living in an urban area in ward w, within TAZ t. The columns cratio, uratio and eratio represents the proportion vehicle ownership, urbanised population and employment respectively of a ward w relative to the other wards within each TAZ.

3.5 Vehicle counts

FIGURE 3.8: *Vehicle counting station locations in and around the Cape peninsula*

The 2011 SANRAL vehicle counts are used to evaluate modelled outputs. The counts from stations that had more than 80% uptime during 2011 is captured from the SANRAL 2011

yearbook and processed with image recognition software, Im2Graph [52]. The locations of the counting stations in and around the Cape peninsula can be seen in Figure 3.8.

Figure 3.9 shows the capture taken from the yearbook for vehicle counting station 5027. Each block represents 24 hours. The days are from left to right, Monday to Sunday. The blue and green graphs are the recorded volumes in terms of vehicles per hour for each direction, with the red being the sum of the blue and green lines [6]. The image is then processed with the image recognition software to capture each line and the data is saved in a comma separated value text file with the x values and y values.

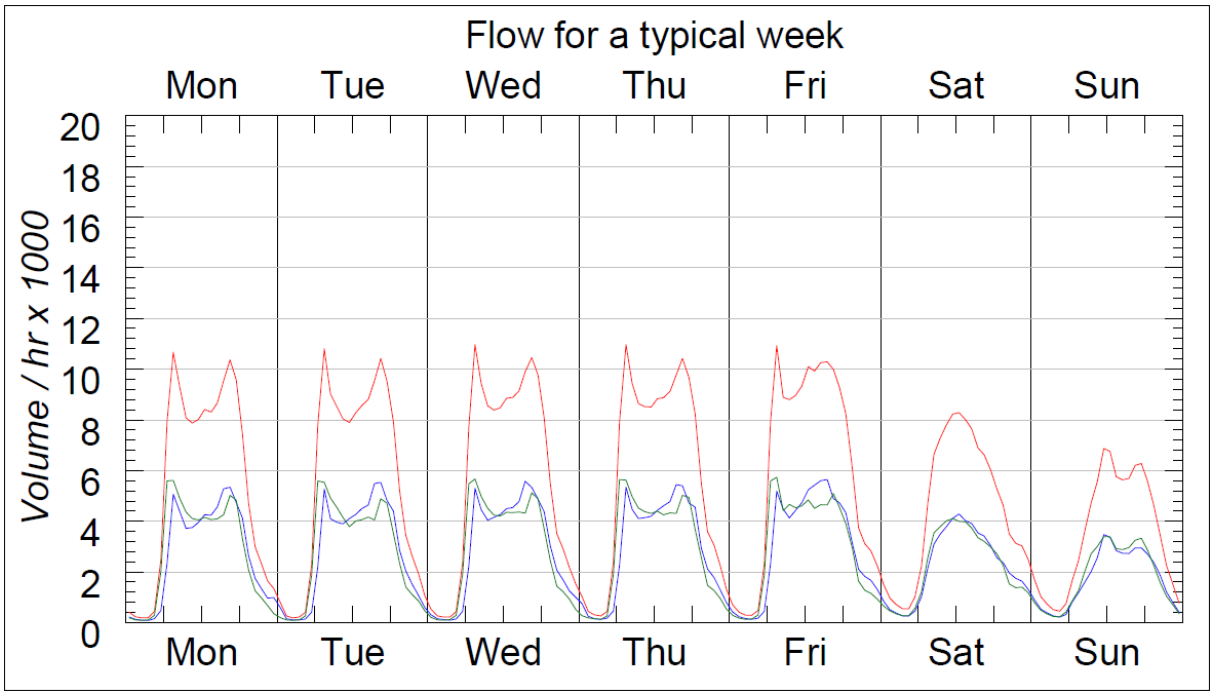

FIGURE 3.9: *The image captured from the SANRAL Yearbook that shows the vehicle counts for counting station 5027.*

To determine the total number of vehicles for any given time period, a Python script takes a Riemann sum over the range required from the data points to approximate the area under the curve.

3.6 Trip generation

The 2011 Census spatial geography and 2011 National Census [44] are used in combination with the GAP to approximate where workers lived and where they worked. Both data sources are aggregated to TAZ (Travel Analysis Zone) level through assigning a ward or GAP zone to the TAZ, based on the largest intersection with a TAZ. The TAZ worker and job data for the Western Cape can be seen in Table Appendix A, A.7. This data is used as the input data for the gravity model that is discussed in the next chapter.

3.7 Kernel density functions

Kernel density functions are fitted to the NHTS TLD and departure data using the *gaussian_kde* function from the Python package *scipy.stats*. Both sets of functions use the default bandwidth factor, *scott*. For the TLD and departure data only a vector of travel times and departure times are passed to the function, respectively, for every TAZ and mode. Figures A.7, A.8 and A.9, in Appendix A, show the fitted kernel density functions for TAZ zone 9020 (Northern Corridor) for the modes, *drive*, *bus* and *taxi* respectively. The density functions for the departure times, Figures A.1, A.2 and A.3 show the binned departure times for the modes *drive*, *bus* and *taxi*.

These density functions fitted to the TLD data are used as the travel of impedance function in the proposed gravity model discussed in Chapter 4. The functions fitted from the departure data are used to disaggregate the number of workers departing from a TAZ into 15 minute intervals.

3.8 Simulation

In the simulation, fleets of vehicles are represented by a list of variables. This list contains information of the

- assigned route b,
- current position on the route at vertex number k,
- fleet size,
- origin TAZ,
- destination TAZ,
- current simulation time interval,
- time left on road,
- estimated time to complete current segment,
- departure time and
- mode.

The assigned route b is a list of network vertex Ids The variable k is the index of b and stores the vertex which was most recently passed by the fleet.

The traffic simulator produces a trace of each fleet on route assignment that contains the

- origin TAZ,
- destination TAZ,
- fleet size,
- mode and
- list of traversed vertices.

Once a fleet has completed its trip the following entries are saved:

- Origin TAZ,
- destination TAZ,
- trip time,
- fleet size,
- departure time and
- mode.

The former trace is used to evaluate if the routes are converging. The end trace is used to create distance tables for the next iteration of the gravity model. A table is constructed for each mode based on the recorded travel times from the completed trips' entries. The table contains

- origin TAZ,
- destination TAZ and
- average travel time,

where the travel time is the weighted average travel time between the origin and destination TAZs.

3.9 Chapter conclusion

The CSIR's GAP can be used to estimate D_i, the number of trips demanded at or destined for TAZ i by aggregating the GAP zones to a TAZ level. The 2011 Census data can be used to calculate O_i, the number of trips supplied by or trips originating from TAZ i by adding the active working population from the wards contained within the TAZ.

The NHTS data discussed in this chapter is deemed to be usable at a TAZ level. It can be used to generate departure and as a measure to compare the trip distributions and modelled TLDs. It should be noted that the survey has previously under estimated the number of intra-zonal trips. However, the density of the data points are not sufficient to be used to derive TLDs for periods shorter than a day.

Both the GAP and NHTS does not fulfil the data requirements to construct an ABA modelling framework. Although the GAP does identify where exactly people work, it does not give any information of where they come from or when they arrive at work. The NHTS data is compiled from surveying a stratified sampling of the population – its findings are therefore aggregate in nature. The data discussed in this chapter is used as input and the basis from which the framework described in the next chapter is designed. The traffic modelling framework will therefore be limited to a disaggregated top-down approach (a FSM).

It should be noted that the assumptions pertaining to the number of lanes, directional split of intersections and speed limits of the road network obtained from Open Street map, could skew model outputs due to the nature of transportation modelling.

CHAPTER 4

Modelling framework

Contents

The previous chapter was a summary of all data which is used as input for the framework described in this chapter. The models and techniques that are discussed in Chapter 2 share a common limitation assumption. They are predominantly used to model the traffic within an area which is small relative to the area that is encompassed by the study. This is achieved by estimating the inter-zonal trips. Assumptions for where these trips enter and leave the smaller area can be made based on vehicle counts. The drawback of using traffic counts to estimate these trips is that they are origin and destination blind. Vehicles are only observed when passing a vehicle counting station. Even with a high density of inductor loops to count the number of vehicles within the study area, their origins and destinations remain unknown. Without information on where inter-zonal trips are coming from or going to, forecasting traffic demand for an area might lead to building inaccurate future scenarios.

A gravity model can be used to estimate the composition of inter-zonal trips from the larger aggregated zones falling outside the area of interest. The shortcoming of this method is that the behaviour of travel for a large area is estimated through a single cost function $f(C_{ij})$ in equation (2.1.2). This means that every area in the study region follows the same distribution of trips which is consistently used through the study period. This could lead to building incorrect scenarios. The travel behaviour of people living within a central business district differs from those who live far outside it. The 2013 NHTS shows that even at a provincial aggregate there are differences in the behaviour of different modes of transport. The kernel density functions fitted from the 2013 NHTS illustrate how different TAZs have different travel time length distributions.

Alternatively, impedance of travel functions can be calibrated for each TAZ. This would however require the simultaneous calibration of all the impedance of travel functions, which will result in

an exponentially growing parameter space. The model proposed in this chapter seeks to address the aforementioned potential temporal stability and trip distribution concerns and is specifically designed to improve its scalability.

4.1 Trip distribution

The proposed gravity model makes use of traffic analysis zones, census and survey data to model the origins and destinations of commuter traffic on a macroscopic level. Interactions between TAZs are influenced by the number of employed residents, the number of people who work within the boundaries of a TAZ (henceforth referred to as jobs) and the cost associated with travel between zones. The calibration of the commuter demand model is achieved by comparing its output to survey data.

The survey data was used to estimate the number of workers who drove all the way to work or used a bus or a taxi for each TAZ. The travel fractions for transport mode m and TAZ i, p_{mi}, was calculated as a percentage of the total number of respondents who indicated their mode of travel. The number of workers per mode was calculated by multiplying the travel factors with the employed population within a TAZ. Departure times, Figures A.1, A.2 and A.3 were fitted through Gaussian kernel densities to determine the expected number of workers who will leave for work within a specific time window.

A travel impedance function for every TAZ for every time period was derived through fitting Gaussian kernel densities to the travel times, the difference between the departure and arrival times. By using the fitted TLD for each TAZ as the impedance of travel function, for inter- and intra-TAZ travel, estimates individual TAZ behaviour, rather than finding a single function that, when distributed with a gravity model, fits the aggregated travel behaviour over all TAZs. A potential pitfall of using individual TLDs is that the iterative process may not find a stable or equilibrium distribution.

4.1.1 Gravity model

A gravity model that calibrates a single travel impedance function to distribute trips between multiple zones may, in principal, not produce accurate results, given that the travel impedance function could have a significant influence in the distribution. A gravity model with a single travel impedance function, calibrated over the aggregated time length distribution, is equivalent to assuming that the travel patterns of individuals in each zone are similar. The calibration of a single impedance function to model the behaviour of a large area is biased towards zones with more trips. If there are a higher relative number of trips originating from a zone it skews the aggregate trip length distribution towards such a zone. The same skewing effect happens when such a model is calibrated on the RMSE of trip distributions. A larger zone will have a more significant contribution to the RMSE.

Figure 4.1 shows the differences in travel patterns for the mode *drive* between TAZs 9023 and 9012, a single travel impedance function calibrated on the average time length distribution and RMSE would be more skewed in favour of zone 9023. The proposed gravity model is introduced to address this shortcoming of the traditionally used gravity model to compensate for modelling a larger area spanning multiple TAZs.

A negative correlation was found between departure times and trip lengths across all modes (driving, bus and taxi), each with a respective R-squared value of 0.86, 0.88 and 0.79. To model

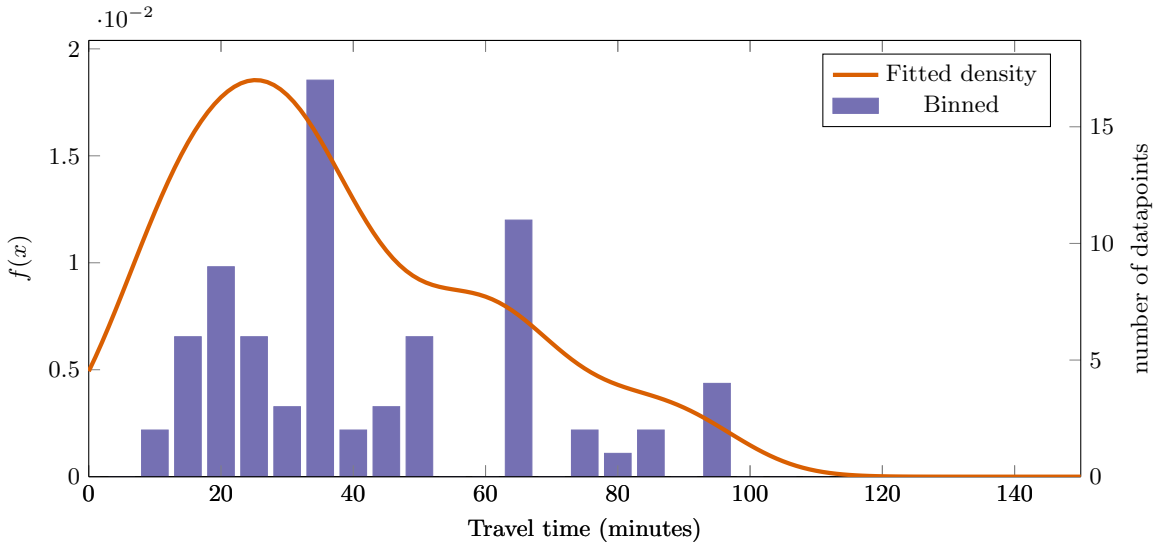

(a) *TAZ 9023*

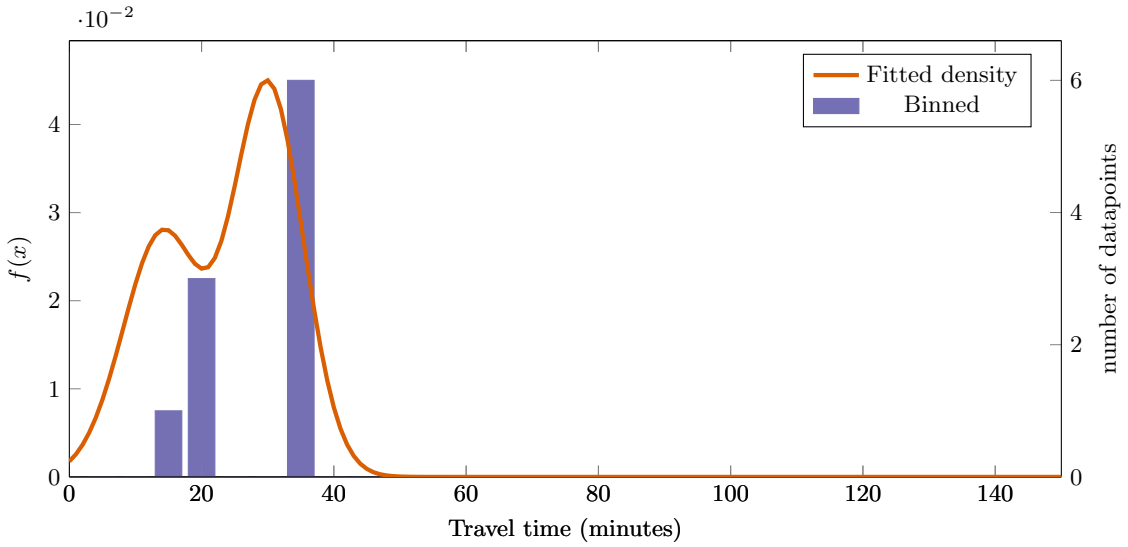

(b) *TAZ 9012*

FIGURE 4.1: *Fitted kernel density functions with binned data histograms for mode* drive.

the behaviour, that commuters who leave for work earlier have on average longer trips, the kernel density function values where further adjusted. Krygsman et al. [35] found that the 2003 NHTS severely underestimated the number of intra-zonal trips. Intra-zonal trips start and end in the same TAZ. This shortcoming is addressed by adding the intra-zonal and temporal calibration parameters α_{m} and τ_{m}.

The temporal parameter τ_{m} adds additional relative weight depending on when the trip started. If the estimated trip length falls within one standard deviation of the average trip length for the period that is currently being evaluated by the kernel density function, the function value $f(C_{ij})$ is adjusted to a higher value. Trips with estimated trip lengths falling outside this band's function value, returns a lower value. Given that O_i is the total number of trips originating at TAZ i, D_j is the total number of jobs in TAZ j, $C_{ijt\mathrm{m}}$ is the cost of travelling from TAZ i to j

during the time t for mode m. The number of trips T_{ijtm} can be expressed as

$$T_{ijtm} = K_{itm}K_{jtm}O_{itm}D_{jtm}G_{ijtm}, \tag{4.1}$$
$$\tag{4.2}$$

with

$$K_{itm} = \frac{1}{\sum_j K_{jtm}D_{jtm}G_{ijtm}}, \tag{4.3}$$
$$K_{jtm} = \frac{1}{\sum_i K_{itm}O_{itm}G_{ijtm}}, \tag{4.4}$$
$$O_{itm} = p_{im}O_i \int_t^{t+1} S_m(x)dx, \tag{4.5}$$
$$D_{jtm} = p_{im}D_j \frac{\sum_i O_{itm}}{\sum_j D_j} \text{ and} \tag{4.6}$$
$$G_{ijtm} = f_{im}(C_{ijtm})\alpha_m\tau_m, \tag{4.7}$$

where

$$\alpha_m = \begin{cases} \alpha_m \text{ for } i = j \\ \alpha_m^{-1} \text{ for } i \neq j \end{cases}, \tag{4.8}$$
$$\tau_m = \begin{cases} \tau_m \text{ for } C_{ijtm} \in [\mu_{tm} - \sigma_{tm}, \mu_{tm} + \sigma_{tm}] \\ \tau_m^{-1} \text{ for } C_{ijtm} \notin [\mu_{tm} - \sigma_{tm}, \mu_{tm} + \sigma_{tm}] \end{cases} \tag{4.9}$$

and f_{im} is a time length distribution function of zone i for mode m with C_{ijtm} the cost of travelling from zone i to j for period t using mode m. S_m is the distribution fitted from the departure times in Figures A.1, A.2 and A.3 and p_{im} is the proportion of workers from TAZ i who indicated they used mode m to travel to work. B_{tm} is a band of one standard deviation σ_{tm} around the average travel time μ_{tm} for period t, illustrated in Figures 4.2, 4.3 and 4.4.

4.1.2 Gravity model parameter calibration

The gravity model parameters are calibrated through a line search method similar to Celik's [9] implementation. A gravity model is iteratively solved for each combination of the calibration parameters during the line search procedure which enumerates the parameter space. The final parameters α_m and τ_m are selected by: Firstly, selecting the parameters that produced the lowest average difference between the OTLD and modelled TLD for each mode m. Secondly, by selecting the parameters that produced the lowest RMSE between the observed and modelled trip distributions for each mode m from the first selection. The RMSE used for calibrating the gravity model parameters is defined as,

$$\text{RMSE}_m = \sqrt{\frac{1}{|T||O||D|} \sum_{t\in T} \sum_{i\in O} \sum_{j\in D} (o_{ijtm} - T_{ijtm})^2} \tag{4.10}$$

where o_{ijtm} being the number of observed workers and T_{ijtm} the modelled number of workers travelling from TAZ i to TAZ j during time period t for mode m.

A traditional gravity model,

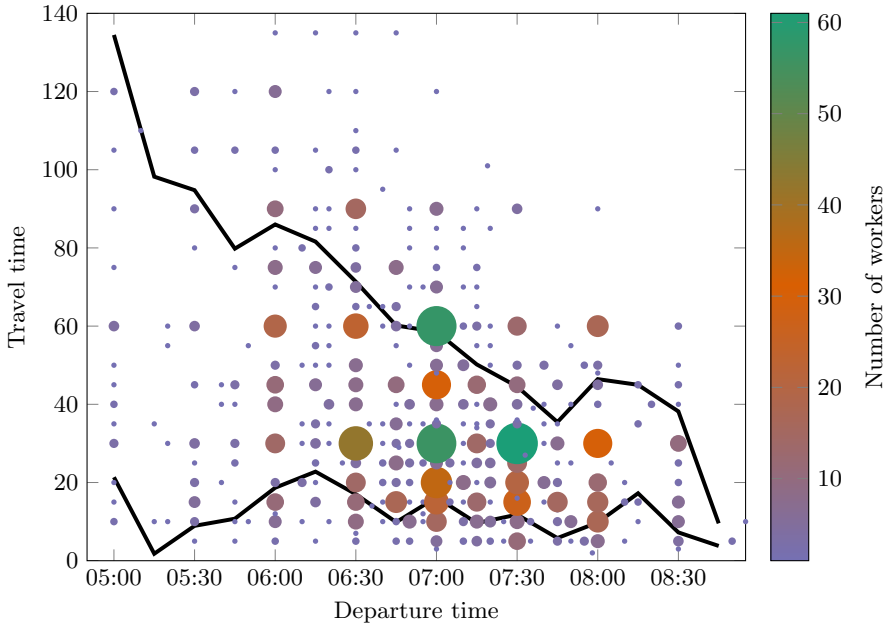

FIGURE 4.2: *The standard deviation band around the mean travel time for workers who drove all the way to work, combined with a scatter plot of the underlying travel times plotted against departure times.*

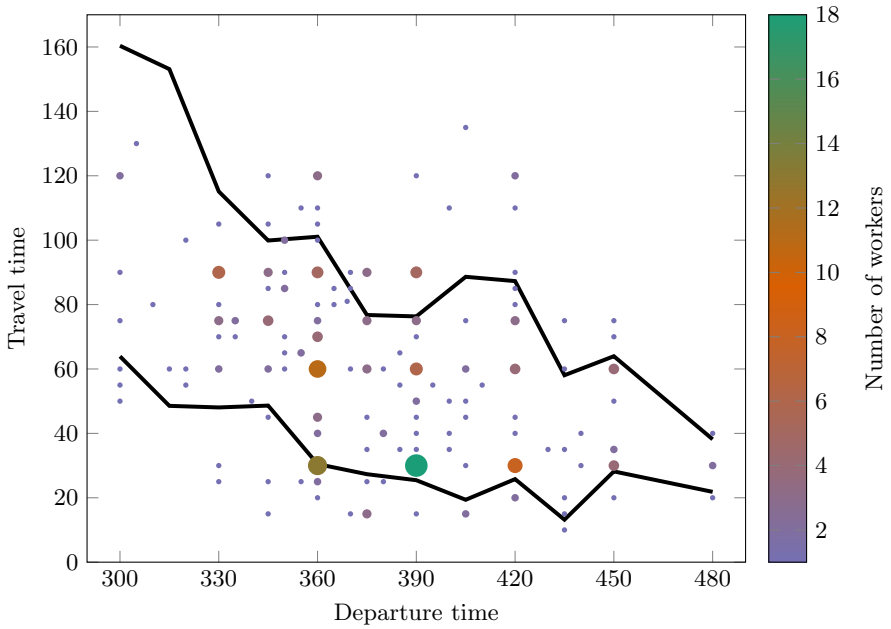

FIGURE 4.3: *The standard deviation band around the mean travel time for workers who took a bus to work, combined with a scatter plot of the underlying travel times plotted against departure times*

$$T_{ijm} = K_{im}K_{jm}O_{im}D_{jm}f_m(C_{ijm}), \tag{4.11}$$

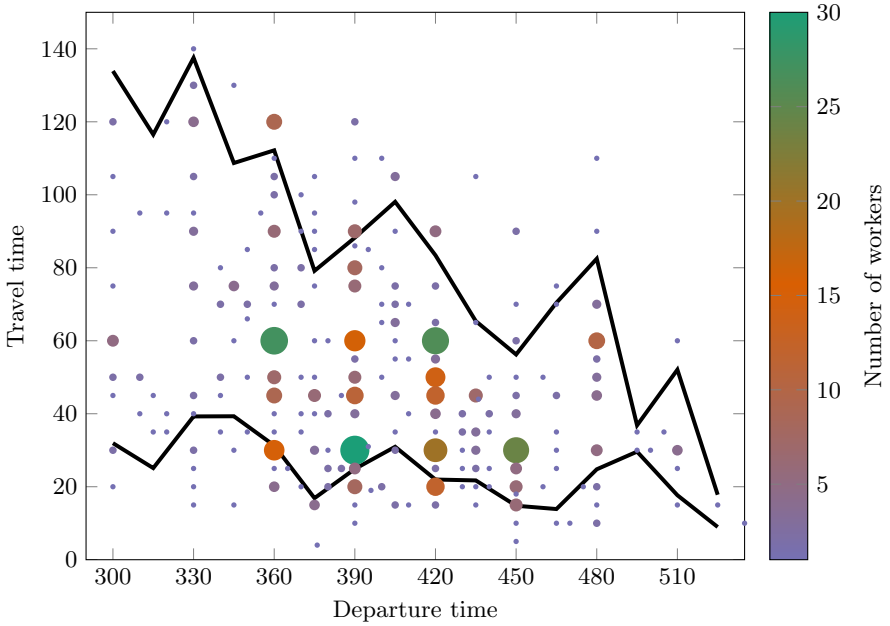

FIGURE 4.4: *The standard deviation band around the mean travel time for workers who took a taxi to work, combined with a scatter plot of the underlying travel times plotted against departure times*

with

$$K_{i\mathrm{m}} = \frac{1}{\sum_j K_{j\mathrm{m}} D_{j\mathrm{m}} f_{\mathrm{m}}(C_{ij\mathrm{m}})} \text{ and} \tag{4.12}$$

$$K_{j\mathrm{m}} = \frac{1}{\sum_i K_{i\mathrm{m}} O_{i\mathrm{m}} f_{\mathrm{m}}(C_{ij\mathrm{m}})}, \tag{4.13}$$

with a tanner function ($f_{\mathrm{m}} = C_{ij\mathrm{m}}^{-\eta_{\mathrm{m}}} e^{-\zeta_{\mathrm{m}} C_{ij\mathrm{m}}}$) is used for comparison.

The tanner function parameters are calibrated on the intervals $0 \leq a \leq 1$ and $0 \leq b \leq 4$ with a step-size of 0.01. The proposed model was calibrated on the intervals $0.25 \leq \tau_{\mathrm{m}}, \alpha_{\mathrm{m}} \leq 10$ for all m with a step-size of 0.25. The parameters with the lowest RMSE were selected from the top five percent of parameter combinations which had the lowest differences between the observed and modelled average trip lengths. This selection protocol favours parameterisations that produce trip length distributions that match observed trip distributions.

4.2 Dynamic traffic assignment

Gravity models require a measure of impedance between TAZs to produce a trip distribution. In the proposed gravity model, average travel times between TAZs are used to measure this impedance. The travel times are in reality dependent on the transportation network and the interaction of all the individuals (traffic) using the network. DTA provides a solution to obtaining average travel times through modelling time-varying networks.

The travel times of individuals in a DTA model can only be determined after arriving at their destination. It is therefore necessary to iteratively load the transportation network. The gravity model is therefore given free flow travel times as an initial input in order to produce the first trip distribution. This distribution of trips is then simulated and produces new average travel

times between TAZs. These travel times are then used as input for the second iteration of trip distribution.

The initial distribution will route all the trips as if there were no congestion present and in doing so, create artificially high congestion in some parts of the network. The next iteration of trips distribution, produced by the gravity model using the first iterations simulation output will then be different than the preceding one due to the high congestion on some roads which affected the travel time between certain TAZs. This process is repeated until the changes between trip distributions become stable. When such a state is achieved, the gravity model parameters are recalibrated and the process is repeated using the most recent travel times produced by the last traffic simulation, before parameter recalibration.

The iterative process can be terminated when subsequent trip tables are sufficiently similar. It is then assumed that the final trip distribution has reached a state that is close enough to that of Wardrop's equilibrium. This is a DTA approach wherein each individual effectively has perfect information on the network he is entering and chooses the path with the lowest time through the network. For this thesis a predefined number of iterations are executed in order to evaluate the effectiveness of the proposed gravity model compared to that of the traditional gravity model.

4.2.1 Assumptions

The DTA framework, implemented in this thesis, is built on the assumption that all individuals who drive to work drive alone. Buses and taxis are always full, given that there are enough individual trips to fill them.

All network facilities are considered uninterrupted traffic facilities. Due to a lack of road network data, capacity splits at signalised intersections and stop streets could not be calculated. The physical constraints of all intersections were therefore relaxed to allow crossing roads to operate at their respective, maximum theoretical capacities.

Consider two one-way roads, both with a theoretical capacity of 1600 vehicles per hour (veh/h). If these two roads were to intersect, and vehicles could pass through other vehicles without colliding. Figure 4.5(a) shows the maximum combined theoretical capacity of the intersection would be 3200 veh/h. Vehicles are required to yield or stop at an intersection to prevent collisions, therefore the maximum theoretical capacity of an intersection is the maximum capacity of both roads and will happen when no traffic is present on the road with capacity.

The capacities of roads that intersect are proportional to the time vehicles are allowed to flow through them, over the intersection. Figure 4.5(b) is a simplified example of the capacity assuming a green light uptime of 75% for one direction. Due to the lack of data for the location and directional uptime of signalised intersections, stop streets and yields it is assumed that all network facilities supply the maximum theoretical capacity in terms of veh/h at all times.

This assumption minimizes the maximum error of the maximum flow through an intersection. If for example the real directional uptime was 10/90, and the assumption was made that all intersections have a 50/50 directional uptime, the road that had 90% uptime would appear more congested than it should. As a consequence routes can be chosen through a path that now has 40% more directional uptime than it should have. This is predominantly a cause for concern in urban residential areas and on- and off-ramps to and from large roads.

It is further assumed that

- each vehicle for mode *drive* takes up 1 passenger car equivalent (PCE)
- each vehicle for mode *bus* takes up 3 PCE

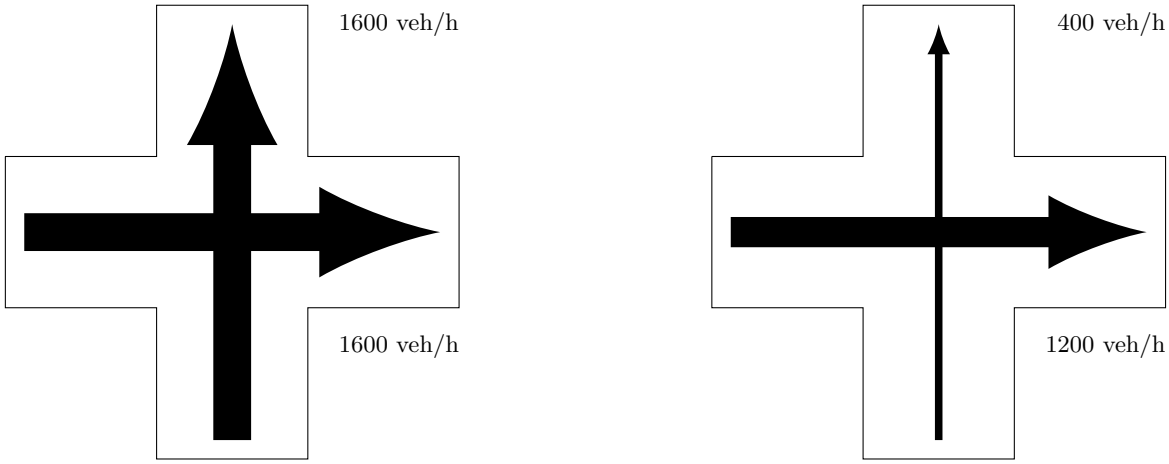

(a) *Unhindered flow* (b) *75/25 signalised intersection*

FIGURE 4.5: *Schematic representation of the effect of signalised intersections on road facilities.*

- each vehicle for mode *taxi* takes up 1.5 PCE

The framework consists of two phases. The first phase (trip distribution) is a gravity model that creates a trip matrix which serves as input for the second phase, route selection (DTA). Modal split is incorporated through using a gravity model for each of the modes.

4.2.2 Traffic simulator

A traffic simulation was coded in Python [21] to model the effect of congestion on the road network and to serve as a method for root selection. Each fleet is flowed through the network at discrete time intervals, updating the data fields for the road segments as they utilise them. The interval, represented by T_f, used was 15 minutes, the same time frame that is used by the Highway capacity manual to calculate level of service on road network facilities. If the flow limit (veh/h) is reached on a road segment within a time period, all vehicles arriving at the segment will be placed into a vertical queue. This process is repeated until all the trips are flown. Figures 4.6 and 4.7 contain flow diagrams of the simulation logic.

The modelled trips are then assigned to routes on a road network. The total trips from TAZ i to TAZ j are gradually depleted through assigning small fleets to random combinations of origin TAZ connectors and destination TAZ connectors. The network capacity is updated to reflect the marginal contribution of the assigned fleets.

4.2.3 TAZ connector selection

A pair of origin and destination TAZ connectors are selected randomly with replacement from a pool of origin and destination nodes. The nodes are grouped together per census ward within a TAZ. The probability of selecting a specific ward from a TAZ is based on the mode currently being flowed, the vehicle ownership percentage of the underlying ward and the proportion of urban residents and jobs. The likelihood that a specific ward is selected for a mode is proportional to the percentage vehicle ownership and the number of workers in the ward.

Given that p^v_{iw} is the percentage of vehicle ownership and p^e_{iw} is the proportion of workers in ward w, both within TAZ i, the probability that ward w will be selected to choose an origin

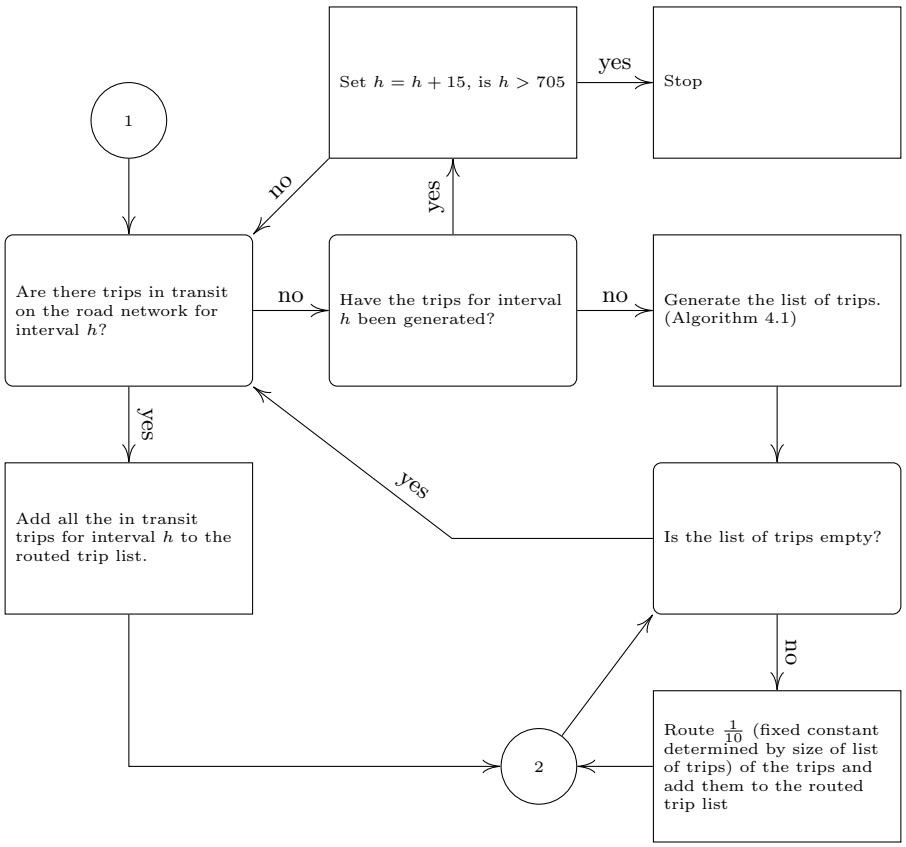

FIGURE 4.6: *A flowchart representing the discrete temporal progression of the mesoscopic simulator.*

TAZ connector is

$$p_w^O = p_{iw}^e \frac{p_{iw}^v}{\sum_{k \in W} p_{ik}^v} \tag{4.14}$$

for the mode *drive* and $1 - p_w^O$ for *taxi* and *bus*. Wards for destination connectors are selected based on the percentage of jobs, present in the ward relative to the number of jobs present in the TAZ. Given j_w is the number of jobs located in ward w, within TAZ i, the probability that ward w will be selected to choose a destination TAZ connector is,

$$p_w^D = \frac{j_w}{\sum_{k \in W} j_k}. \tag{4.15}$$

Once a ward is selected the probability to choose a vertex from the pool of urban vertices as the TAZ connector is the percentage of workers living (origin) and working (destination) in an urban enumeration area within the ward.

4.2.4 Route selection

A set number of trips for each mode m is subtracted from the total number of trips from TAZ i to j and assigned to the random origin-destination pairing. This is repeated until all the trips from every TAZ i to j for the time period has been assigned. At every assignment a random departure

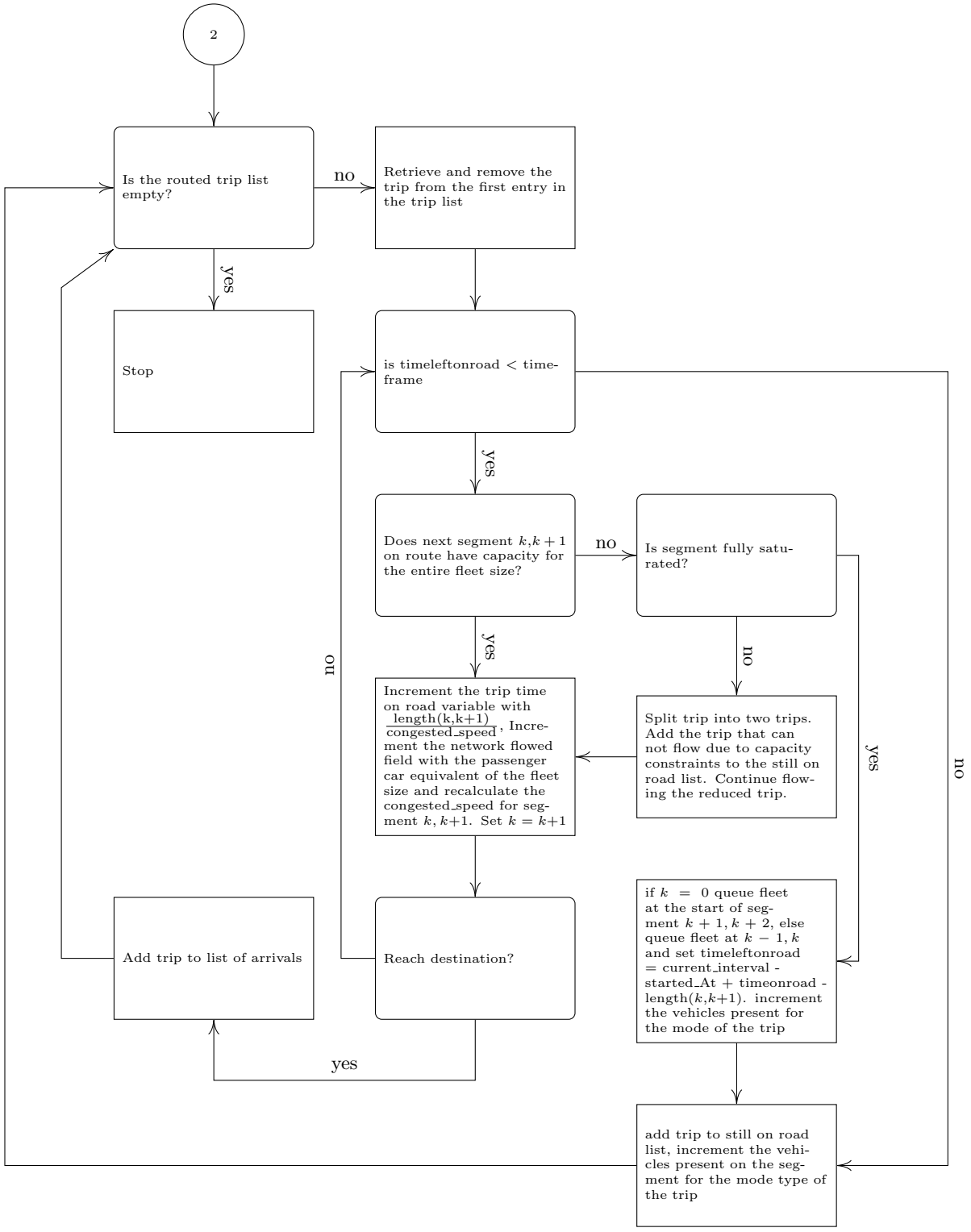

FIGURE 4.7: *A flowchart representing the logic for the mesoscopic traffic simulator.*

time is generated based on the kernel density of the departure times. Every assignment is added to a list of trips. Algorithm 4.1 contains the pseudo-code for this process.

Trips can now be processed into a fleet size that has to travel between two vertices on the network. Trips are selected in chronological departure order from the list, and assigned to a

Algorithm 4.1: Trip list generation at the start of each time interval

Input : OD Matrix T for time t with trips from every TAZ i to every TAZ j
Output: List of fleets that are to be flown from TAZ i to TAZ j with the accompanying TAZ connectors

```
1  Initialize empty list of trips List;
2  foreach i in list of TAZs do
3      foreach j in list of TAZs do
4          foreach m in list of modes do
5              Fleet ← Select_Fleet_Size(m,T(i,j));
6              Start_Time ← Generate_Start_Time(m);
7              Start ← Select_Origin_TAZ_connecter(i);
8              End ← Select_Destination_TAZ_connecter(j);
9              Add_To_List_Of_Trips(Fleet,Start_Time,Start,End,Mode);
10         end
11     end
12 end
13 Sort_List_Of_Trips(List);
```

route.

Route selection criteria is randomly selected to choose either the shortest path in terms of travel time or distance travelled with the probability c and $1 - c$, respectively. After the travel criteria is selected the shortest path through the network is determined with a bi-directional implementation of Dijkstra's shortest path algorithm [13].

The average flow speed on each segment is determined with equation (A.1) discussed in Akcelik's paper [2]. The average flow speed for a time period is a function of the hourly passenger car equivalent flow rate through a segment and the queued demand at the start of each time period.

The distance matrix containing the cost from TAZ i to TAZ j that departed in time period t is updated with the average travel times produced by the commuter flow model. This initializes the gravity model with the updated distance matrices and begins the iterative process with the output feeding back into the gravity model.

The calibrated gravity model trip distribution is then used for three more iterations before the gravity model parameters are recalibrated. This process is illustrated in Figure 4.8.

4.3 Chapter conclusion

The framework discussed in this chapter is shaped by the available data for the South Africa context. Due to the disaggregate nature of the available data, a FSM-like framework is conceptualised. Trip distribution is performed through the implementation of a traditional and proposed doubly constrained gravity model. The proposed gravity model is an extension on the traditional model and uses the data from the NHTS to temporally adjust the trip distributions. Because of a lack of data to derive accurate capacity for the road network, each road segment is assumed to have unconstrained capacity based on an estimated number of lanes and its speed limit in an effort to minimize the maximum error.

The gravity model parameters are calibrated based on a the RMSE and TLD selection criteria. These gravity models are then used for four iterative simulation runs before the parameters are recalibrated. The Modelling framework combines the trip distribution, modal choice and route assignment into an iterative process to find a trip distribution that is nearing equilibrium.

Route assignment is performed through a DTA approach, which is implemented with a traffic

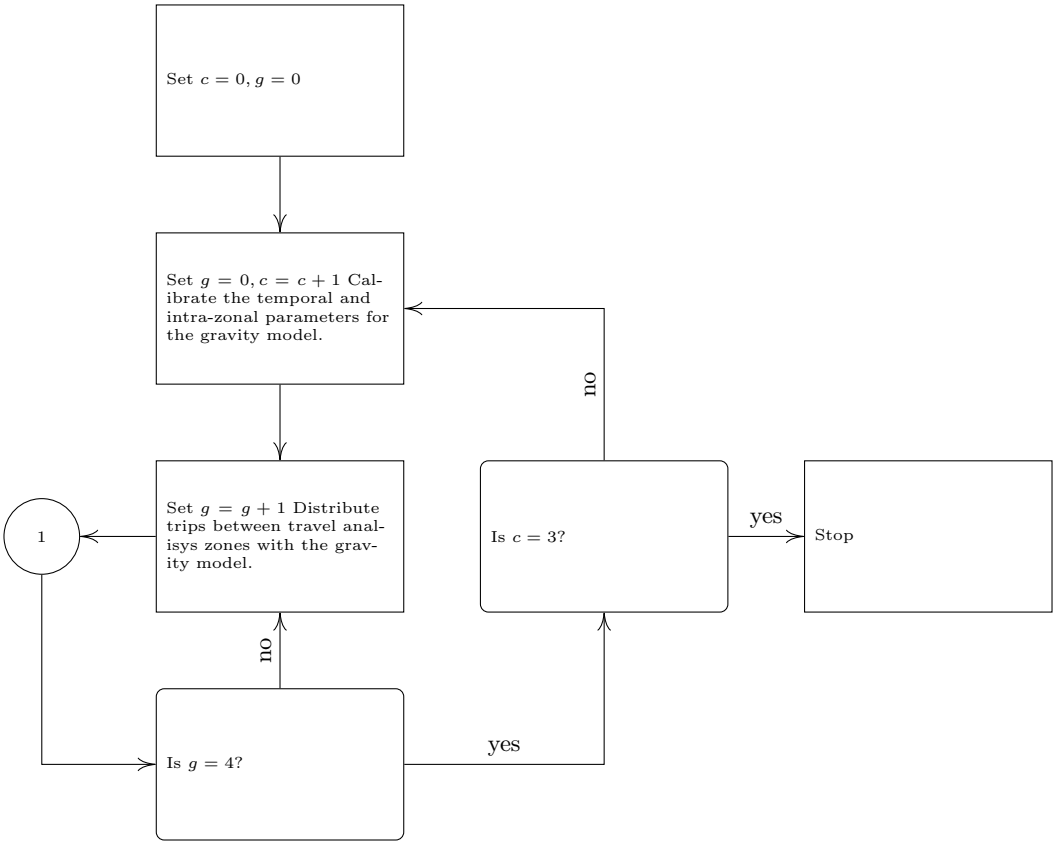

FIGURE 4.8: *Flowchart of the iterative gravity model calibration.*

simulator, coded with Python. The traffic simulation is used through iterative interaction with the gravity model. The output of the gravity model is used as the input for the simulation. Once all trips have been reached their destination and the simulation has terminated, its output is parsed into trip length tables. These trip length tables are then used in turn as the input for the gravity model within the iterative framework. The framework is an iterative feedback loop which combines the trip distribution, modal split and route assignment through the use of a dynamic time varying network.

This chapter discussed the models and techniques used in constructing the traffic modelling framework, which is shaped by the data discussed in Chapter 3. The next chapter compares the proposed and traditional gravity models' effectiveness within the framework.

CHAPTER 5

Gravity model comparison

Contents

The previous chapter described a proposed gravity model and the accompanying mesoscopic traffic simulator. This chapter compares the outputs produced by the proposed model and the traditional gravity model, as described in Chapter 4 which is calibrated for each mode. The models are compared through:

- their respective calibration criteria during each parameter recalibration and the final gravity model iteration,
- trip length distribution (TLD) convergence,
- inter-iteration differences between trip distributions and distance matrices,
- differences in the routes, trips used between iterations,
- differences between the observed and simulated departure and arrival times and
- vehicle counts.

An integral part of the gravity modelling is the parameter calibration. After each iteration the trip distribution will change given that equilibrium has not been reached yet. If the gravity model is not recalibrated to the latest average trip length table, the gravity model would be distributing the trips according to a network under free flow conditions.

5.1 Parameter calibration

The calibration procedure, as described in Chapter 4.1.2, is used to determine the gravity model parameters. The first gravity model parameter calibration is performed with the shortest distance under free flow conditions in the network. The first set of iterations, before the second parameter calibration, is essentially an attempt to distribute trips between TAZs, testing that a

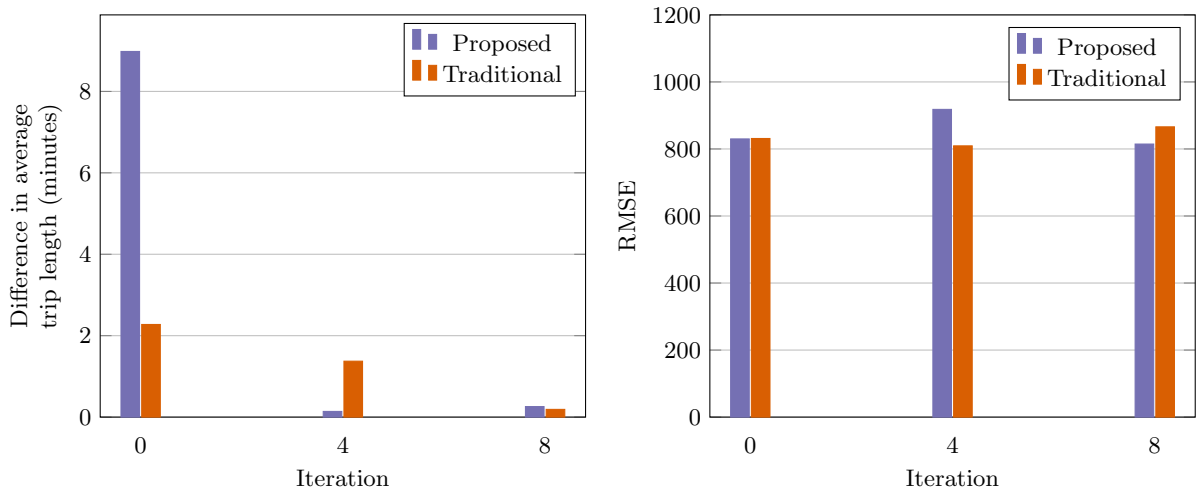

(a) *TLD* (b) *RMSE*

FIGURE 5.1: *Recalibration of gravity model parameters for mode drive.*

trip distribution that avoids congestion could exist. Subsequent calibrations are performed after a predetermined number of iterations, using the distance table from the preceding iteration.

The calibration selects the parameters based on the modelled time length distribution and the RMSE of the trip distribution assignments. Figures 5.1(a) and 5.1(b) show an improvement in the difference between average trip lengths and an increase in the RMSE for mode *drive* from the first to second parameter calibration. This is consistent with expectations. The distance table that is used for the first parameter calibration was determined under free flow conditions. The first gravity model parameters therefore distributed the trips with a gravity model that is calibrated for a network under free flow conditions. More vehicles are therefore assigned to places that are usually further away in terms of travel time, given sufficient levels of congestion on the road.

In each following iteration the distance table produced from parsing the arrivals of the previous iteration is used to perform the trip distribution for the current iteration. With each iteration the gravity model distribution changes as the distances between trips vary. After the second parameter calibration the difference between average trip travel time for the proposed model is reduced to 8 seconds, yet the RMSE increased to 918. This occurs because now the gravity model could find parameters that produces a similar average trip length in the network with the distance table obtained from a congested network. This came at the price of an increase in the RMSE which means that although the trip lengths are now on average following a similar TLD, they are distributed to places different from what is observed in the NHTS.

The drop in RMSE from 918 to 814 between the second and to third parameter calibration is offset by an increase of 0.119 minutes or 7.15 seconds. The trip distribution and distance tables are fairly consistent with distributing trips in regard to average trip length. It is assumed that congestion has stabilised at this stage and trip distribution is approaching equilibrium at a slower rate of change. The gravity model parameter calibration selected parameter values that had the smallest RMSE from the 10% of parameters that had the lowest difference in average times. A parametrisation with a lower RMSE can therefore be selected during calibration, due to the rate of change in the distance table, which decreased.

The first parameter calibration for the traditional gravity model has a lower difference in average

travel time, 2 minutes 17 seconds, than for the proposed gravity model 8 minutes 59 seconds, for the mode *drive*. This is because the impedance of travel function that was produced by the line search procedure was calibrated to estimate the aggregate travel distribution of all the TAZs. At the second and third parameter calibration the difference in average trip length decreased with 54 and 71 seconds, respectively. Both models found parameters that were within 15 seconds of the average trip length of the observed data by the third iteration. All the trips are distributed with the same impedance of travel function with the traditional gravity model. This produces trip distributions that are on average similar to the observed average trip length. As the trip distribution stabilizes during each iteration the modelled TLD approaches the observed TLD resulting in a smaller difference between the average trip lengths. The RMSE of the traditional gravity model increased from 809 to 866 from the second to third parameter calibration. This is explained by the deviations of the observed TAZ TLD from the aggregated TLD. The trips originating from a TAZ with a significantly different TLD will be distributed to TAZs different to that of the observed data because its trips are distributed partially according to the aggregate TLD.

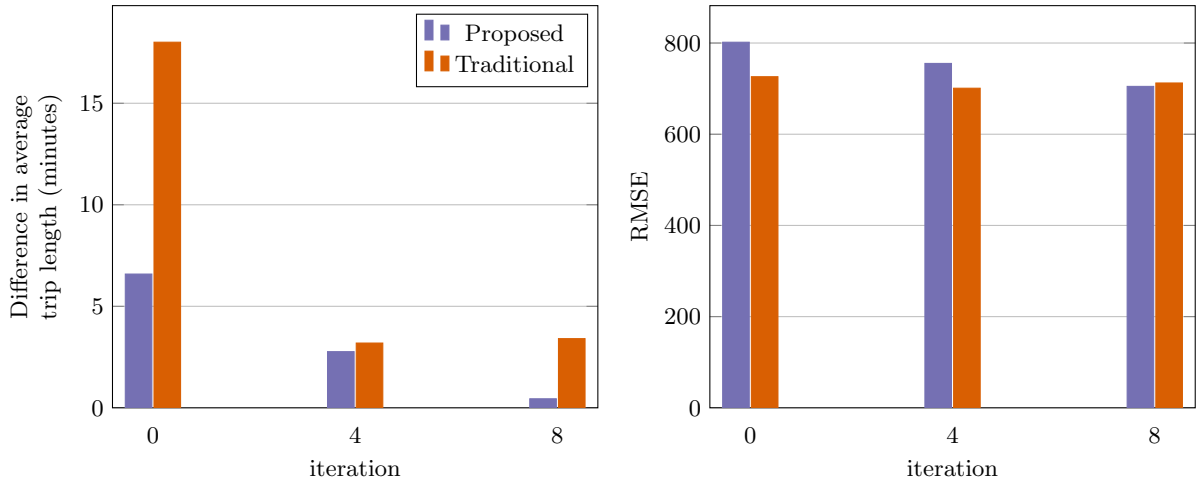

(a) *TLD* (b) *RMSE*

FIGURE 5.2: *Recalibration of gravity model parameters for mode bus.*

Figure 5.2 shows that the trip distribution for the proposed gravity model has a smaller difference in average trip lengths than the traditional gravity model for the mode *bus* for each parameter calibration. The parameter calibration procedure could not find a traditional gravity model trip distribution such that difference in average trip length is smaller than 3 minutes. The proposed model has a higher RMSE, but lower difference in average trip length than the traditional model for the first and second parameter calibrations. After the third parameter calibration difference in average trip length between the OTLD and the proposed model's TLD is 26 seconds. This is 3 minutes and 2 seconds less than the difference between the average trip length of the OTLD and the TLD of the traditional gravity model. The proposed model's RMSE after the third parameter calibration of 704 is lower than the 712 of the traditional model. This illustrates the capability of the proposed model to produce more accurate trip distributions during parameter calibration than the traditional model for the mode *bus*. Commuters travelling with a bus to their place of work have on average less freedom to travel and are less than the total number of commuters driving to work. This illustrates a shortcoming of the one size fits all approach to distributing trips on a large scale in the traditional model: When travel patterns differ between TAZs a trade off has to be made between RMSE and difference between average trip length.

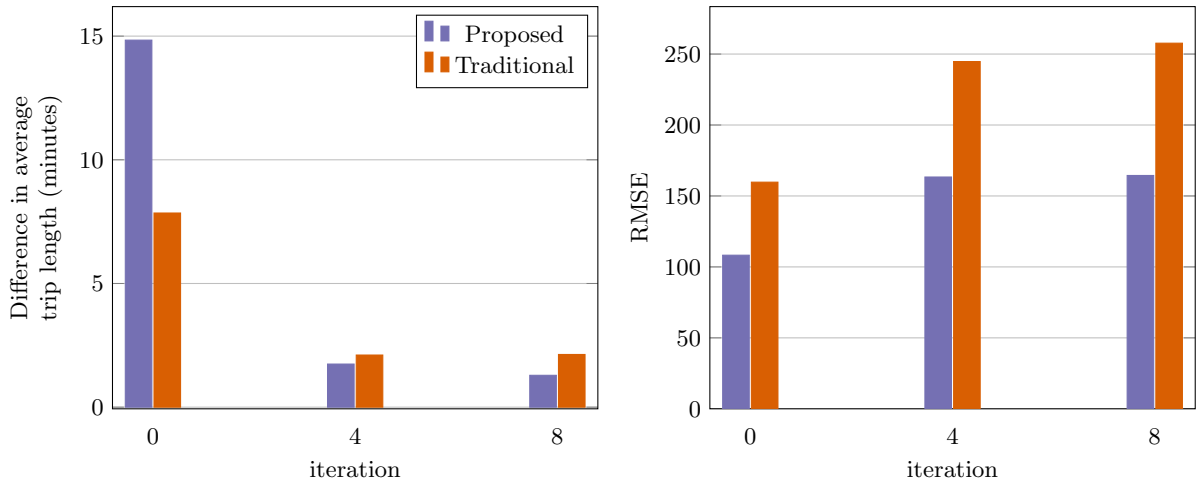

(a) *TLD* (b) *RMSE*

FIGURE 5.3: *Recalibration of gravity model parameters for mode taxi.*

Mode	Traditional	Proposed
drive	11 (0.5%)	16 (0.7%)
bus	204 (5.8%)	27 (0.8%)
taxi	128 (4.2%)	77 (2.6%)

TABLE 5.1: *Deviation of gravity model distribution from observed travel times (seconds).*

The proposed gravity model trip distribution for mode *taxi*, in Figure 5.3, has an average trip length that is 14 minutes 50 seconds longer than the OTLD after the first parameter calibration. The difference in average trip length decreases to 75 and 48 seconds, respectively during parameter calibrations two and three. Compared to the 7 minutes 50 seconds, 2 minutes 6 seconds and 2 minutes 8 seconds of the traditional gravity model.

A trade off between difference in average trip length and RMSE is evident in the traditional and proposed gravity model for the mode *taxi*. The RMSE for the three parameter calibrations are 160, 245, 258 and 108, 164, 163, respectively. This trade off is smaller for the proposed model.

Table 5.1 shows how the traditional and proposed gravity models performed when their respective output is compared to the observed NHTS data, after the second parameter calibration. The proposed model is on an average 5 seconds less accurate than the traditional gravity model for the mode *drive*. This means that the proposed model is on par with the traditional gravity model which is specifically designed to match the aggregate observed TLD through the calibration of the impedance of travel function. This proves the viability of fixing a unique TLD for each TAZ from survey data. This is a powerful result and starts to address the critique that disaggregate methodologies does not represent true underlying behaviour. This result is confirmed by the smaller deviations in the proposed model for the modes *bus* and *taxi*.

The gravity models could find a trip distribution such that the average trip lengths or aggregate TLD match, but still not distribute these trips to the correct places. RMSE analysis, Table 5.2 of both gravity model trip distributions show that the proposed gravity model has an improved accuracy over that of the traditional model, especially for the mode *taxi*.

Figures 5.4 plots the calibration space for the gravity model parameters for the proposed and traditional models for the mode *drive*. The parameter space changes significantly between the

Mode	Traditional	Proposed	Improvement
drive	866	815	6%
bus	712	705	1%
taxi	258	164	36%

TABLE 5.2: *RMSE comparison between gravity models.*

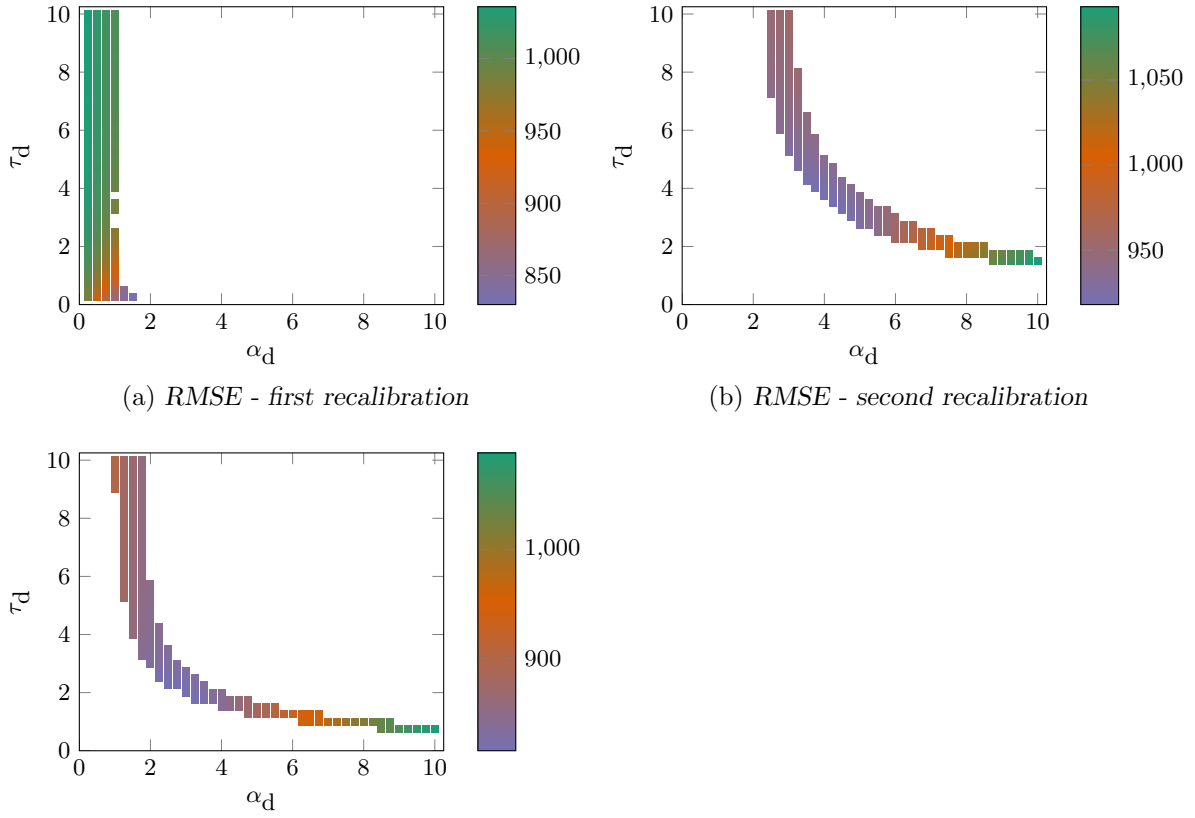

(a) *RMSE - first recalibration*

(b) *RMSE - second recalibration*

(c) *RMSE - third recalibration*

FIGURE 5.4: *Calibration criteria values for the solution space of calibration parameters for the proposed gravity model for mode* drive.

first and second calibration iterations when evaluated in terms of the average trip length distance and RMSE. The changes are more subtle between iterations two and three. Figure 5.4(c) shows how calibration of the proposed gravity model can produce an aggregate trip length distribution that has the same average trip length than the observed data. This can be achieved with a set of parameters that are close to the line

$$\tau = \frac{10.338}{\alpha^{1.208}} \tag{5.1}$$

which illustrates a trade-off between the intra-attraction parameter τ and the temporal adjustment parameter α. The interaction of these two parameters on the average trip length appears to be consistent. Trips can be distributed with a similar average trip length by assigning more vehicles to the TAZ which in general reduces the trip lengths as more trips are limited to a TAZ. The temporal adjustment parameter progressively reduces the gravity of TAZs that are falling outside of one standard deviation of the average trip lengths for the specified time period. Therefore an increase in the intra-attraction parameter can be offset by decreasing the temporal

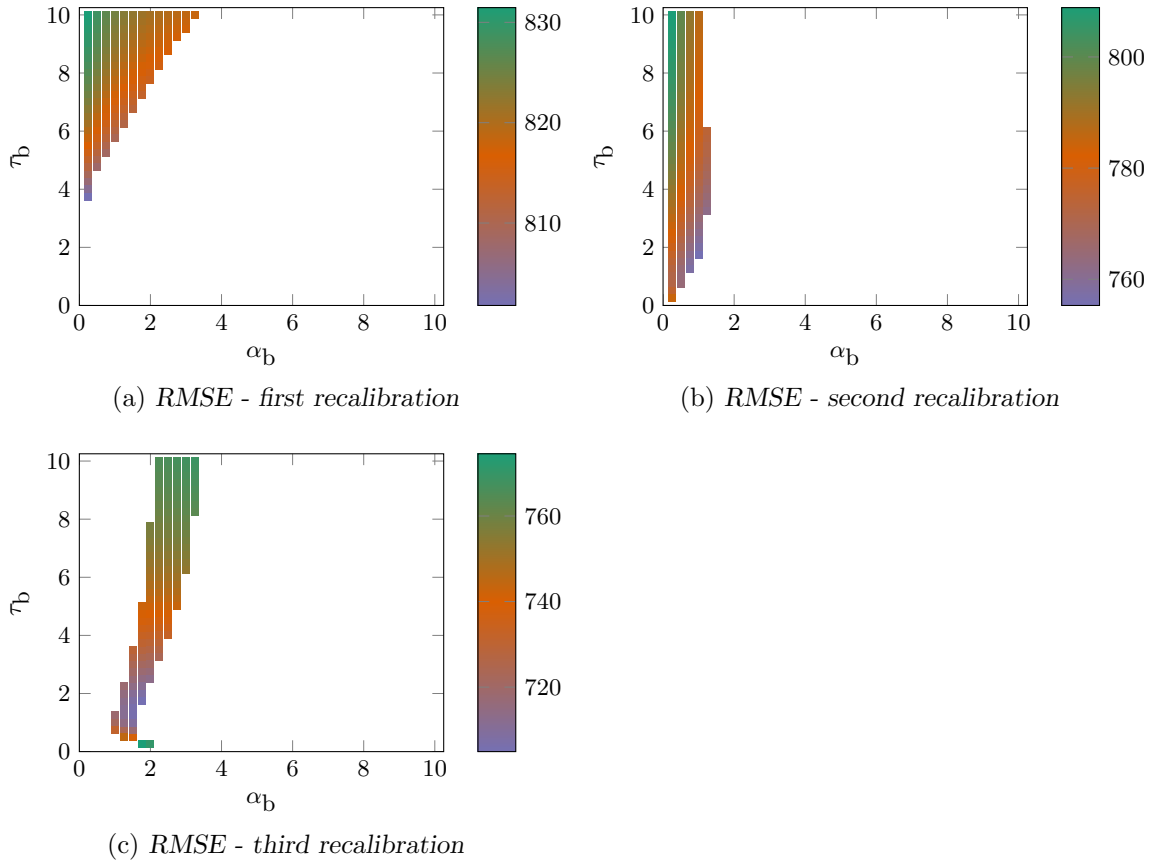

(a) *RMSE - first recalibration*

(b) *RMSE - second recalibration*

(c) *RMSE - third recalibration*

FIGURE 5.5: *Calibration criteria values for the solution space of calibration parameters for the proposed gravity model for mode* bus.

adjustment parameter so that trips that are distributed can continually be attracted distant TAZs. Data suggests that people leaving for work later in the morning tend to not travel as far as those leaving earlier.

Figures 5.5 and 5.6 show the parameter space for the modes *bus* and *taxi*. The first calibration iteration for both modes show that the temporal adjustment parameter has a more significant effect on the difference of average trip length than the intra-attraction parameter. The top parameter space from which the parameters with the lowest RMSE are selected can be approximated by triangles, each with a slope of $\tau_b = \frac{11}{4}\alpha_b$ and $\tau_t = \frac{5}{3}\alpha_t$. The second and third recalibration of the parameters show that both modes are significantly more sensitive to changes in the intra adjustment parameter rather than temporal adjustment parameter.

The RMSE parameter space, is confined to a width of 2.5 and 1.25 for the modes *bus* and *taxi* respectively. Therefore the underlying trip length distributions per TAZ for these modes effectively force the intra adjustment parameter calibration to fall within a small bound. This implies that people who drive can in general travel more freely, the movements of cummuters who take the bus are much more constrained with people using taxis, having the most constraints on where and especially when they are able to travel. Table 5.3 contains the selected parameter values from each calibration iteration.

The NHTS indicates that 49.2%, 34.3% and 55.7% of people who drive, take a bus, or a taxi to work, work in the same TAZ in which they live. These percentages are based on the smaller subset, as discussed in Section 3.3. The upper bound and lower bounds of these percentages,

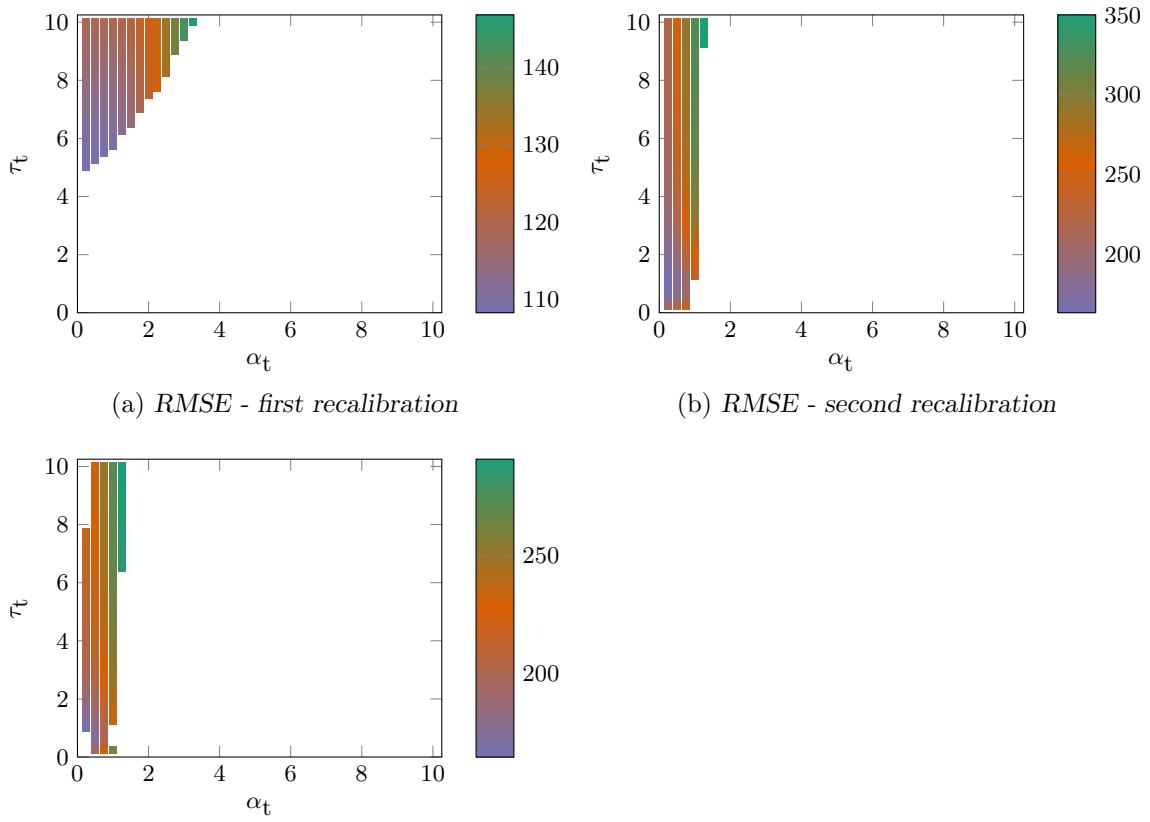

(a) *RMSE - first recalibration*

(b) *RMSE - second recalibration*

(c) *RMSE - third recalibration*

FIGURE 5.6: *Calibration criteria values for the solution space of calibration parameters for the proposed gravity model for mode* taxi.

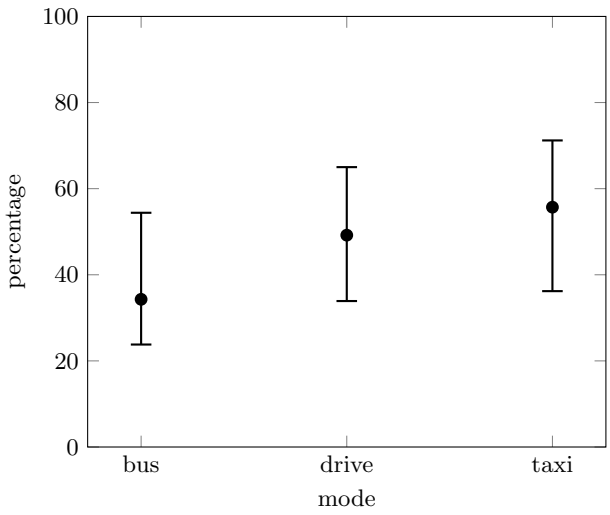

FIGURE 5.7: *The percentange of workers living in the same TAZ in which they work per mode.*

Figure 5.7, are obtained if all the data points that did not indicate the destination TAZ are either within the TAZ or outside it.

Figures 5.5 and 5.6 show that the NHTS dataset that is used to determine the RMSE underestimates and slightly overestimates the number of people who live and work in the same TAZ for

Model	Parameter	Mode	Calibration iteration		
			First	Second	Third
Proposed	α_d	*drive*	1.5	4	3
Proposed	α_b	*bus*	0.25	1	1.75
Proposed	α_t	*taxi*	0.25	0.25	0.25
Proposed	τ_d	*drive*	0.25	3.75	2
Proposed	τ_b	*bus*	3.75	1.75	1.75
Proposed	τ_t	*taxi*	5	1	1
Traditional	η_d	*drive*	1	0.25	0
Traditional	η_b	*bus*	0.65	0	0.05
Traditional	η_t	*taxi*	0	0	0
Traditional	ζ_d	*drive*	0.6	3.95	4
Traditional	ζ_b	*bus*	0.2	1.3	1.2
Traditional	ζ_t	*taxi*	0.5	1.75	1.55

TABLE 5.3: *The calibrated parameters for the traditional and proposed gravity model.*

modes *bus* and *taxi*, respectively, given the observed trip length distributions. Figure 5.4 shows that the subset of data used to determine the NHTS underestimates the number of intra-TAZ trips. However the error might be overstated with this set of data because the model only takes commuter traffic into account. Adding trips with an academic destination, such as a school or university, will increase residential congestion, effectively reducing such an over-estimation.

5.2 Aggregate TLD convergence

Trip length distribution is an effective measure of how well the gravity model distributes trips compared to the observed data. The modelled TLD should converge to the observed TLD. The theoretical TLD is compared to the observed TLD for all iterations.

TLD comparison

Figure 5.8 shows the TLD and cumulative TLD from the traditional gravity model for parameter calibration iterations 1, 2 and 3. During the first iteration the gravity model overestimates the number of trips that are between 10 and 30 minutes in length and underestimates the number trips of 30 to 60 minutes. This is due to the free flow distance table that is used for the first parameter calibration. At iterations 2 and 3 the models are unable to find distributions for the gravity model that have a high frequency of 5 to 10 minute trips. This causes an slight overestimation of the remainder of the trips, when compared to the observed TLD for mode *drive*.

The same behaviour is observed from the proposed gravity model during the parameter calibration iterations. The proposed model overestimates the number of trips between 15 and 55 minutes. This is a result of using the average trip length as calibration criteria. The calibration algorithm selects those parameters that produce on average a similar trip distribution which in this instance resulted in an underestimation of trips that range between 5 and 15 minutes. Another reason for this underestimation is that the distance table only gives a point estimate of the intra-TAZ trip lengths for a TAZ. The trips might be recorded in the arrival data but are then skewed towards the longer 15–35 minute trips that are very common in congested networks within a TAZ.

The traditional gravity model, Figure 5.10, overestimates the number of trips that are less

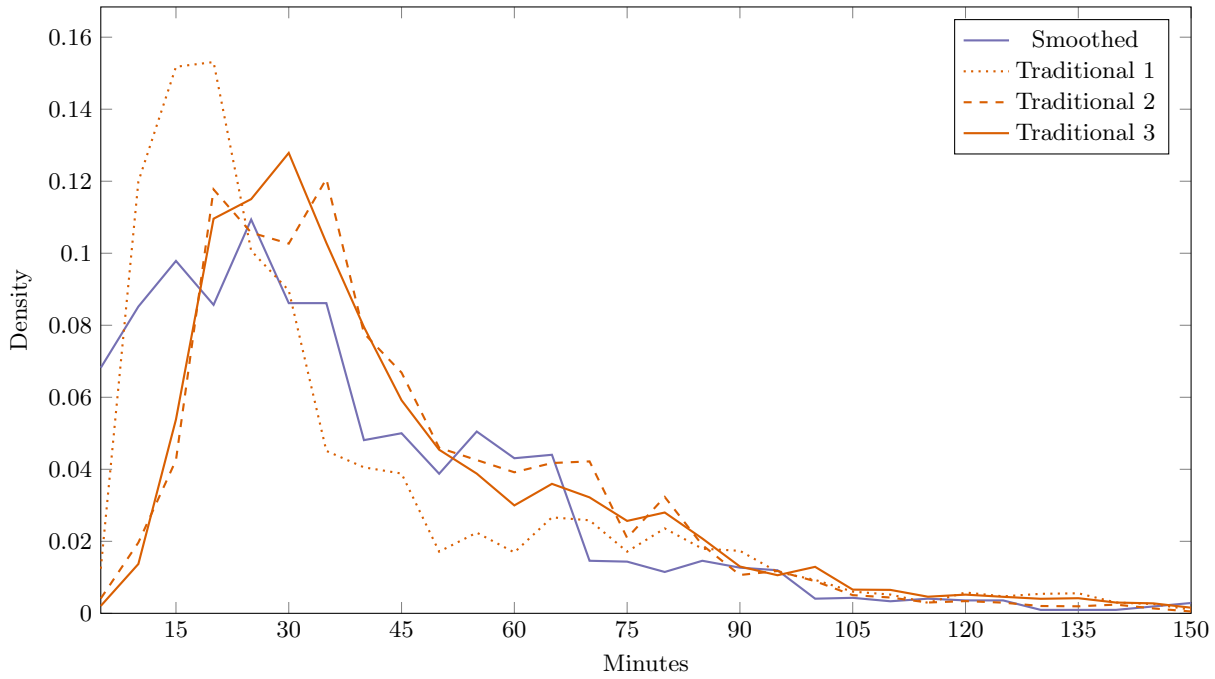

(a) *TLD for the traditional model after parameter calibration iterations 1, 2 and 3*

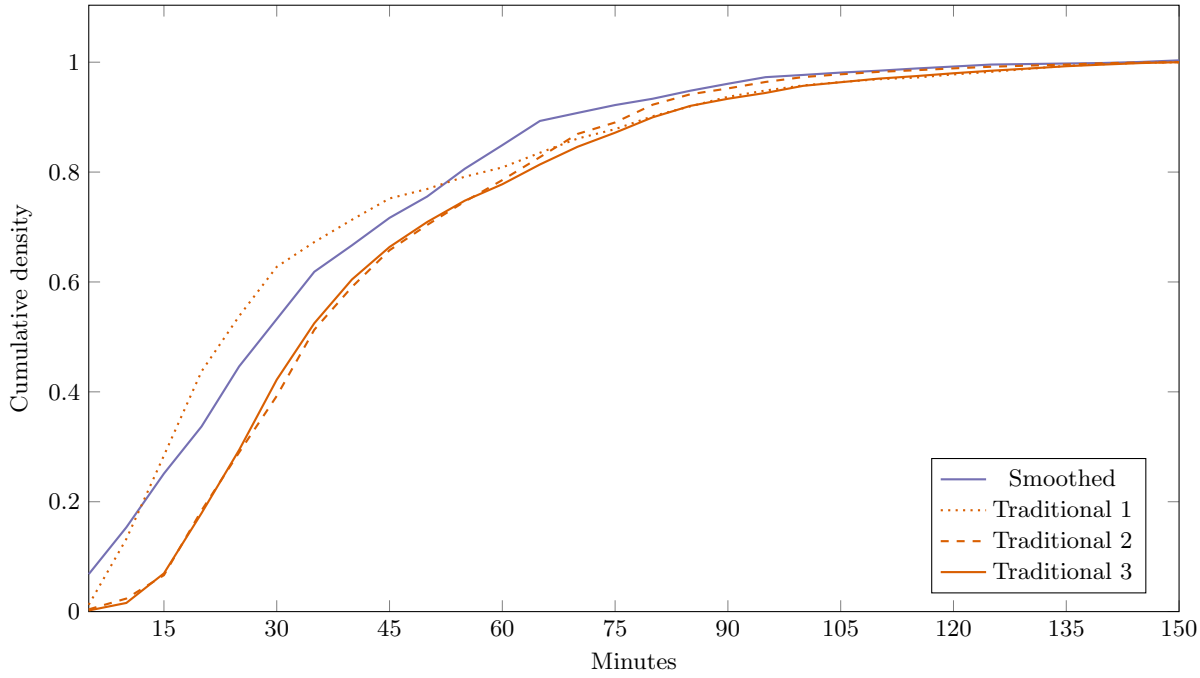

(b) *Cumulative TLD for the traditional model after parameter calibration iterations 1, 2 and 3*

FIGURE 5.8: *Smoothed TLD compared to the traditional gravity model TLD for mode* drive.

than twenty minutes and underestimates the trips that are 40 to 95 minutes for the mode *bus*. The overestimation is compounded during the first calibration iteration that uses the free flow distances between TAZs. This large deviation is reduced with subsequent parameter calibration iterations two and three.

The proposed gravity model overestimates the number of trips that are 70 to 80 minutes for the mode *bus* at the first calibration iteration. The number of trips that fall between 80 to 100

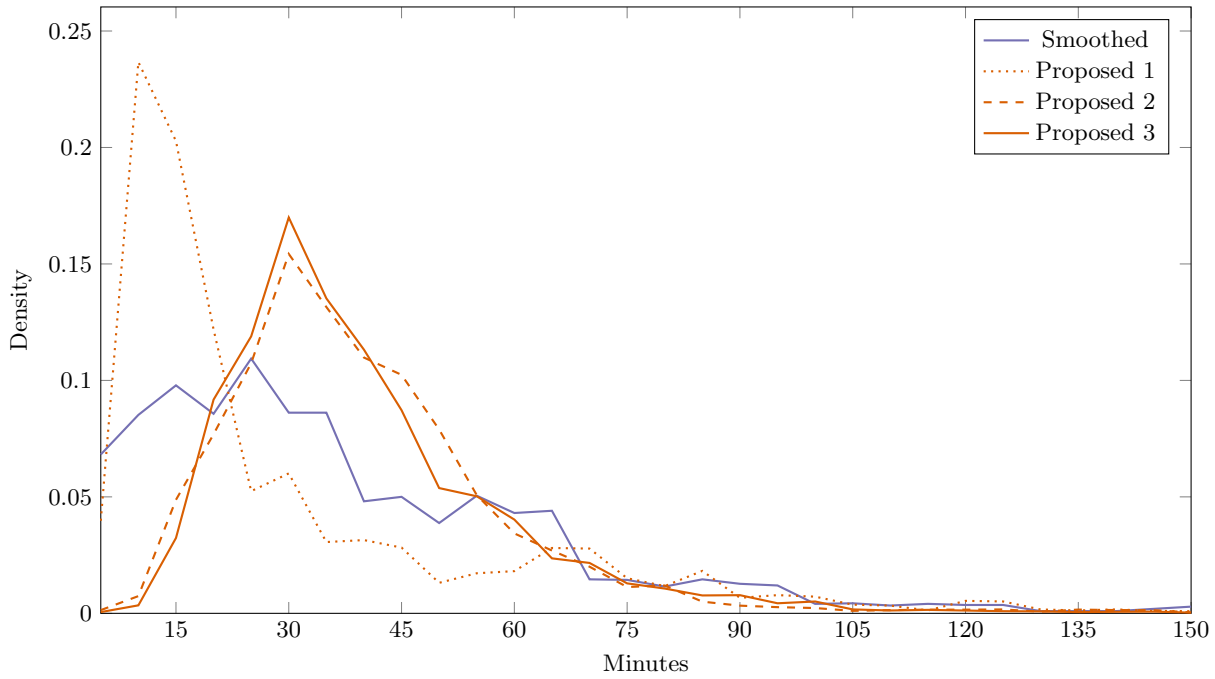

(a) *TLD for the proposed gravity model after parameter calibration iterations 1, 2 and 3*

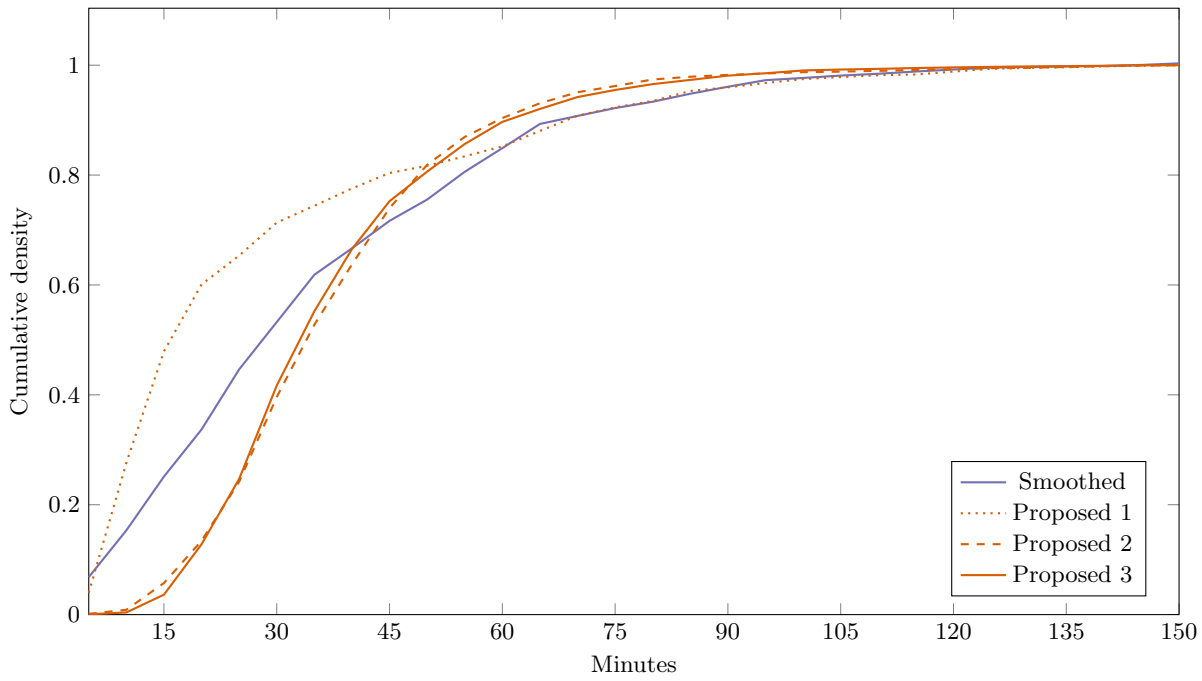

(b) *Cumulative TLD for the proposed gravity model after parameter calibration iterations 1, 2 and 3*

FIGURE 5.9: *Smoothed TLD compared to the proposed gravity model TLD for mode* drive.

minutes are underestimated. This deviation is noticeably smaller at second and third parameter calibration iterations. The more stable modelled trip length distribution coincides with the overlap in the parameter space, in Figure 5.5, for the second and third calibrations for low relative RMSE values.

Figures 5.12 and 5.13 show that both the traditional and proposed gravity models overestimated the number of shorter trips and underestimates the amount of longer trips during the first

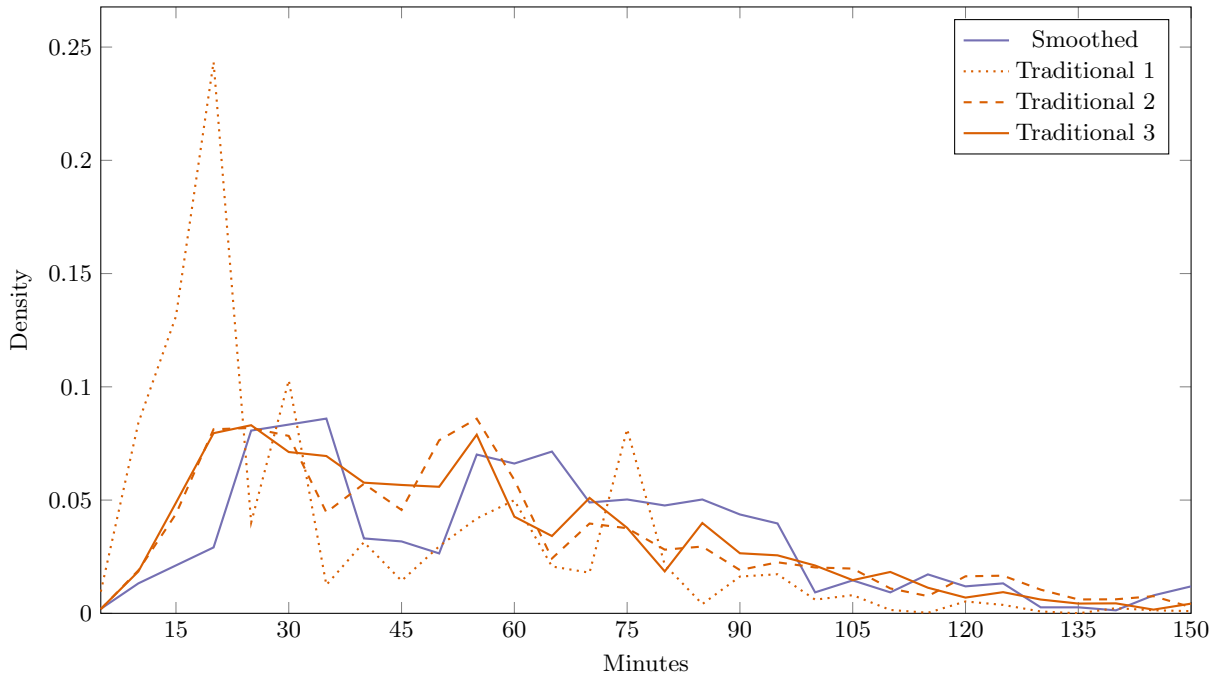

(a) *TLD for the traditional model after parameter calibration iterations 1, 2 and 3*

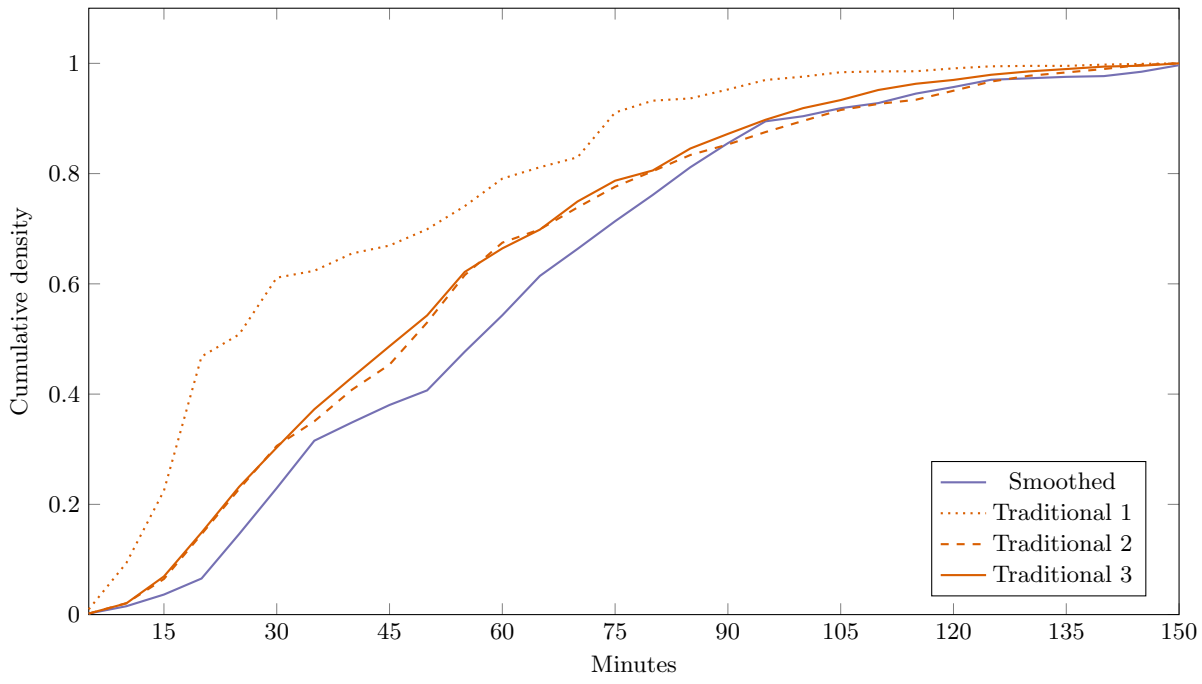

(b) *Cumulative TLD for the traditional model after parameter calibration iterations 1, 2 and 3*

FIGURE 5.10: *Smoothed TLD compared to the traditional gravity model TLD for mode* bus.

parameter calibration iteration for mode *taxi*. The traditional model underestimates the number of trips that travel less than 70 minutes both in the second and third parameter calibration iterations. The proposed model's modelled trip length distribution underestimates the number of trips that are shorter than 30 minutes and overestimates the trips that are 30 to 55 minutes. Slight deviations are noticeable for trips between 60 and 70 minutes long. The remainder of the proposed model's trip length distribution fits the observed data better than the traditional

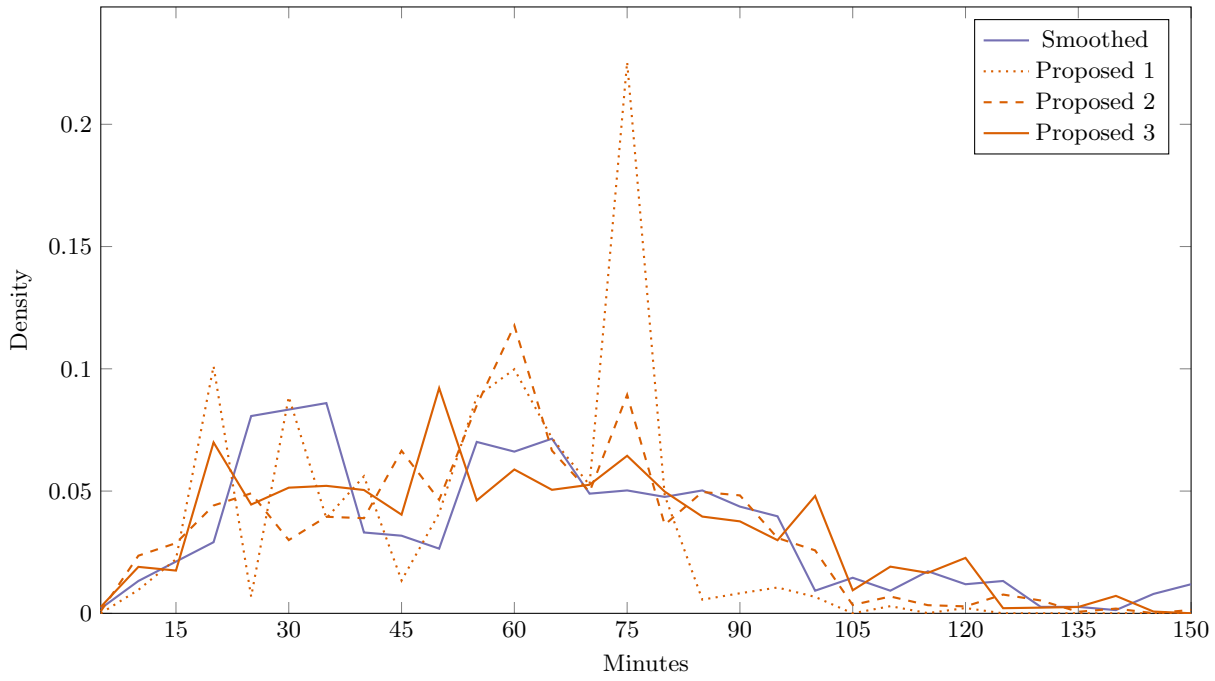

(a) *TLD for the proposed gravity model after parameter calibration iterations 1, 2 and 3*

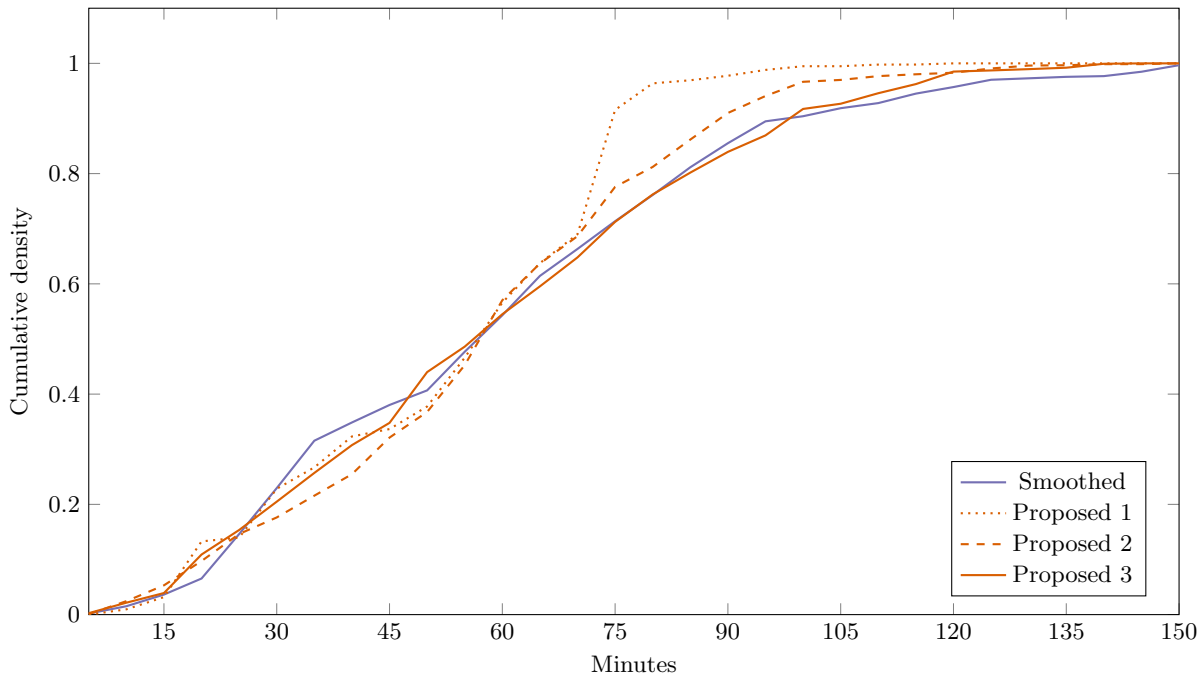

(b) *Cumulative TLD for the proposed gravity model after parameter calibration iterations 1, 2 and 3*

FIGURE 5.11: *Smoothed TLD compared to the proposed gravity model TLD for mode* bus.

model.

RMSE analysis

The parameter calibration iterations that have been evaluated up until this stage produce estimated distributions based on point estimates of the average travel distance between difference

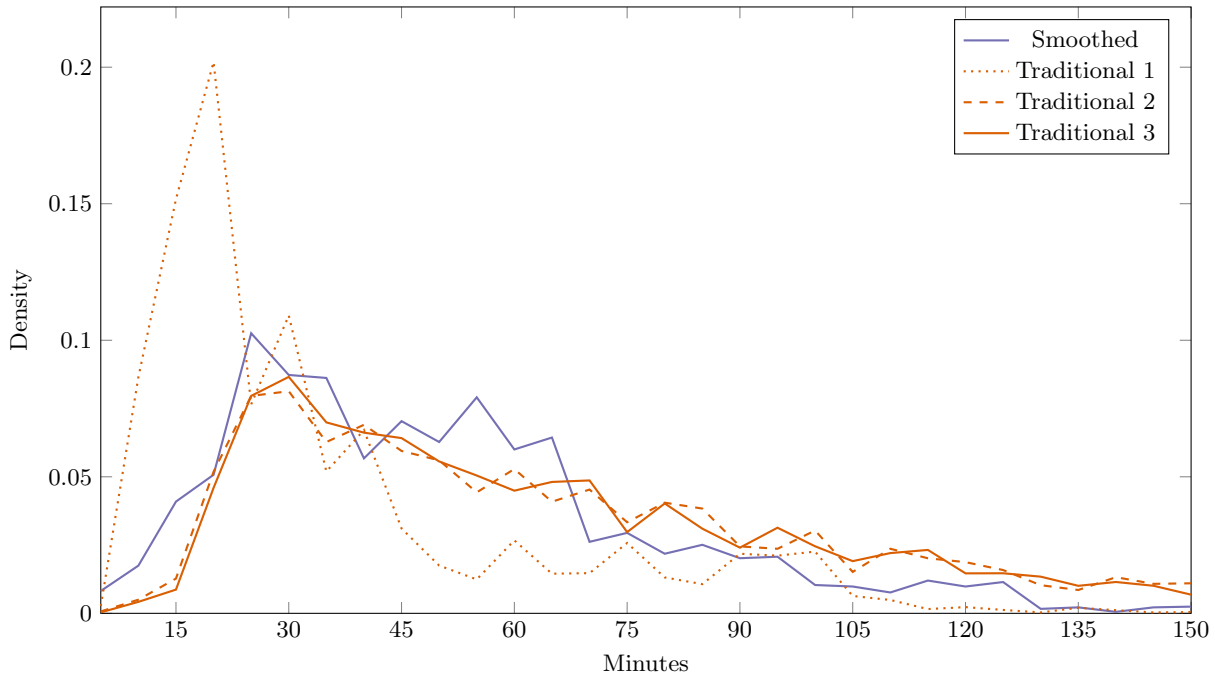

(a) *TLD for the traditional model after parameter calibration iterations 1, 2 and 3*

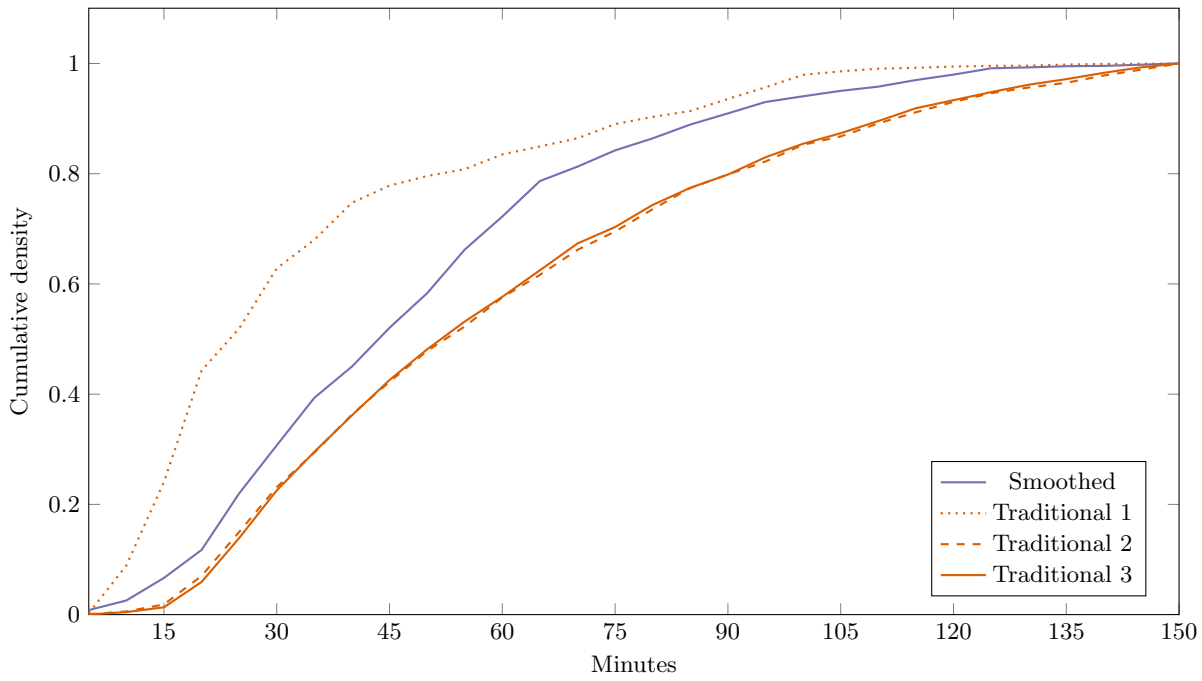

(b) *Cumulative TLD for the traditional model after parameter calibration iterations 1, 2 and 3*

FIGURE 5.12: *Smoothed TLD compared to the traditional gravity model TLD for mode* taxi.

TAZs from the previous iteration. In order to establish whether the travel time distributions are converging to a stable solution the arrival data from the traffic simulator need to be analysed. For each iteration the RMSE between the OTLD and trip length distribution, obtained from parsing the arrival data, is calculated.

The travel times parsed from the traffic simulator arrival output, in Figure 5.14, show that for the first four iterations, the RMSE of the trip length distribution of the simulated traffic

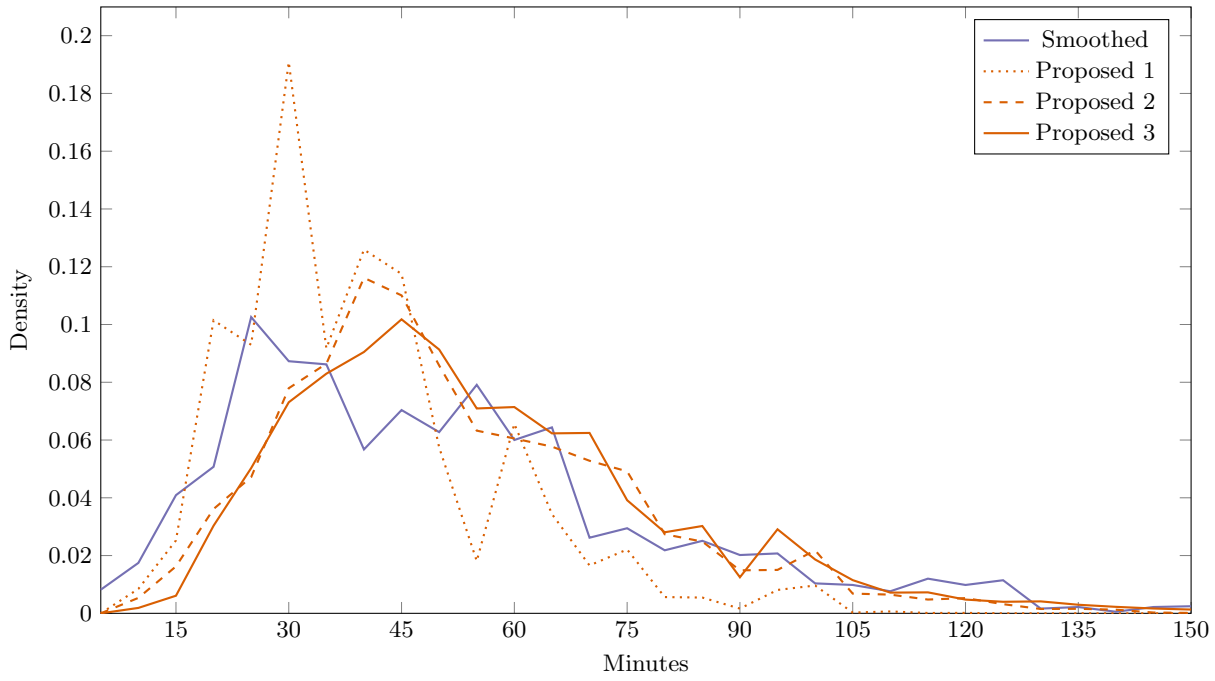

(a) *TLD for the proposed gravity model after parameter calibration iterations 1, 2 and 3*

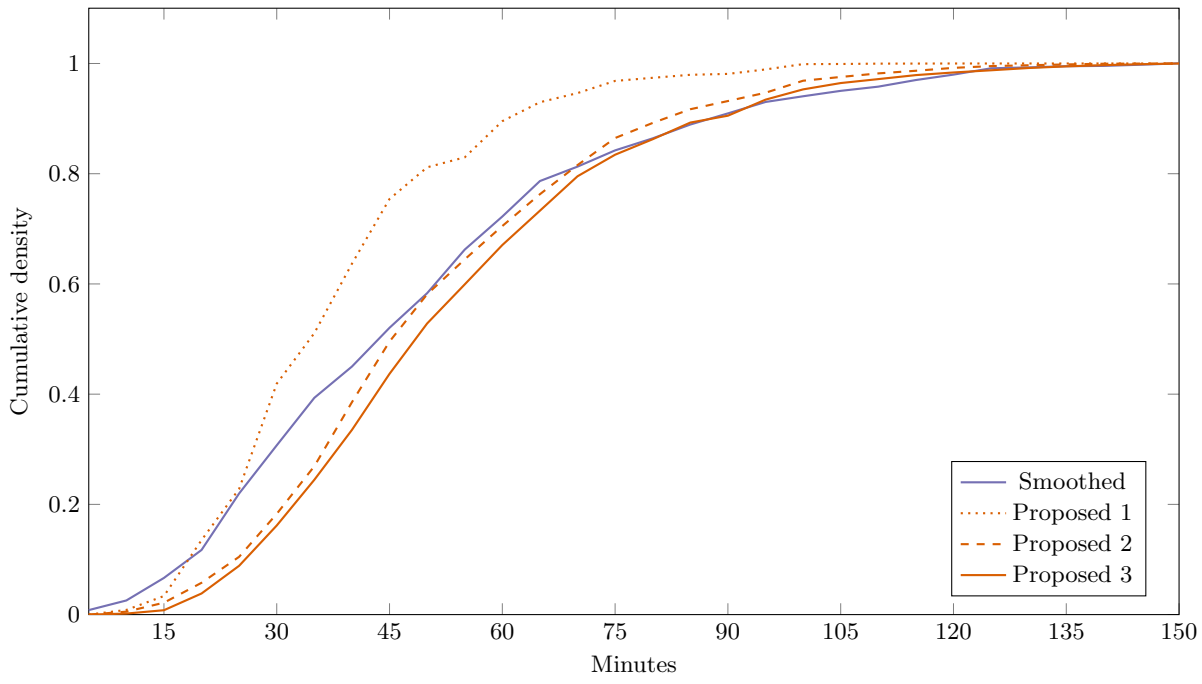

(b) *Cumulative TLD for the proposed gravity model after parameter calibration iterations 1, 2 and 3*

FIGURE 5.13: *Smoothed TLD compared to the proposed gravity model TLD for mode* taxi.

increased from 0.0139 to 0.0188 when the proposed gravity model is used for mode *drive*. The gravity parameters were calibrated based on the free flow distance matrix during this period. This explains the increase in the RMSE in the second iteration. The first trip distribution caused an over assignment of trips to TAZs that fit the aggregate travel distribution of the parameters, under free flow conditions. Figure 5.4 shows that the parameter space from the first calibration is confined to $\alpha_{\mathrm{d}} \leq 1.5$. This means that the model distributed few intra-TAZ

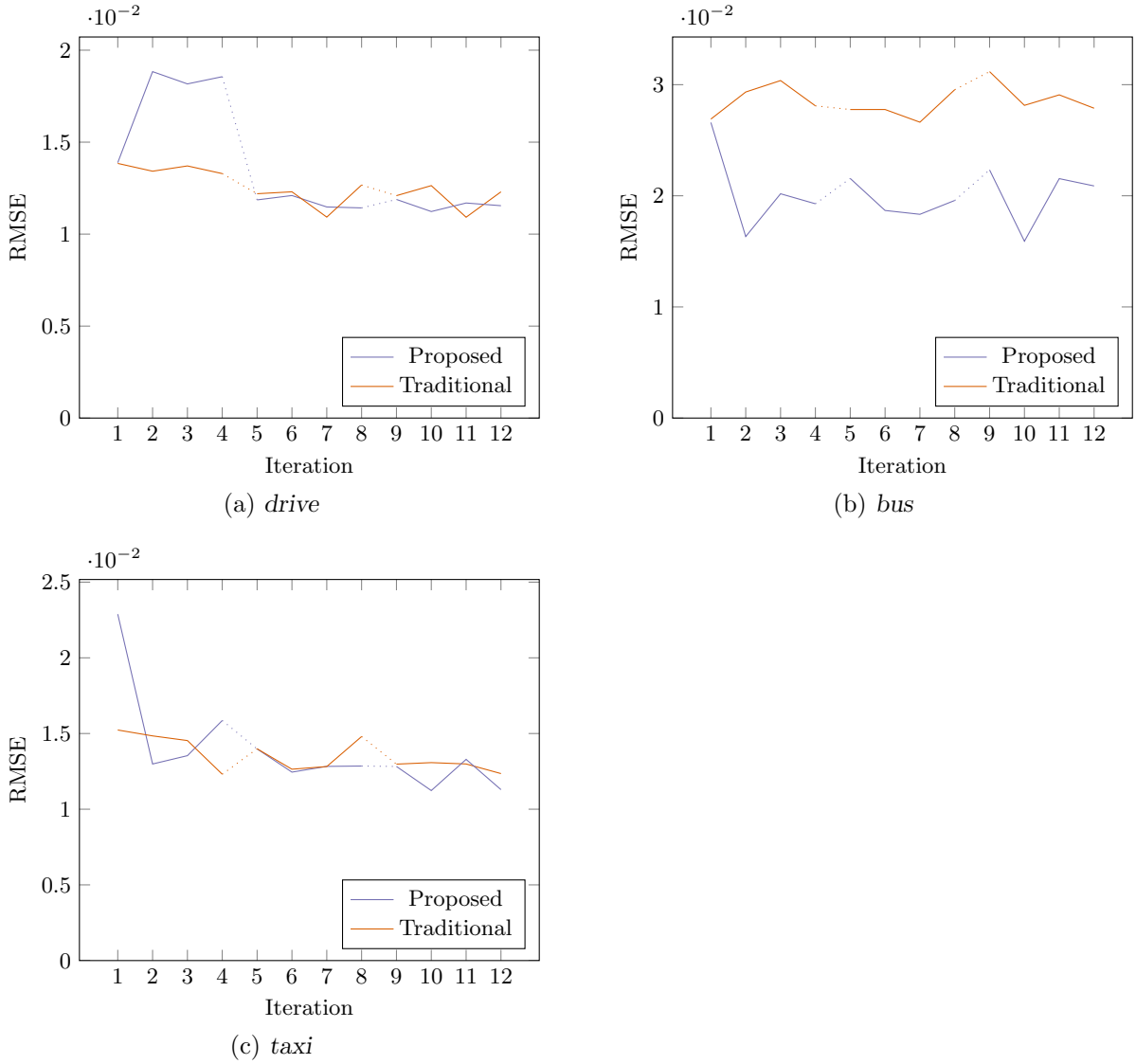

FIGURE 5.14: *Graph of the RMSE of the travel time distribution compared to the arrival data parsed from the traffic simulation data output.*

trips and more inter-TAZ trips. This assignment of trips produced new distance matrices, in which the congestion en route to these TAZs is overestimated due to the higher number of trips distributed to them, as a result of using the free flow trip matrix from the previous iteration.

In iteration three the RMSE decreases from 0.0188 to 0.0182 - The opposite of what happened between iterations one and two. The over-congested TAZs have 'less gravity' to attract trips from other TAZs. This effect persists between iteration three and four with the RMSE increasing from 0.0182 to 0.0186. The average RMSE for the iteration intervals (1–4, 5–8 and 9–12) is 0.0174, 0.0117 and 0.0116 respectively.

The same see-saw pattern is present in the arrival data from the traffic simulator that used the traditional gravity model. The variation between iterations is on average smaller, 0.00038, for the first four iterations than the second and third intervals which are 0.0011 and 0.012 respectively. The average RMSE for the three intervals for the traditional gravity model is 0.0136, 0.012 and 0.0119 which is slightly, but not significantly, higher than the proposed model.

The RMSE values for mode *bus* at the first iteration were 0.0266 for the proposed and 0.0269 for the traditional model. The RMSE of the proposed model decreased to 0.016 after the second iteration while the RMSE of the traditional model stayed above that of the first iteration 0.0293. On average the RMSE for the three iteration intervals were 0.0206, 0.0195, 0.0202 and 0.0287, 0.0279 and 0.0291 respectively for the proposed and traditional models.

The output produced from the traffic simulation for the mode *taxi* shows a decrease in the RMSE from 0.0229 to 0.0130 for the proposed model between iterations one and two. This is consistent with the parameter calibration analysis in Section 5.1 and is due to the initial free flow distance matrix input. The proposed model had on average an RMSE of 0.0163, 0.0130, 0.0121, which is lower in the second and third iteration intervals than the 0.0142, 0.0136 and 0.0128 of the traditional model.

Analysis of the arrival data shows how the inputs produced by both gravity models lead to similar outcomes when the trip distributions are simulated. A large change in the RMSE value is observed between the first and second iterations, relative to the average change across all iterations within the aforementioned intervals. The first to second iteration changes were 5.44, 2.94 and 4.57 times larger than the average absolute change in RMSE for the modes *drive*, *bus* and *taxi*. In contrast, the largest differences between iterations for the traditional model were between iterations 7 and 8 for mode *drive*, 9 and 10 for *bus* and 7 and 8 for *taxi* which were 1.95, 1.834 and 2.742 times larger, respectively. The traditional model inherently calibrates a single Tanner function that, in combination with the trip matrix, produces an aggregate trip distribution that is similar to the observed aggregate distribution. This explains the limited response to recalibration of its parameters and the iterations that follow thereafter, as seen in Figure 5.14.

The RMSE of the output produced by the traffic simulator using the trip distribution performed by the traditional gravity model steadily decreases (*drive* and *taxi*) or increases (*bus*). The standard deviation of the average iteration-on-iteration change in RMSE of the proposed model is 2.44, 2.42 and 2.54 times more for the modes *drive*, *bus*, *taxi* respectively than that of the traditional model. Despite this increased variability, the RMSE after the final iteration is lower for all modes when using the proposed model. This can be attributed to the use of each individual TAZ's observed trip length distribution, as well as adjusting how the time of day influences the average trip lengths of commuters. By introducing a temporal shift and an intra-TAZ trip adjustment parameter, the proposed gravity model can calibrate to a set of parameters that produces a distribution that, when it is simulated, results in an aggregate trip length distribution that matches the observed trip length distribution better than the traditional model.

A well-modelled aggregate trip length distribution is in itself not a sufficient condition for reaching a traffic equilibrium. The approach used in this thesis attempts to find trip distributions which match the observed TLD at an aggregate level. Finding such a distribution could mean that the underlying trip distributions from and to each TAZ could be significantly different from one iteration to the next.

5.3 Trip table stability

The trip distribution for either gravity model is a function of the travel costs C_{ij}. The RMSE between iterations in Figure 5.15 is therefore a response to the variation observed in Figure 5.16. This relationship indicates how sensitive a gravity model is to a change in C_{ij}.

The tables containing all the trips T^t_{ijh} and costs C^t_{ijh} from each TAZ i to TAZ j during iteration

h for time interval t, were compared based on the RMSE between iterations h and $h-1$. The RMSE for the trip table, RMSE_h^x, and cost matrix, RMSE_h^c, is calculated as

$$\text{RMSE}_h^x = \sqrt{\frac{1}{mn}\sum_{i=1}^{n}\sum_{j=1}^{m}\sum_{t=1}^{16}(T_{ijt}^h - T_{ijt}^{h-1})^2} \text{ and} \tag{5.2}$$

$$\text{RMSE}_h^c = \sqrt{\frac{1}{mn}\sum_{i=1}^{n}\sum_{j=1}^{m}\sum_{t=1}^{16}(C_{ijt}^h - C_{ijt}^{h-1})^2}. \tag{5.3}$$

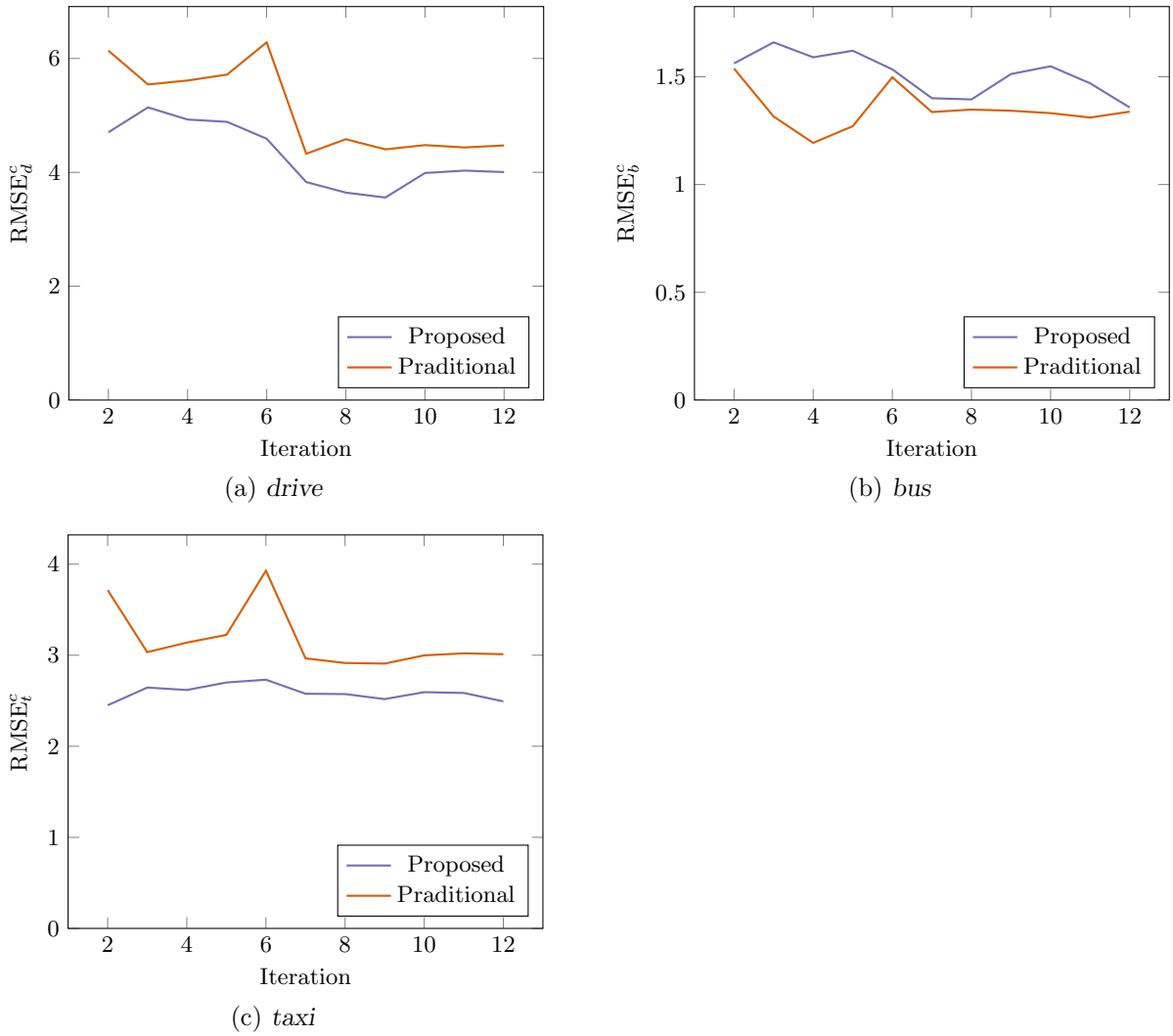

(a) *drive* (b) *bus*

(c) *taxi*

FIGURE 5.15: *Graphs that illustrate the average trip length stability for each mode.*

If there are no trips assigned to a TAZ, the free flow speed is used for the next iteration. This can be amended by assigning at least one trip from every TAZ to every other TAZ. Figure 5.17 shows the number of TAZs that were assigned to trips in iteration $h+1$ to which no trips were assigned in iteration h. The variation in the trip lengths decreases as the number of TAZs that trips are assigned to becomes more consistent.

The gravity models converge on the aggregate trip length distribution for each mode and the

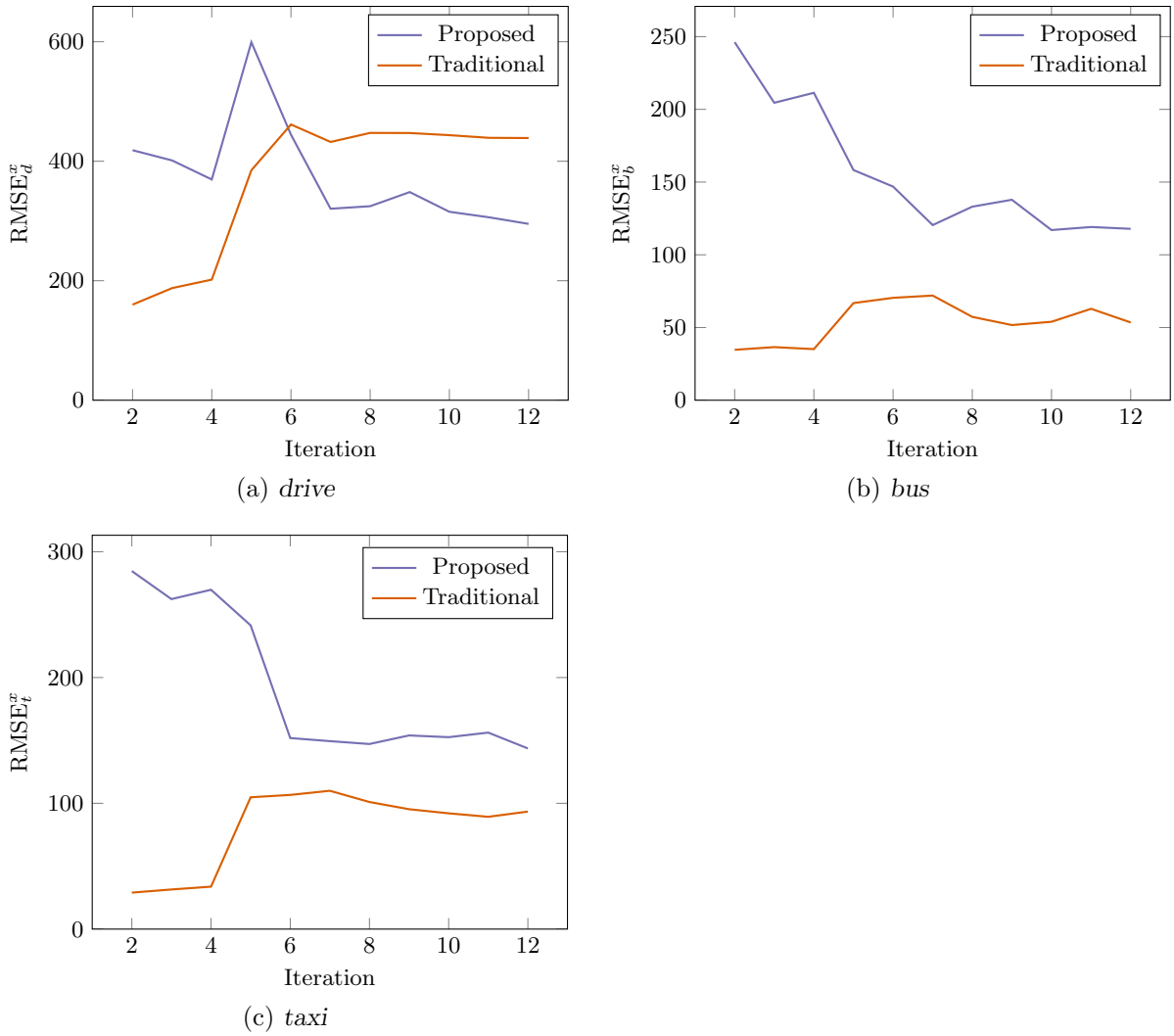

(a) *drive* (b) *bus*

(c) *taxi*

FIGURE 5.16: *Graphs that illustrate the trip table stability for each mode.*

changes in the trip tables are explained by the changes in the cost matrices. Variations in cost matrices could be due to the traffic simulator. Trip distributions might be consistent for each iteration, but trip distances can vary due to how traffic is routed through the network, which is influenced by congestion. It is therefore important to evaluate if the routes taken between any TAZ i to TAZ j converges to a stable collection.

The travel cost matrix, produced by the simulation of the trip distribution from the first iteration, is used to generate the trip distribution for the second iteration. Therefore a relationship should exist between the difference in travel costs of iterations 1 and 2, and the differences between the trip distribution in iterations 2 and 3. More formally, there should exist some relationship between RMSE_t^c and RMSE_{t+1}^x.

Table 5.4 contains the correlation coefficients for both the traditional and proposed gravity models for each mode. When interpreted in isolation these correlation coefficients can not be considered significant. However, the differences are dependent on the cost matrix as well as the number of workers and jobs originating from, and destined to, each TAZ. If the R-squared statistics are interpreted within this context, 39%, 32% and 6% of the inter iteration variance of the trip distribution of the proposed model is explained by the changes in the cost matrix

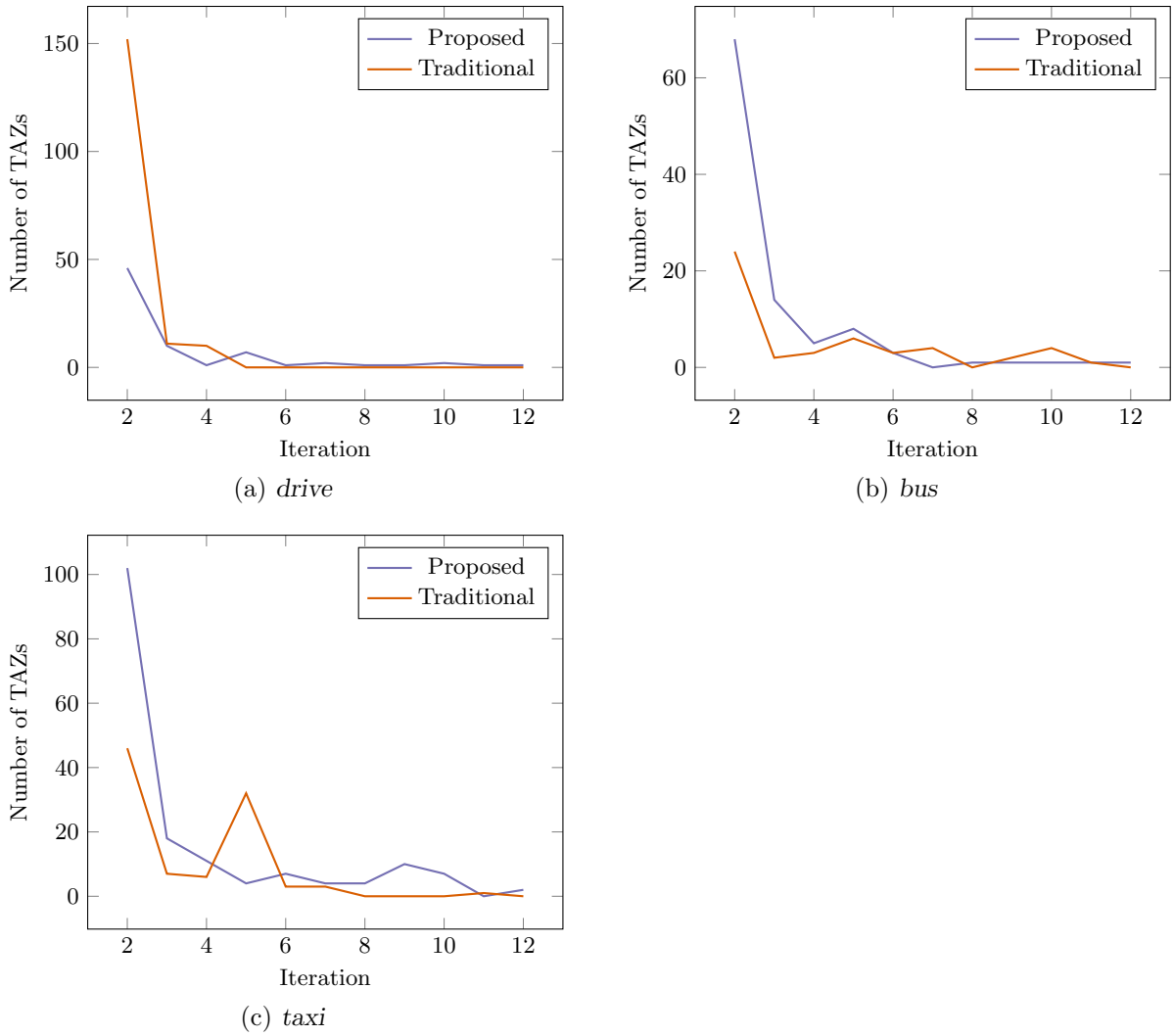

(a) *drive* (b) *bus*

(c) *taxi*

FIGURE 5.17: *The number of TAZs to which trips are assigned, which did not have trips assigned to the previous iteration and vice versa.*

Mode	*drive*		*bus*		*taxi*	
Gravity Model	proposed	traditional	proposed	traditional	proposed	traditional
Correlation Coefficient	0.62	-0.51	0.56	-0.3	-0.25	-0.14
R-squared	0.39	0.26	0.32	0.09	0.06	0.02

TABLE 5.4: *Correlation coefficients for the trip table and distance table for all modes.*

for the modes *drive*, *bus* and *taxi*, respectively. This is consistent with expectations. The travel patterns of workers who drive to work are less constrained than those travelling by bus, which is in turn less constrained than those workers travelling to work by taxi. This relationship holds for both the traditional and proposed gravity models.

5.4 Route convergence

The route convergence analysis is an integral step in verifying the framework as a sufficient method for modelling traffic. If routes do not converge to a large extent, any calibration that is performed in terms of TLD convergence is meaningless, seeing as it would mean that the underlying traffic behaviour is nonsensical.

To test the stability of the collection of routes, the total number of routes from and to every TAZ is evaluated within each mode during every iteration. The number of routes from TAZ i to TAZ j is determined by merging paths between the two TAZs according to the number of edges (road segments) they share. First, the paths are sorted in a descending order according to the number of edges it is comprised of. The longest path is chosen as the first route. The second-longest path is compared with the first route, and if the proportion of its edges that are also in the first route is greater than the specified overlap criteria, that path is assigned to the first route. If the proportion of edge overlap is smaller than the overlap criteria for all the routes established up until the evaluation of that path, that path becomes a new route. This process is followed until all paths are clustered into routes.

Route overlap for mode *drive*

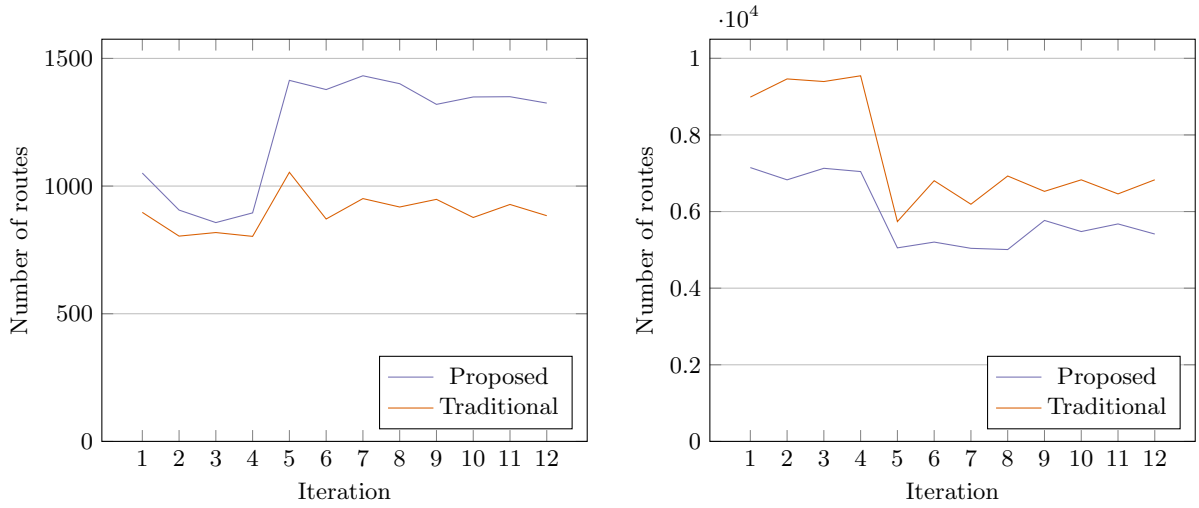

(a) *Intra-TAZ* (b) *Inter-TAZ*

FIGURE 5.18: *Total number of intra- and inter-TAZ routes, given a 50% overlap for mode* drive.

The total number of intra- and inter-TAZ routes at every iteration, for mode *drive*, is shown in Figure 5.18. Similar patterns are observed for both the proposed and traditional gravity model based simulations. The number of routes decrease between the first and the second iterations for the proposed model. In contrast, the decrease in the number of routes in the traditional model from iteration 1 to iteration 2 is offset by an increase in the inter-TAZ routes for the same iteration. The trip distribution for the first iteration is based on the free flow distance between TAZs. When this distribution is simulated each fleet tries to find the shortest way through the network. As the network becomes overly congested due to the assignment under free flow conditions these fleets find alternative shortest routes through the network, different to the routes of fleets originating from and destined to the same TAZs. For the first four iterations the number of intra- and inter-TAZ routes are strongly negatively correlated with a (R-squared

of 0.98). The proposed model reacts differently during the first four iterations. Both the number of intra- and inter-TAZ routes decrease between iterations 1 and 2. Every TAZ has a unique distribution according to which the trips, per mode, are distributed from. The proposed model could therefore produce a trip distribution based on the first iteration that reduced both the number of intra- and inter-TAZ during the traffic simulation of second iteration. There was no significant correlation (R-squared of 0.094) between the changes in intra- and inter-TAZ trips for the routes produced by the simulations of the proposed gravity model during iterations one to four for the mode *drive*.

The number of routes increased from 895 to 1414 between iterations 4 and 5, showing the effect of the intra-TAZ trip adjustment parameter α_{d}. The parameter value was adjusted from 1.5 to 4 after the second parameter calibration, thereby increasing the effective gravitational pull of a TAZ on the trips originating from it while at the same time reducing the pull from all other TAZs. The number of intra-TAZ routes decreased from 1401 to 1320 between iterations eight and nine, after the third parameter calibration selected $\alpha_{\mathrm{d}} = 3$. The average number of routes during each of the four-iteration periods were 927, 1406 and 1336 for the proposed model and 831, 949 and 909 for the traditional gravity model.

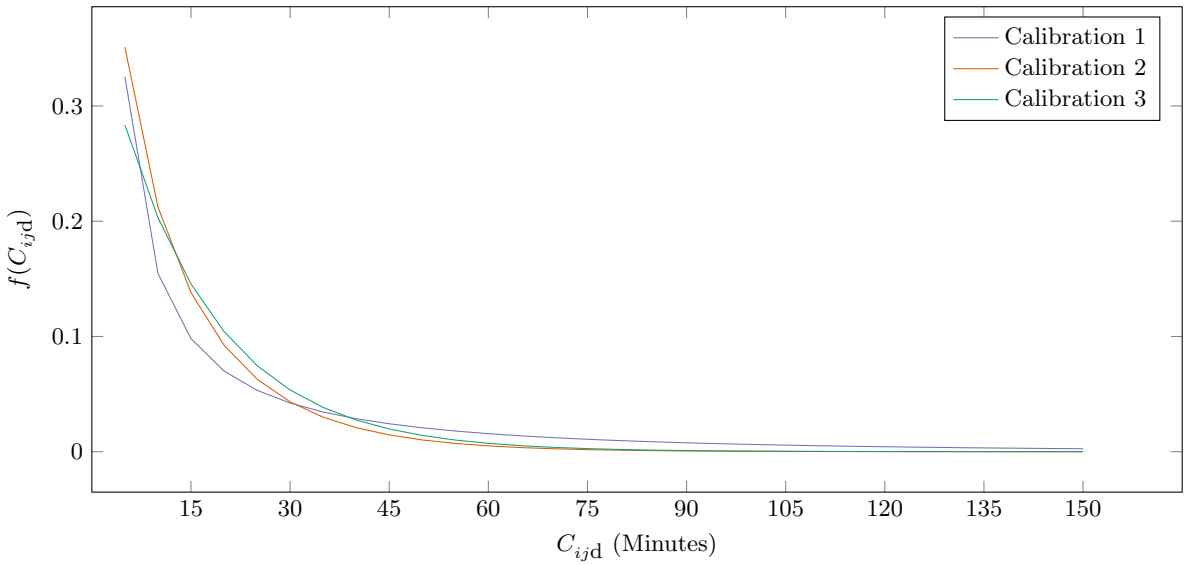

FIGURE 5.19: *Impedance of travel functions for the traditional gravity model for mode* drive.

There is a negative correlation between the number of inter- and intra-TAZ routes for each period between parameter calibrations for the traditional mode, R-square values of 0.98, 0.831 and 0.85. No such correlation seems to exist when evaluating these periods for the proposed model, depictied by R-square values 0.094, 0.54 and 0.021. When the twelve iterations are considered as a whole, the number of inter-TAZ trips are more negatively correlated (R-squared of 0.92 with the number of intra-TAZ trips for the proposed model) than for the traditional model (R-squared of 0.68). After the parameter recalibration, a single impedance of travel function is selected to represent the behaviour of each mode for all the TAZs within the study area with the traditional gravity model. Therefore the fluctuations in the number of inter and intra-TAZ routes is explained by the differences between the impedance of travel functions. Figure 5.19 shows the impedance of travel functions the parameter calibrations selected. As these functions differ from one period to the next, so do the relationships between the intra- and inter-TAZ trips. The impedance of travel functions for each TAZ for the proposed model stays fixed to the function fitted from observed data. The calibration parameter *alpha* just scales the gravity of all TAZs on the trips originating from it, thereby creating a more consistent model than the

traditional gravity model, as illustrated by the correlation between the intra- and inter-TAZ trips for all the iterations combined.

Route overlap for mode *bus*

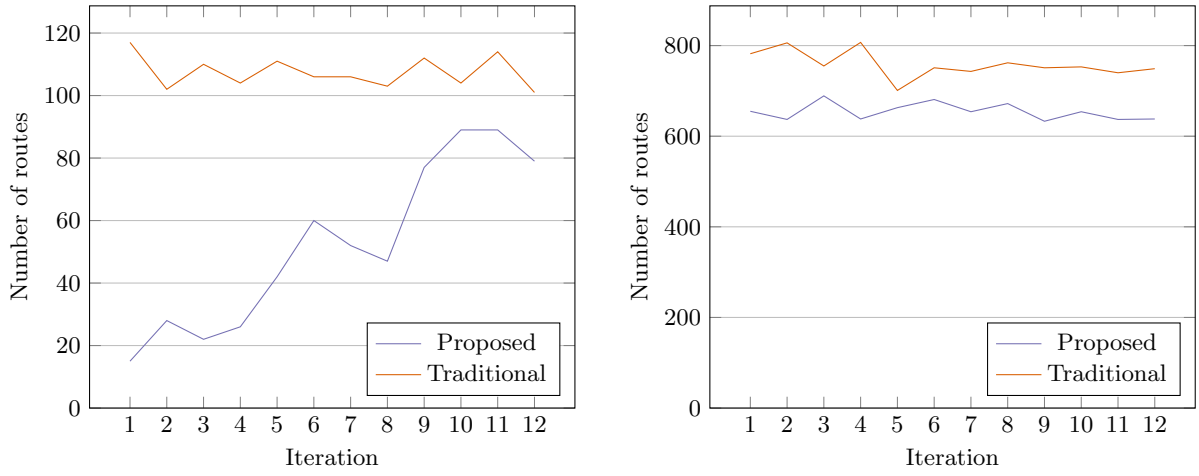

(a) *Intra-TAZ* (b) *Inter-TAZ*

FIGURE 5.20: *Total number of intra- and inter-TAZ routes, given a 50% overlap.*

The increase in intra-TAZ routes for the mode *bus* (in Figure 5.20) are on average 23, 50 and 84 which corresponds to increases in the α_b parameter from 0.25 to 1 and 1.75 after the second and third parameter calibrations for the proposed gravity model. The number of intra-TAZ routes for the traditional model remained fairly the same during each of the periods; 108, 107, 108. With each four-iteration period the variance between successive iterations decreased for the number of inter-TAZ trips for the proposed model. The standard deviations for each of the three aforementioned periods are 21.08, 10.06 and 8.015. The average number of inter-TAZ routes, 788, 739 and 748 correspond to the impedance of travel functions produced by the parameter calibrations for the traditional gravity model, (see Figure 5.21).

There is little to no significant correlation between the intra- and inter-TAZ trips for the mode *bus* for either the traditional or the proposed gravity model, with the exception of the second iteration period (from iterations five to eight) which had a strong negative correlation with an R-squared of 0.96. This can be attributed to the relatively low number of trips that travel by bus as well the small increments in the intra-TAZ adjustment parameter. The temporal adjustment parameter τ_b is 3.75, 1.75 and 1.75.

Route overlap for mode *taxi*

The number of intra- and inter-TAZ routes for the mode *taxi*, shown in Figure 5.22, are negatively correlated for the traditional model when evaluated over the whole twelve iteration period with a R-squared of 0.97. The average number of routes during each of the three iteration periods were 222, 273 and 269 for the traditional gravity model. Figure 5.23 shows the impedance of travel functions that were the result of the parameter calibrations. The change between iterations 1 and 2 for the proposed model is explained by the free flow trip distance table that is used for the first iteration. Thereafter the standard deviation of the number of intra-TAZ routes for iterations two to twelve is 7.3. The calibration parameter α_t is 0.25 for each of the parameter

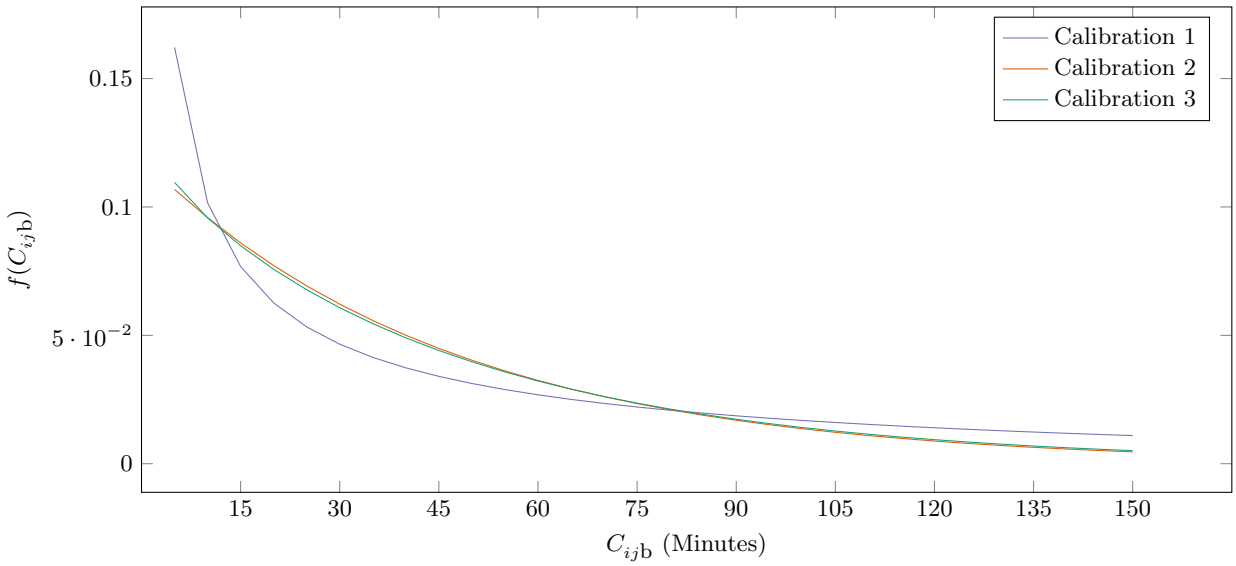

FIGURE 5.21: *Impedance of travel functions for the traditional gravity model for mode* bus.

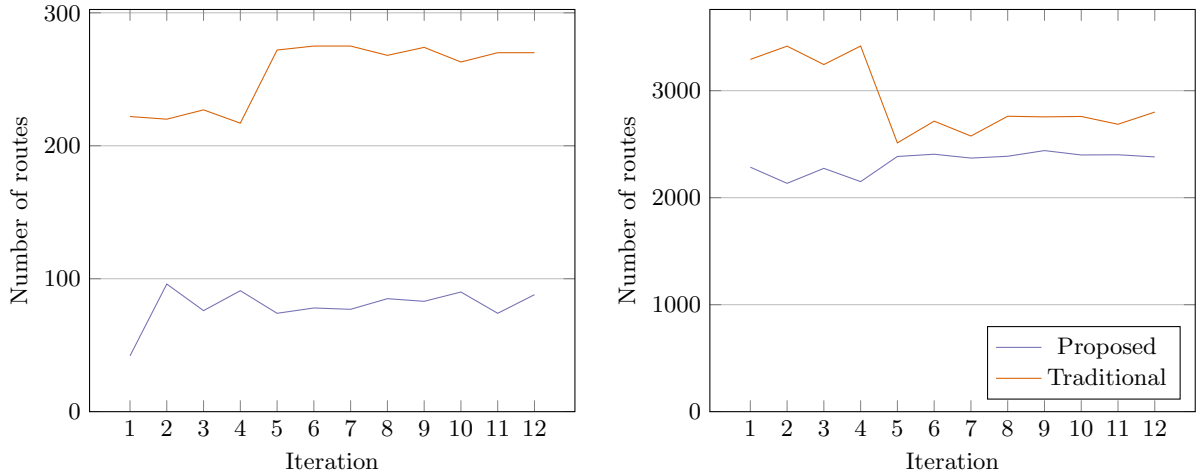

(a) *Intra-TAZ* (b) *Inter-TAZ*

FIGURE 5.22: *Total number of Intra- and inter-TAZ routes, given a 50% overlap for mode* taxi.

calibrations. The number of inter-TAZ routes for the proposed model was on average 2211, 2387 and 2405. This is explained by the parameter τ_{t}, which is 5 after the first parameter calibration and 1 for the second and third calibrations. The number of routes based on a 10% and 90% overlap can be seen in Figures A.10 to A.15.

Route stability

The number of routes is a proxy for route stability for inter- and intra-TAZ trips. As the iterative process continues, the variance between the number of routes in successive iterations decreases on average across all modes for both models. If the number of routes were to stay the same, it would not necessarily mean that the same routes are used during each iteration. To test for route stability additional information is necessary. It is assumed that if the same routes are being used consistently throughout the iterative process, then the edges through which the most

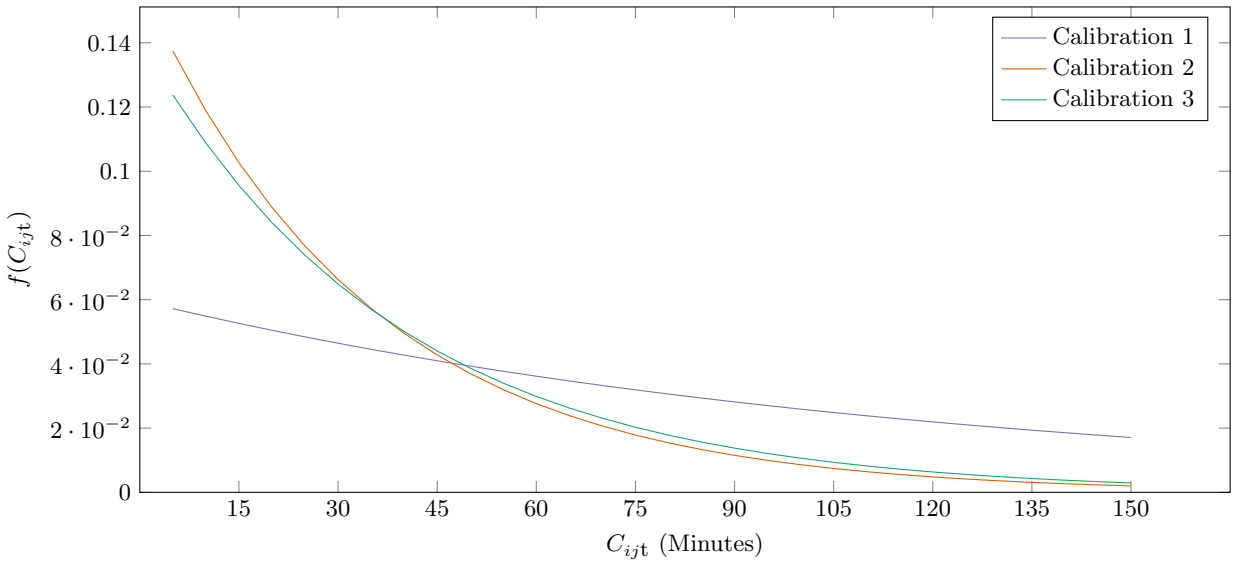

FIGURE 5.23: *Impedance of travel functions for the traditional gravity model for mode* taxi.

traffic flows on all routes and the volume of traffic through said edges during each iteration, should stay the same. For each iteration the top 20% of edges, A^t_{20}, from all routes through which traffic is flowed between each TAZ i and TAZ j and the volume of trips is recorded and compared to the next iteration's top 20%. Given the volume of trips, v^t_{aij}, that have traversed edge a during iteration t, RMSE^t_{v20} travelling from TAZ i to TAZ j can be expressed as

$$\text{RMSE}^t_{v20} = \sqrt{\frac{\sum_{i \in O} \sum_{j \in D} \sum_{a \in A^t_{20}} (v^t_{aij} - v^{t-1}_{aij})^2}{|O||I||A|}} \tag{5.4}$$

with

$$v^t_{aij} = \begin{cases} v^t_{aij} & \text{for } v^t_{aij} \in A^{t-1}_{20} \\ 0 & \text{for } v^t_{aij} \notin A^{t-1}_{20}. \end{cases} \tag{5.5}$$

Figure 5.24 shows the RMSE^t_{v20} values for both the traditional and proposed models. The largest changes are observed during the first 4 comparisons for each mode. Other than iterations six and seven for the traditional model mode *drive*, proposed model mode *bus* between iteration ten and eleven and mode *taxi* between iterations eight and nine, every succeeding iteration had more throughput in common with the same edges than its preceding iteration. This result shows that when simulated, the routing of the trip distributions from either gravity model will produce routes that are more like the routes from the iteration that preceded it.

A framework that converges to an observed aggregate trip length distribution based on a stable trip distribution might still not be an accurate reflection of the actual traffic within the study area. Trips could be distributed consistently, but to the wrong places. If the framework is a sufficiently accurate enough representation of the traffic within the study area it should produce a similar departure and arrival time distribution as the observed data.

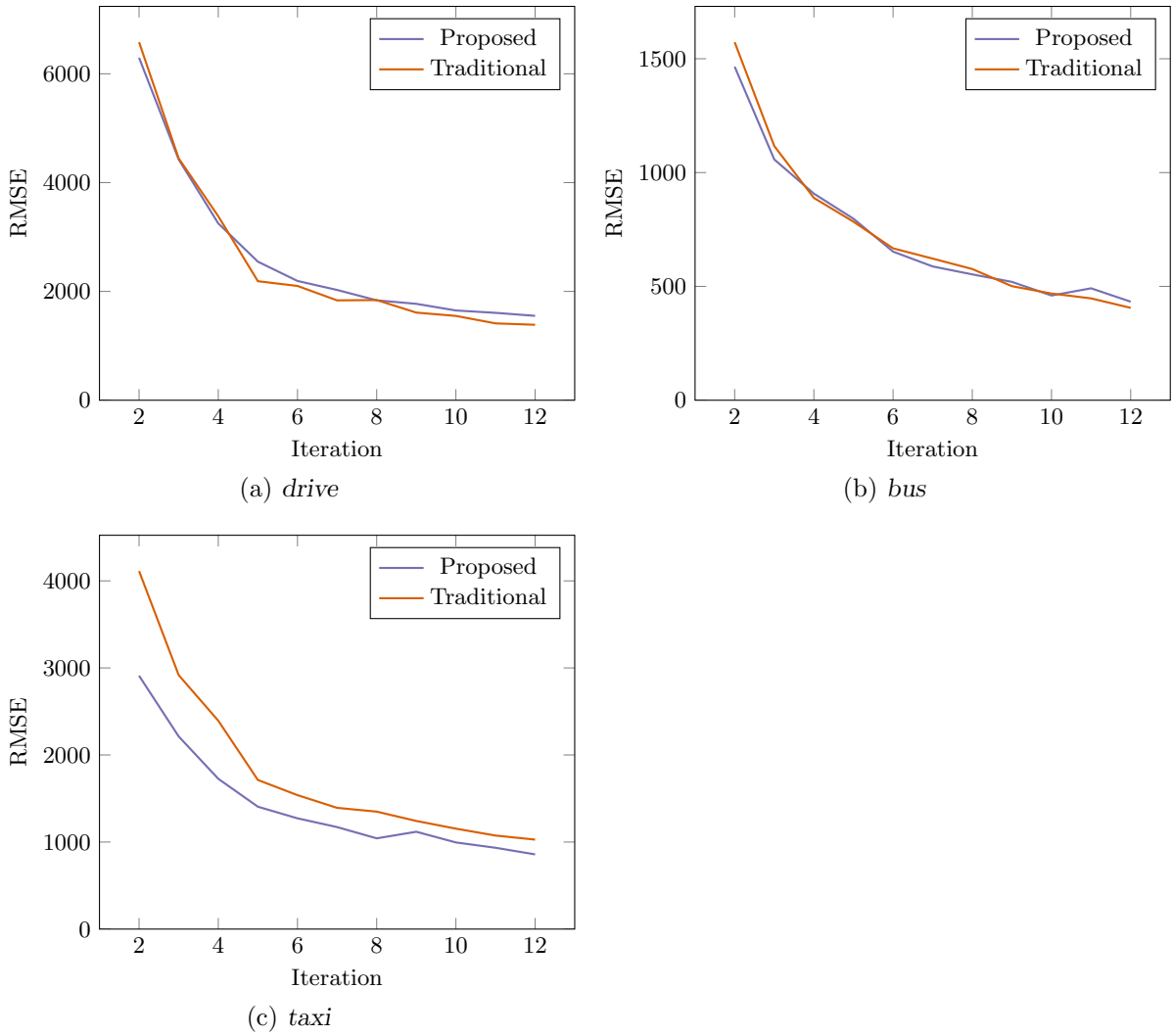

FIGURE 5.24: *Iteration-on-iteration change in traffic volumes to the most-used edges in the network*

5.5 Departures and arrivals

Figure 5.25 compares the modelled and observed binned proportions of trip departure and arrival times for all modes, combined for the last iteration. Given the observed proportion for bin β, U_β, and the modelled proportion, M_β, the deviation, σ^δ, σ^ρ of the simulated departure and arrival times is calculated by

$$\sigma^\rho = \sum_\beta \frac{(U_\beta^\rho - M_\beta^\rho)^2}{U_\beta^\rho} \text{ and} \tag{5.6}$$

$$\sigma^\delta = \sum_\beta \frac{(U_\beta^d - M_\beta^\delta)^2}{U_\beta^\delta}. \tag{5.7}$$

The departures for all trips, irrespective of mode had a deviation value of 0.072 and 0.078 for the traditional and proposed models, respectively. There is no significant observable difference between the departure times produced by the proposed or traditional gravity model.

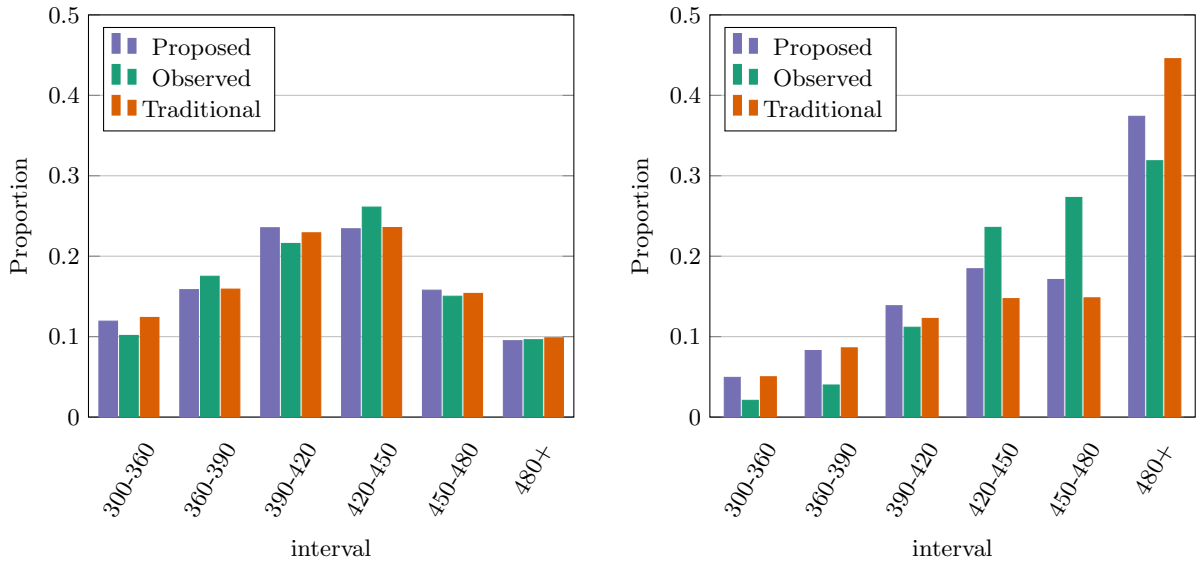

(a) *Departures* (b) *Arrivals*

FIGURE 5.25: *Proportion of arrivals and departures per time interval for all modes combined.*

The departure times of the simulated trips for both the traditional and proposed model is generated through the same process and is expected to be the same. The deviations in the arrival distribution highlights a caveat of disaggregating trip distribution data. The parameters calibrated in such a fashion that the modelled aggregate trip length distribution closely matches the observed aggregate trip length distribution. The traditional model uses the same trip length distribution consequently, irrespective of the time of departure. Therefore every time interval of the trip distribution will have the same distribution of trips. This should underestimate the arrivals that are close to the median, and overestimate the tails of the arrival distribution. The proposed model seeks to rectify this incorrect temporal distribution of trips with the addition of the temporal calibration parameter τ. The arrivals had a deviation value of 0.24 for the traditional model and 0.15 for the proposed model. The proposed gravity model produced a trip distribution in its final iteration such that the deviation from the observed arrival distribution was smaller than that of the traditional model. The increased accuracy of the proposed model is due to less overestimation of the right tail [it is trips that arrive after 08:00 (480+)] and less underestimation of the arrivals around the median [it is trips that arrive between 07:00 and 08:00].

Figures 5.26, 5.27 and 5.28 show the arrival and departure time distribution for the proposed and traditional models compared to the observed data for the modes *drive*, *bus* and *taxi* respectively.

The arrival deviation values for the mode *drive* are 0.16 for the proposed and 1.07 for the traditional gravity model. The largest deviation from the arrivals observed proportions for both models are seen during the period between 07:00 and 08:00. The proposed model estimates the number of trips arriving after 08:00 with greater accuracy than the traditional model. The proposed model's overestimation of the number of trips arriving on before 06:30 is marginally, but not significantly less, than the traditional model. This is because the bands in Figure 4.2 do not constrain trips shorter than 15 minutes during this period. Both models overestimate the departure of trips during 05:00–06:00 and underestimates them during 07:00–07:30.

The departure deviation values for the mode *bus* are 0.83 for the proposed and 1.49 for the traditional gravity model. Similar to the findings for the mode *drive*, the departure of trips

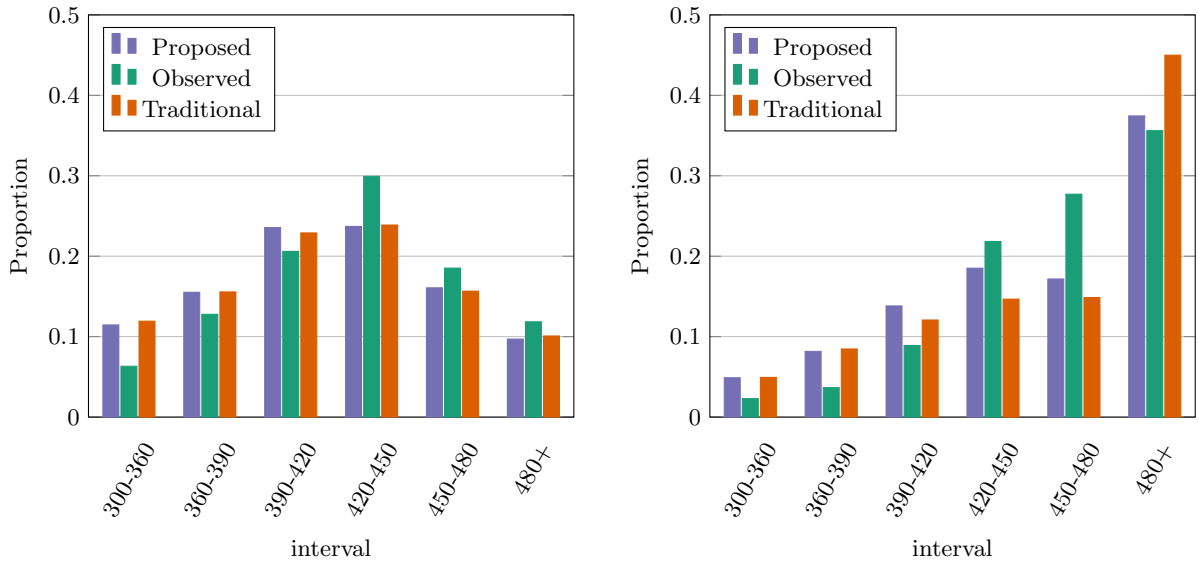

(a) *Departures* (b) *Arrivals*

FIGURE 5.26: *Proportion of arrivals and departures per time interval for mode* drive.

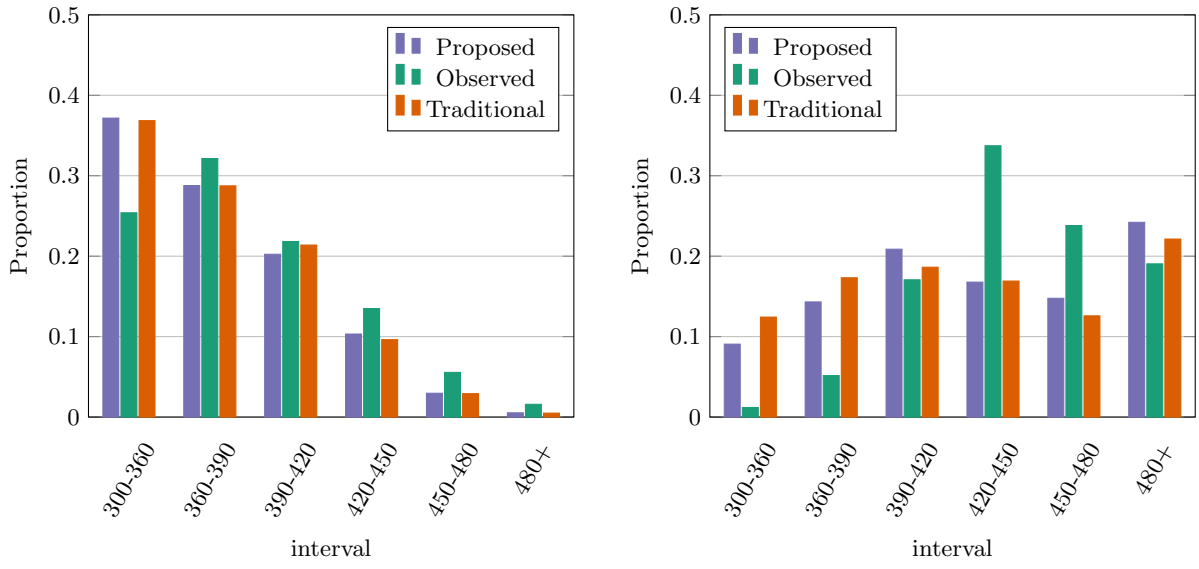

(a) *Departures* (b) *Arrivals*

FIGURE 5.27: *Proportion of arrivals and departures per time interval for mode* bus.

during 05:00–06:00 are overestimated and trips departing during 07:00–07:30 are underestimated. The relative size of the under and overestimations are less for the mode *bus* than for *drive* for the departures before 06:00. The arrival distribution shows a clear overestimation of the trips arriving before 06:30 and after 08:00 and an underestimation of the trips arriving between 07:00 and 08:00. Although the bands in Figure 4.3 constrain trips shorter than 45 minutes before 05:45, τ_b is 1.75, limiting the effect of the temporal constraints.

The arrival deviation values for the mode *taxi* are 0.25 for the proposed and 0.29 for the traditional gravity model. The number of departures for 05:00–06:00 and 06:00–07:00 and overestimates the proportion of departures in 07:00–07:30. This causes the arrivals around the median

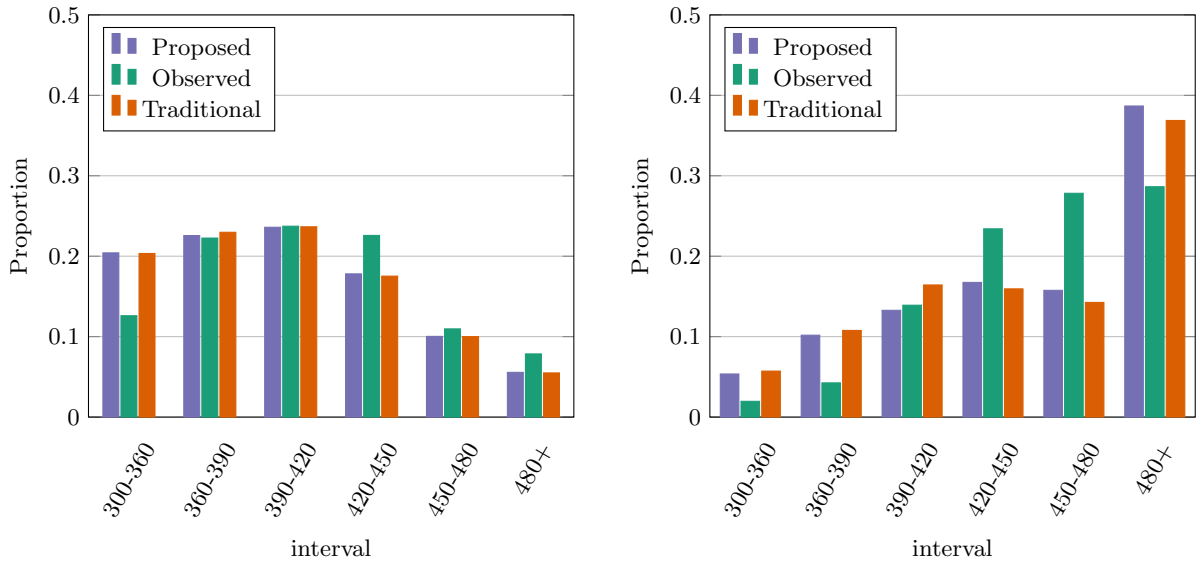

(a) *Departures* (b) *Arrivals*

FIGURE 5.28: *Proportion of arrivals and departures per time interval for mode* taxi.

to be underestimated and the arrivals on the tails to be overestimated. The arrival distributions of the proposed and traditional model are not significantly different, which is attributed to the parameter value of 1 for τ_{taxi}, which means that it has no effect on the trip distribution.

The departure and arrival analysis indicates that the proposed model produces trip distributions that are temporally more aligned to the observed data than the traditional gravity model. The proposed and traditional models have been compared based on aggregate TLD convergence, trip table stability, route convergence, and departure and arrival analysis. The final step is to compare flow volumes to available vehicle counts.

5.6 Flow analysis

The flow analysis is used to validate the traffic simulator. The framework established within this thesis only distributes morning peak hour commuter traffic through the road network. It is therefore not expected to be an accurate reflection of traffic for the whole period as it excludes travel based on other purposes such as attending academic institutions or recreational activities. Figure 5.29 shows the comparison of the simulated traffic of the proposed and traditional models compared to the observed vehicle counts.

The simulated flows are compared to the average annual daily traffic vehicle count data. The difference between simulated and observed data is determined by using a normalised root mean square error. The NRMSE is calculated by comparing the hourly number of observed vehicles for the same road segments. Given the simulated traffic through edge a, for hour η, a^s_η and the observed traffic flow a^o_η the NRMSE is expressed as

$$\text{NRMSE}^{flow}_a = \frac{\sqrt{\sum_{\eta=1}^{4} \frac{\left(a^s_\eta - a^o_\eta\right)^2}{4}}}{\max(a^o_\eta) - \min(a^o_\eta)}. \tag{5.8}$$

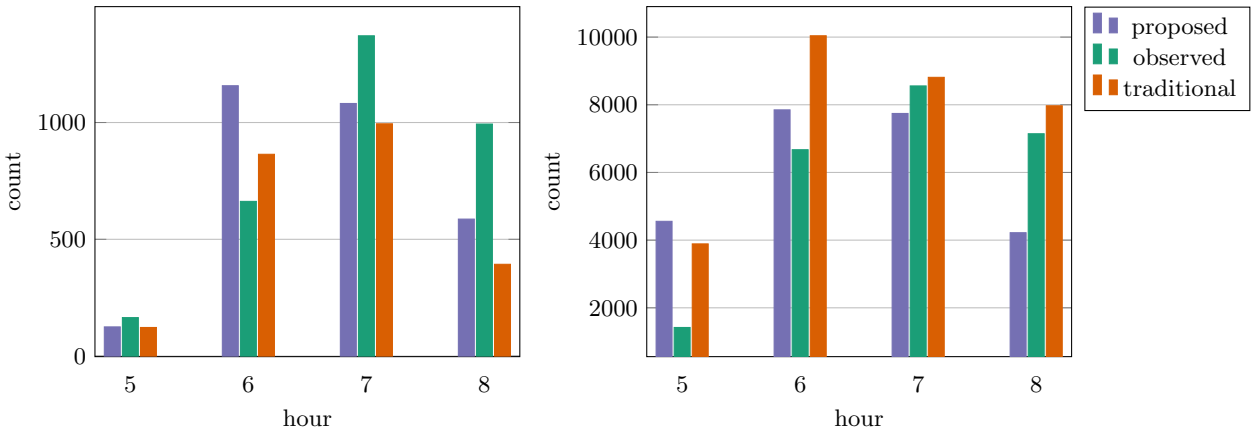

(a) *Station 5008* (b) *Station 5027*

FIGURE 5.29: *Modelled vehicle counts compared to observed vehicle counts for stations 5008 and 5027.*

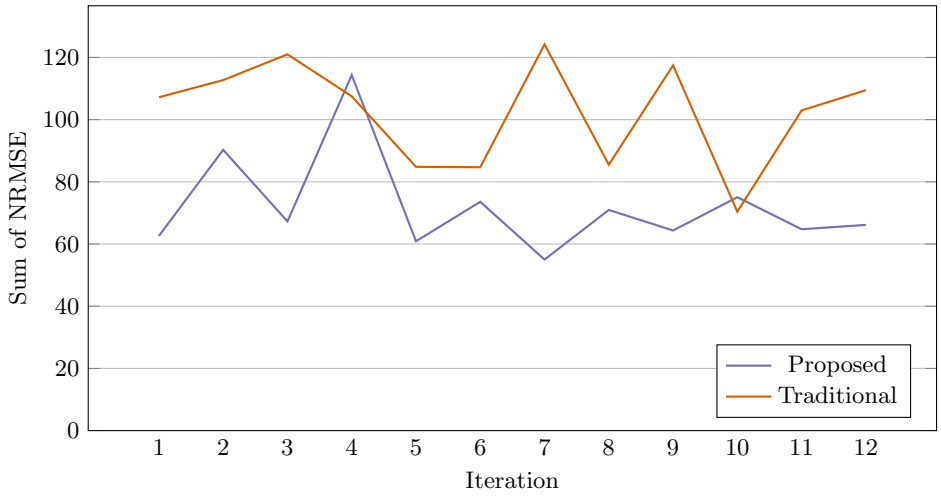

FIGURE 5.30: *The sum of the NRMSE all the vehicle counting stations when compared to the simulated flows.*

An average NRMSE is calculated over all the vehicle counting stations that had more than 80% up time for 2011. The average total NRMSE for the proposed gravity model is 72.1, with a sum over all iterations of 865.3. The traditional gravity model had an average NRMSE of 102.3 with a total sum over all iterations of 1227.9. Figure 5.30 shows the sum of the NRMSE over all the counting stations for each iteration.

5.7 Chapter conclusion

This chapter compared the effectiveness of the traditional gravity model and proposed gravity model through assessing their verification and validation outputs. It is expected that the output produced by these two models should be different and that the differences can be explained.

A comparison of the average trip length derived from the TLD of both gravity models, after each parameter calibration iteration, to the OTLD showed that the proposed gravity model could find better trip distributions than that of the traditional model for the modes *bus* and *taxi*. The

average trip length for the mode *drive* is 15 seconds longer than for the proposed model than the traditional model. The proposed model consistently produced trip distributions with lower RMSE values, especially for the mode *taxi*.

An analysis of the TLD convergence (to the OTLD) gave visual confirmation of the improvement of the trip distributions produced by the proposed model for the mode *bus* and *taxi* over that of the traditional model. These theoretical TLDs are based on the point estimates of average travel time between TAZs, which is aggregated from the simulation output. The TLDs produced from the output of the traffic simulation trip arrival data gave quantitative confirmation that the trip distributions produced by the proposed gravity model fits the OTLD better than the output produced from simulating the traditional gravity model.

The trip table stability comparison shows that the output produced by the traffic simulator has a larger effect on the trip distributions produced by the proposed gravity model. This highlights that the proposed model is more sensitive to variations in the trip length tables. This means that the proposed model would be more effective at evaluating any proposed infrastructure developments that would affect the road network.

The trip distributions of both the traditional and proposed models produce converging, stable sets of routes when simulated. However, the number of inter-TAZ routes produced by the traditional model are consistently more than that of the proposed model. This illustrates the shortcoming in using a single impedance of travel function to distribute the trips of each zone when the underlying behaviour is different than that of the aggregated behaviour.

The arrival analysis shows that the proposed model produces more accurate trip distributions when simulated within the mesoscopic traffic simulation. This is corroborated with the results of flow analysis which shows that the traffic flows of the traffic simulator is closer to the observed traffic counts when using the proposed gravity model.

The proposed gravity model generates trip distributions which scored better on the metrics discussed in this chapter. This shows the advantage of using the TLD for each TAZ rather than calibrating a single function to estimate the underlying behaviour of all the TAZs. The next chapter contains sensitivity analysis of the traffic simulator parameters and the effect that it has on the calibration of the proposed gravity model.

CHAPTER 6

Sensitivity analysis on simulation parameters

Contents

The previous chapter compared the outputs produced by the proposed and traditional gravity models. This chapter tests the sensitivity of the simulation output for different fleet sizes and route selection criteria based on a trip distribution generated by the proposed gravity model.

The trip distributions for the traditional and proposed gravity models were simulated using a mesoscopic traffic simulator. Trips for mode *drive* are grouped into fleets of 50 vehicles, 10 for mode *bus* and 15 for mode *taxi*, finding the shortest travel time through the network. The choice of fleet size and route decision criteria, given a certain trip distribution, might influence the framework's ability to converge toward a stable solution.

Six simulations are compared to see how a change in the fleet size and route decision criteria parameters affect the simulation output when using the proposed gravity model. Table 6.1 contains the parameter settings used in the sensitivity analysis.

Simulation name	Group size (mode) *drive*	*bus*	*taxi*	Route decision criteria
FAST	100	20	30	1
FAST75	100	20	30	0.75
MED	50	10	15	1
MED75	50	10	15	0.75
SMALL	10	2	3	1
SMALL75	10	2	3	0.75

TABLE 6.1: *The parameter settings for the group sizes used in the the different simulations.*

The average trip distance from TAZ i to TAZ j is likely to be more representative of how long it takes to travel between the TAZs when more fleets are simulated. The average cost C_{ij} in

the distance matrix is the average travel time between TAZ i and j the fleet size and weighted by the fleet size. If, for example there are 50 trips between TAZ i and TAZ j during time interval t and the fleet size is 50, C_{ij} will be determined by a single route between TAZ i and TAZ j. The fleet might be fragmented into smaller parts during the simulation it arrives at a fully saturated network segment a. Only a portion of the fleet could be able to travel to the next segment during time period t, while the remainder is put in the vertical queue at a. These smaller fleets will have different trip times, but will still be between the same TAZ connectors. These TAZ connectors might be near a shared border between adjacent TAZs, giving a skewed average, which is not representative of the average weighted time of all trips departing during interval t to travel from TAZ i to j.

Increasing the number of fleets are likely to produce a representative and stable weighted average travel time. To test this expectation and the effect of different fleet sizes the trip length stability is compared for the different parameter settings.

6.1 Average trip length stability

Figure 6.1 shows the normalised RMSE of the change in trip lengths, T_{ij}, between iterations. The trip length tables are more stable after the second parameter calibration iteration, that is after iteration 6. A change in the route selection criteria, c, from 1 to 0.75, results in a lower NRMSE, as expected. When trips between TAZs choose the shortest path in terms of travel distance and not travel time, the choice of route is not affected by congestion. Assigning more trips to the shortest path in terms of travel distance could therefore lead to a more consistent trip lengths. The trip length stability for the mode *drive* reacts as expected. More, smaller fleets translates to improved trip length stability. On average, reducing the route selection criteria parameter, c, from 1 to 0.75 reduces the RMSE, given the same fleet size. The simulations FAST and FAST75 have an average NMRSE of 4.53 and 4.36. The reduction in c is not as effective as reducing the fleet size from 100 to 50. The average NRMSE for MED and MED75 is 4.3 and 4.22. Reducing the fleet size from 50 to 10 reduces the average NRMSE to 4.17 and 3.9 for SMALL and SMALL75, respectively.

The trip length table stability for the mode *bus*, Figure 6.2, is not as susceptible to a change in c as for the mode *drive* across all fleet sizes. The average NRMSE for the mode *bus* is 1.62 and 1.48 for simulations FAST and FAST75, a difference of 0.14, compared to the 0.03 for the simulations MED, MED75, SMALL and SMALL75, which have NRMSE of 1.51, 1.54, 1.47 and 1.44, respectively. This could be caused by the large fleet size. The largest number of trips, for example, departing between 06:00 and 06:15 from a single TAZ is 2761, from TAZ 9027 to 9020. Given that 33 trips are clustered into a single bus and that buses are clustered into fleets of 20 for the FAST and FAST75 iterations, only 5 fleets of buses would be simulated from TAZ 9027 to 9020 during 06:00 to 06:15. The next largest number of trips is 1338 from TAZ 9028 to 9020, which would only generate three fleets. Less fleets means fewer TAZ connectors are used which leads to a skewed average trip length between TAZs, which leads to more variation between iterations.

The same behaviour of the NRMSE is observed in Figure 6.3 for the mode *taxi* than for the mode *bus*, but just to a lesser extent. On average the NRMSE for FAST, FAST75, MED, MED75, SMALL and SMALL75 are 2.69, 2.48, 2.59, 2.50, 2.54 and 2.26.

This increased stability is more than likely skewed towards the shortest path between TAZs. With a c of 1, the fleets choose the shortest travel time during the simulation. If c was set to 0, all the trips would choose the shortest path in terms of travel distance, ignoring congestion. The

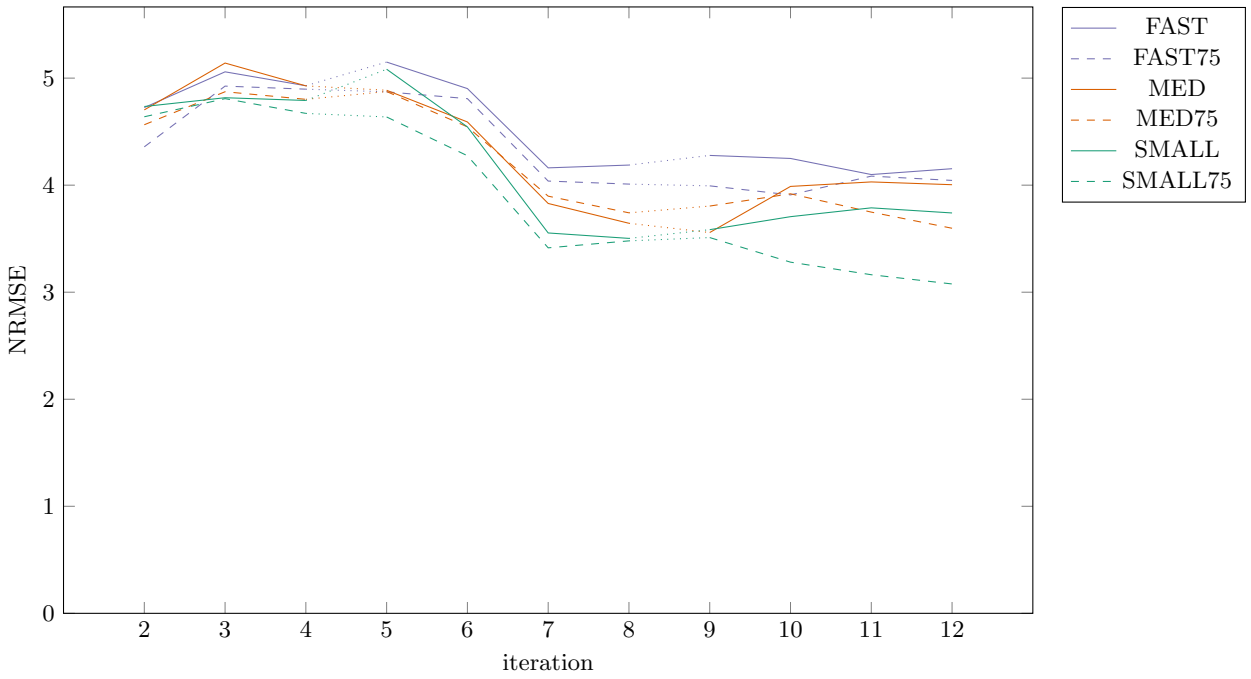

FIGURE 6.1: *NRMSE of the iteration-on-iteration change in trip distance tables for mode* drive.

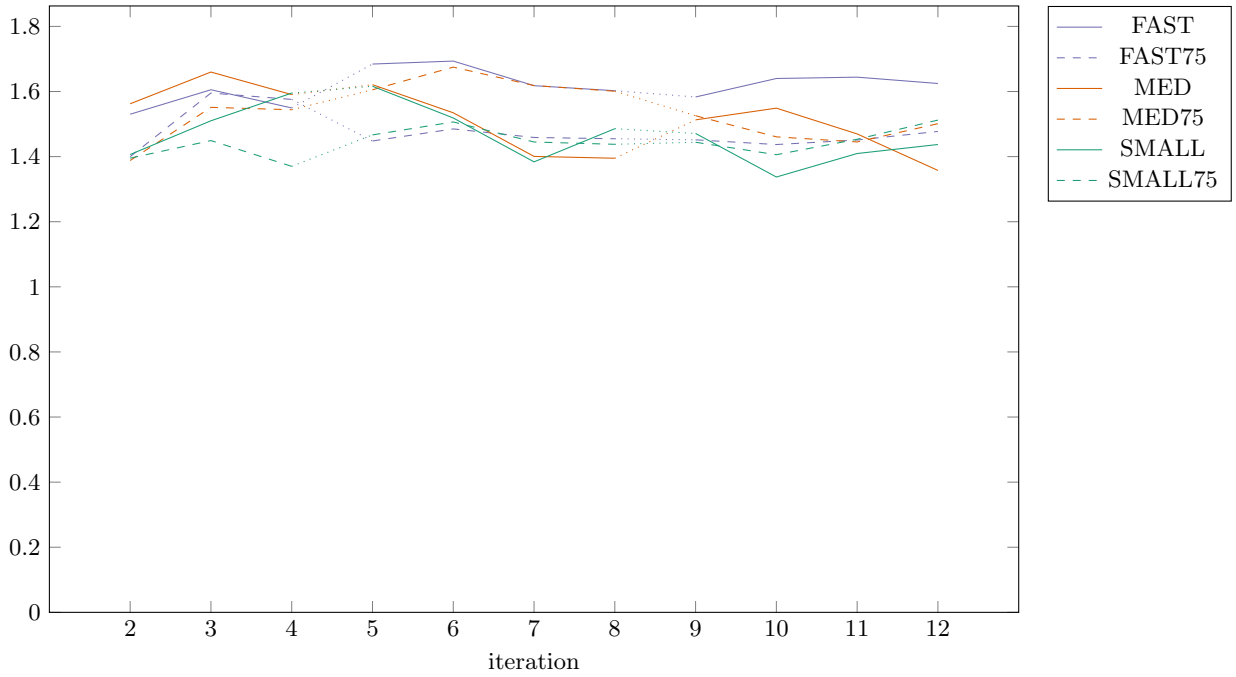

FIGURE 6.2: *NRMSE of the iteration-on-iteration change in trip distance tables for mode bus.*

travel times parsed from the arrival data from such a simulation will have artificially high trip lengths due to all the trips between TAZs being forced through the shortest path. This causes the next iteration to have a different trip distribution from the previous one, as it is based on the trip length distribution of all TAZs.

Reducing the fleet size, and fixing a portion of routes to the shortest path in terms of length corresponds to an increase in trip length stability. A smaller fleet size is more effective at

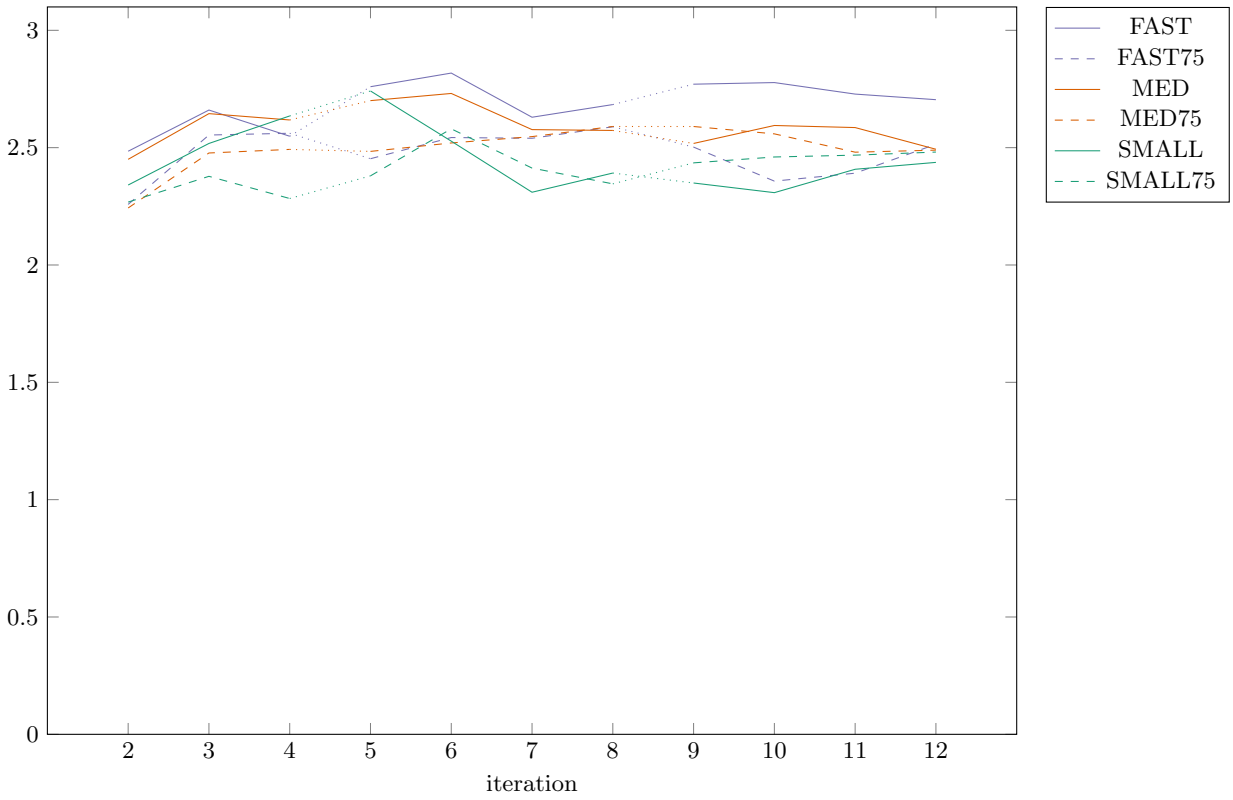

FIGURE 6.3: *NRMSE of the iteration-on-iteration change in trip distance tables for mode taxi.*

increasing trip length stability for all modes except when reducing the fleet size to a number which does not significantly increase the number of fleets that are simulated.

6.2 Trip table stability

Trip length stability should lead to stable trip distributions between TAZs. However, a stable trip distribution could still be skewed towards an average trip length between TAZs, which is not representative of actual trip times. This would cause the gravity model to calibrate towards skewed trips times, which over time will cause the framework to destabilise. The stability of the trip distributions is evaluated on the same criteria as the trip length stability, using the NRMSE of the trip tables. This gives an indication of how much trip distributions change from one iteration to the next.

Figure 6.4 shows the trip stability in terms of the NRMSE between trip tables for the mode *drive*. A reduction in NRMSE is seen between iterations 1 to 4. The large increase at iteration 5 is due to the second parameter calibration. The NRMSE then decreases during iterations 6, 7 and 8 until the next parameter calibration at iteration 9. The NRMSE at iteration 12 is lower than the NRMSE at iteration 9 for MED and SMALL.

The trip stability for the mode *bus* in Figure 6.5 improves until iteration 6. The NRMSE increases between iteration 9 and 12 for the simulations FAST, FAST75 and MED75. On average the NRMSE for the simulations FAST, FAST75, MED, MED75, SMALL and SMALL75 is 174, 151, 156, 160, 135 and 137. Except for the larger fleet size in simulations FAST and FAST75, fixing a portion of trips to a shortest path route is detrimental to trip stability.

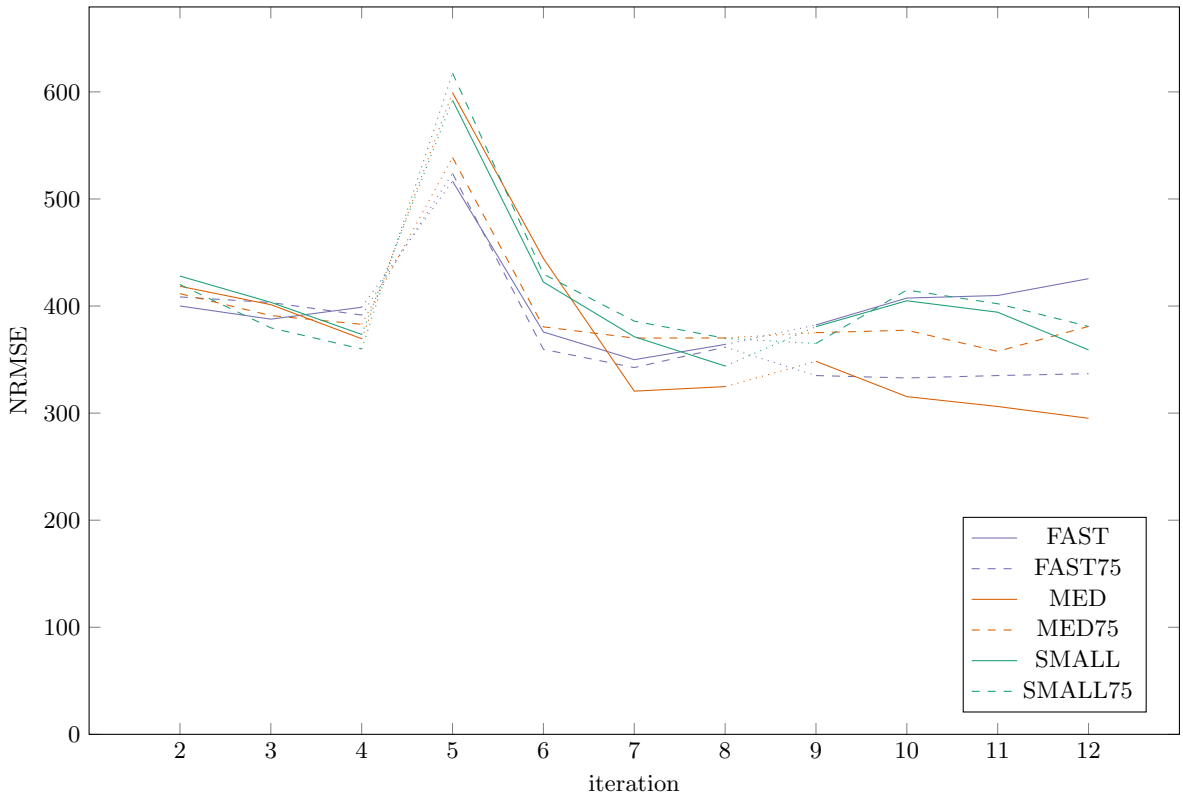

FIGURE 6.4: *Trip table stability for mode* drive.

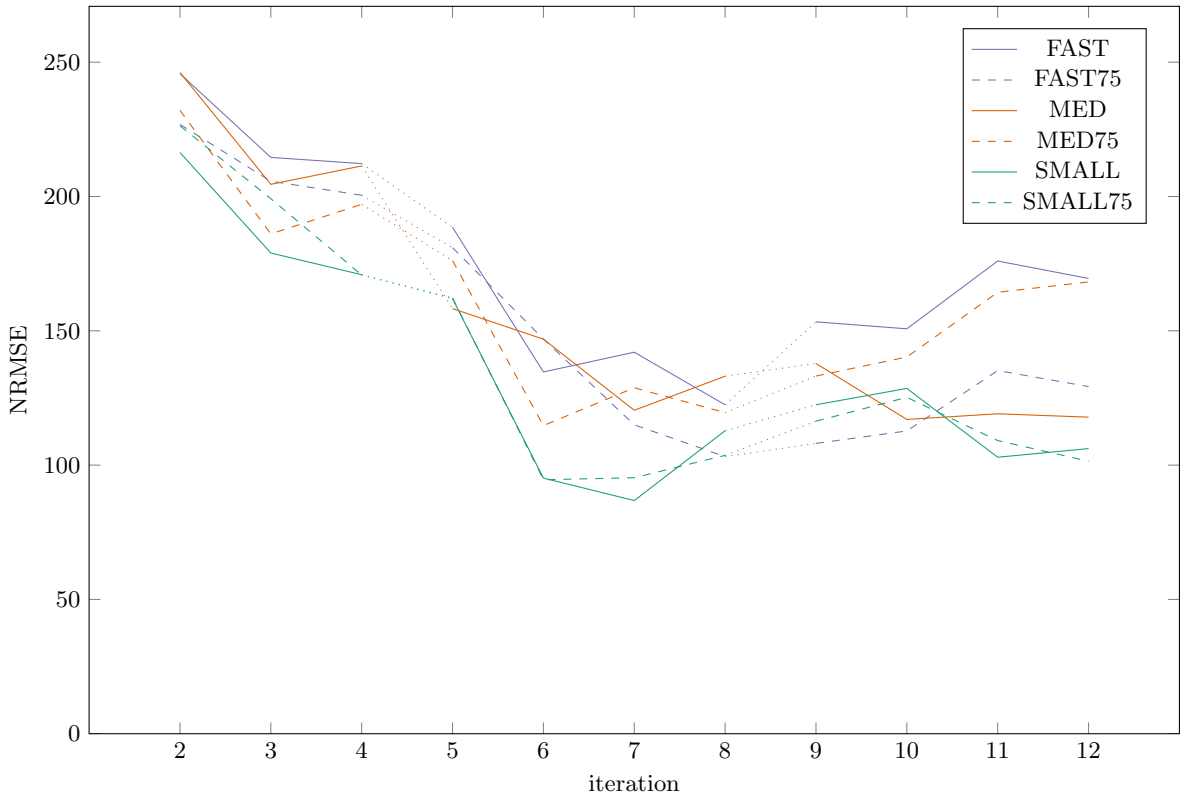

FIGURE 6.5: *Trip table stability for mode* bus.

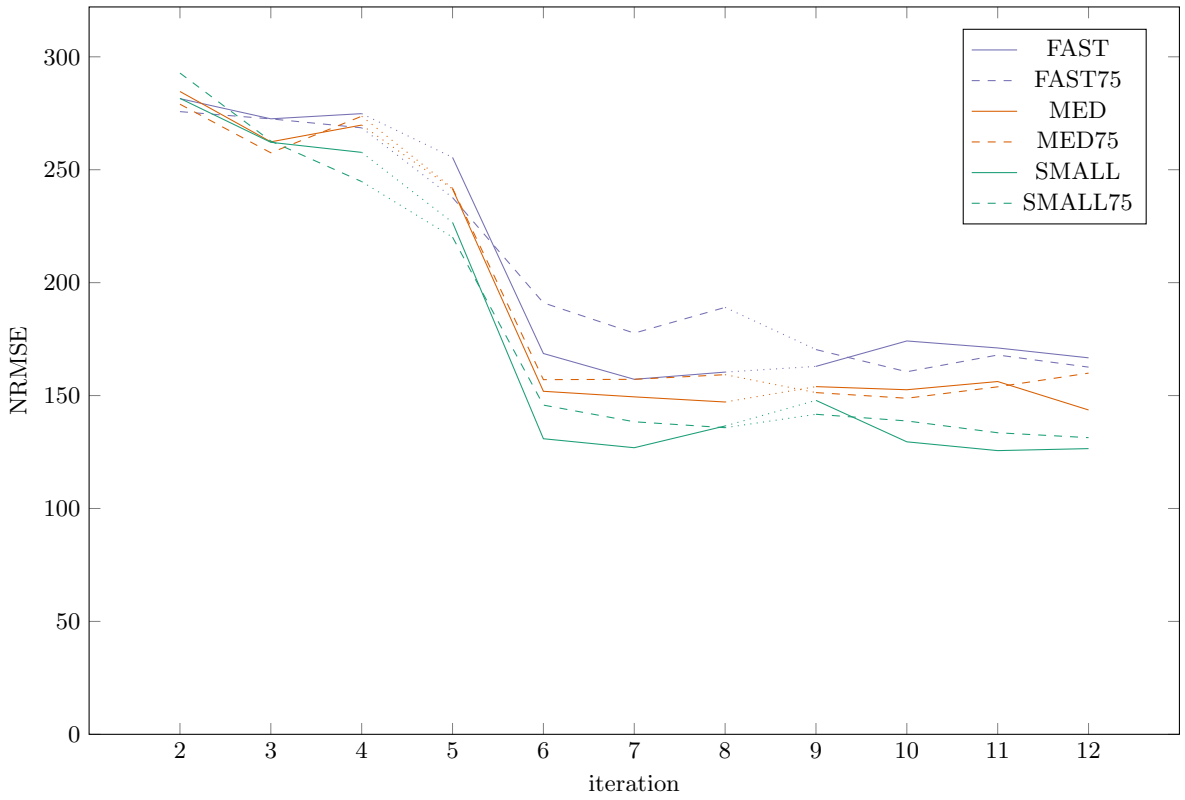

FIGURE 6.6: *Trip table stability for mode* taxi.

The trip distributions stability for the mode *taxi* in terms of the NRMSE in Figure 6.6 shows that like with trip stability for the mode *bus*, on average reducing the fleet size is beneficial for trip stability. With an average of 204 and 207 for simulations FAST and FAST75, the increased stability at larger fleet sizes is absent compared to the other modes. Fixing routes to the shortest path is marginally detrimental to trip stability for the mode *taxi*. The average NMRSE for simulations MED, MED75, SMALL and SMALL75, are 192, 194, 177 and 181, respectively.

The trip table stability should not be interpreted as only a measure for convergence of the trip distributions. It also gives insight into the underlying behaviour on a per mode bases in this instance. A less stable trip distribution means that the process that generated the distribution is more sensitive to changes in trip lengths than a more stable trip distribution. Individuals who drive to work have a larger degree of freedom in their travel choices and where they work. Of the individuals that use public transportation, those who use buses are less constrained in their travel preferences than those using taxis. It is therefore expected that the iterative trip distribution for the mode *drive* should be less stable than for the mode *bus*, which should be less stable than for the mode *taxi*.

6.3 Route convergence

Sensitivity analysis on the route convergence provides insight into how the framework reacts to a change in the fleet size and route decision criteria. If the routes converge to a stable set of network segments, it implies that the routing is nearing an equilibrium. This sensitivity analysis investigates if different parameter settings have an effect on the convergence speed of the trip

routing.

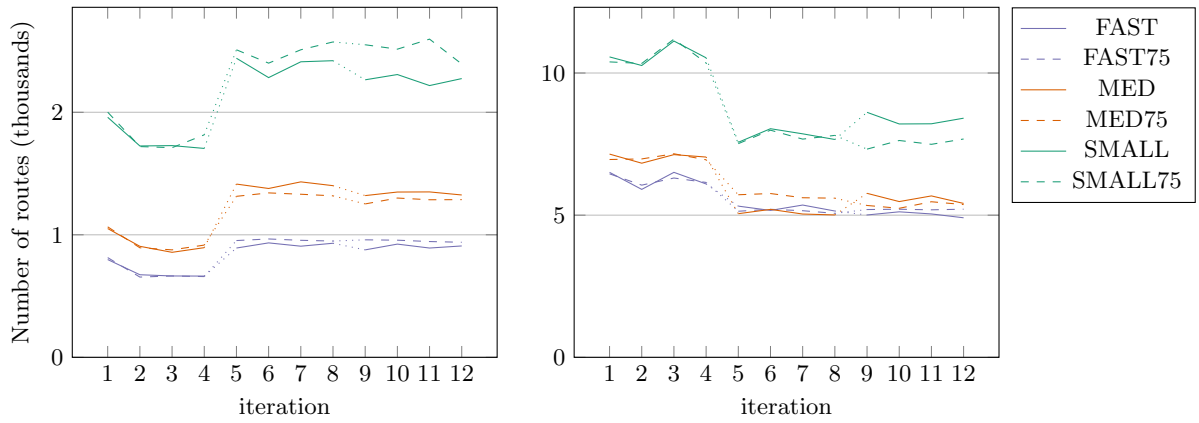

(a) *intra* (b) *inter*

FIGURE 6.7: *Total number of intra- and inter-TAZ routes, given a 50% overlap for the mode* drive.

The number of routes, based on a 50% overlap, is strongly correlated for both inter and intra trips for the mode *drive*. There exists a strong positive correlation between the number of intra routes for all the simulations (15 pairs) with an average R-squared of 0.95 with a standard deviation of 0.02. The inter-TAZ trips are also positively correlated with an average R-squared of 0.9 and standard deviation of 0.06. A negative correlation is observed between the number of inter- and intra-TAZ routes with an average R-squared of 0.85 and standard deviation of 0.07 (36 pairs). Figure 6.7 shows the number of intra- and inter-TAZ routes for each simulation. The fleet size for the mode *drive* does therefore not have a large enough effect on the trip distribution to change the split between inter and intra trips. The route selection parameter does however increase the number of intra-TAZ trips due to the inflated congestion on the shortest distance routes. It also generates more routes due to the higher utilisation of the TAZ connectors.

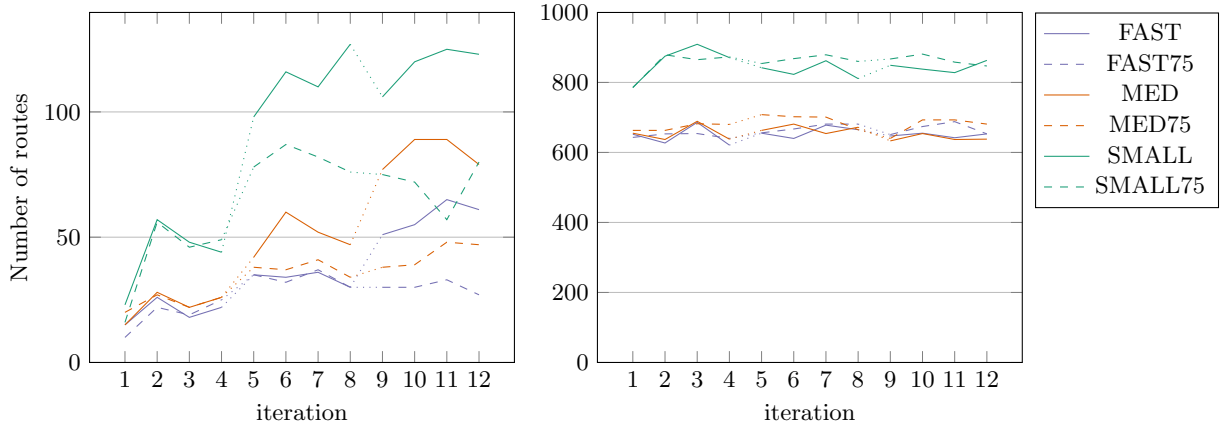

(a) *intra* (b) *inter*

FIGURE 6.8: *Total number of intra- and inter-TAZ routes, given a 50% overlap for mode* bus.

Figure 6.8 increasing the c to 0.25 offsets the effect of a decrease in fleet size for the mode *bus*. The shortest distance distance routed *bus* traffic through congested parts of the network within the TAZ, thereby skewing the average intra trip travel time for the mode. This causes subsequent iterations to have more inter-TAZ routes.

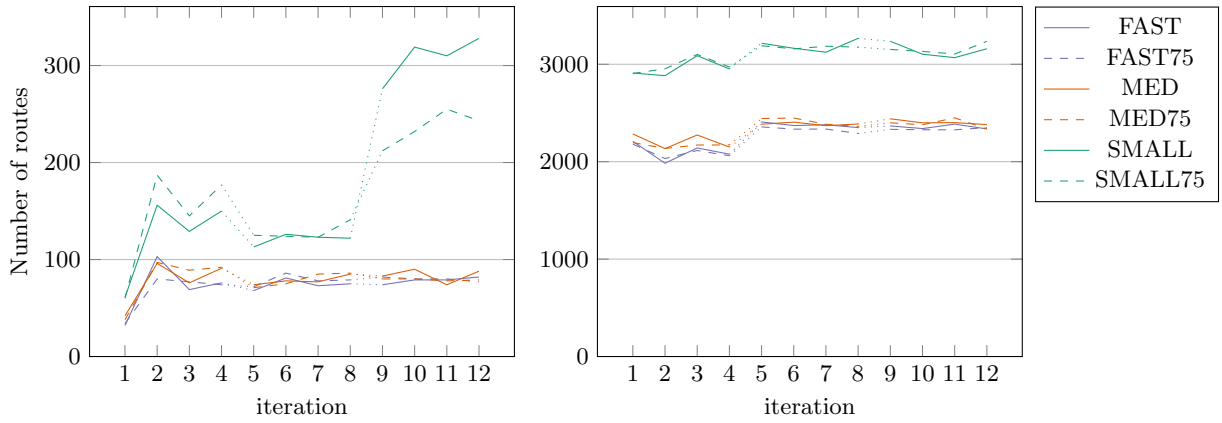

(a) *intra* (b) *inter*

FIGURE 6.9: *Total number of intra- and inter-TAZ routes, given a 50% overlap for the mode* taxi.

The number of *taxi* routes are stable after the second parameter calibration for simulation configurations FAST, FAST75, MED and MED75. The number of intra-TAZ routes increase after the third parameter calibration for simulations SMALL and SMALL75. The increase in fleet size resulted in a calibration of $\alpha_t = 0.75$ for SMALL and $\alpha_t = 0.5$ for SMALL75. Based on the trip table stability sensitivity analysis for the mode *taxi* of the previous section, the higher number of smaller fleets resulted in a less skewed average trip time. The more accurate average trip times translated to the intra-TAZ trip adjustment parameter increase from 0.25 to 0.5 and 0.75 for the simulations SMALL and SMALL75, respectively. The increase in intra-TAZ trips can be seen in Figure 6.9. The number of routes with 10% and 90% overlap can be seen in Figures A.16 to A.21.

Even if the number of routes are stable it is not a sufficient condition for route convergence. The total number of routes might remain the same, but they could be changing location within the network itself. If the routes are converging, then there should be continuity in the set of network segments that these routes are comprised of. To test for this convergence the betweenness centrality for each segment is calculated for every iteration [22]. That is, the number of routes from TAZ i to j that passed through a specific segment. The set Ω is defined as the top 20% of segments with regards to their betweenness centrality and is selected for each iteration, for all combination of TAZs.

These sets of segments are compared by calculating the RMSE^k_{t20} which, given iteration number $k \geq 2$ and betweenness centrality γ^{ka}_{ij} for a segment $a \in \Omega$, the set containing the top 20% of segments can be expressed as,

$$\text{RMSE}^k_{t20} = \sqrt{\sum_i \sum_j \sum_a \frac{(\gamma^{ka}_{ij} - \gamma^{(k-1)a}_{ij})^2}{\sum_i \sum_j \sum_a 1}}. \tag{6.1}$$

Figure 6.10 shows that the edges with the highest total flow volumes are not significantly sensitive to a change in either fleet size or route selection criteria.

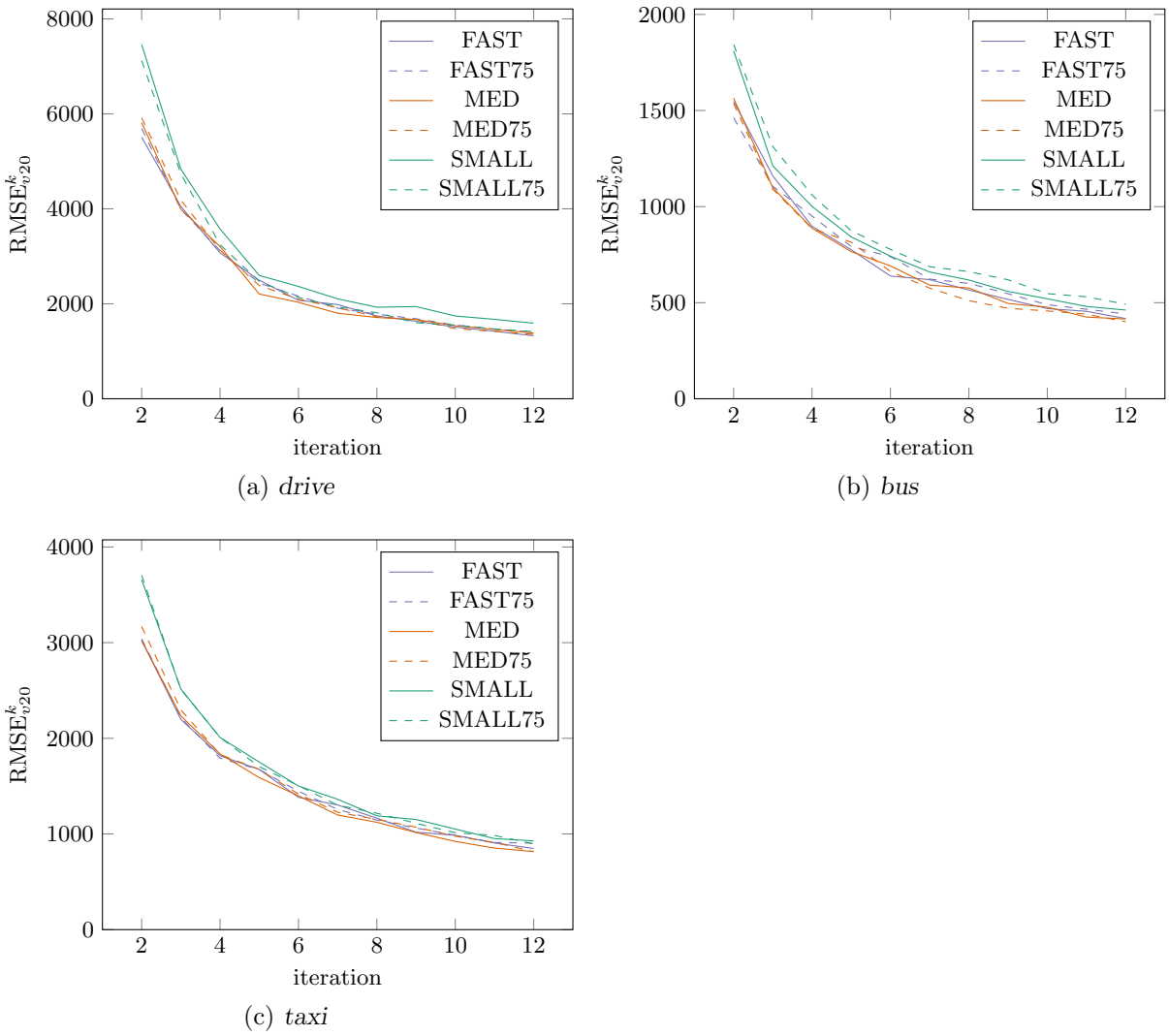

(a) *drive* (b) *bus*

(c) *taxi*

FIGURE 6.10: *RMSE of the on iteration change to the top 20% used edges in terms of flow volumes.*

6.4 Flow analysis

The vehicle counts are compared to the simulated flows for each of the simulations. The average sum of the NRMSE over all the vehicle counting stations are 81.3, 79.2, 72.1, 73.2, 73.8, 68.5 for simulations FAST, FAST75, MED, MED75, SMALL and SMALL75 over all iterations. The sum of the NRMSE over all iterations are 975.4, 950.3, 865.3, 878.6, 885.9, 822.2 for FAST, FAST75, MED, MED75, SMALL and SMALL75. Figure 6.11 shows the sum of the NRMSE over all vehicle counting stations for each iteration.

The iterative process is observable in the difference between the observed counts and the simulated flows which oscillates between higher and lower NRMSE values. Increasing c to 0.25 does increase the accuracy of the flows for the simulations FAST and SMALL. On average, smaller fleet sizes translate to simulated traffic flows that matches traffic count data better.

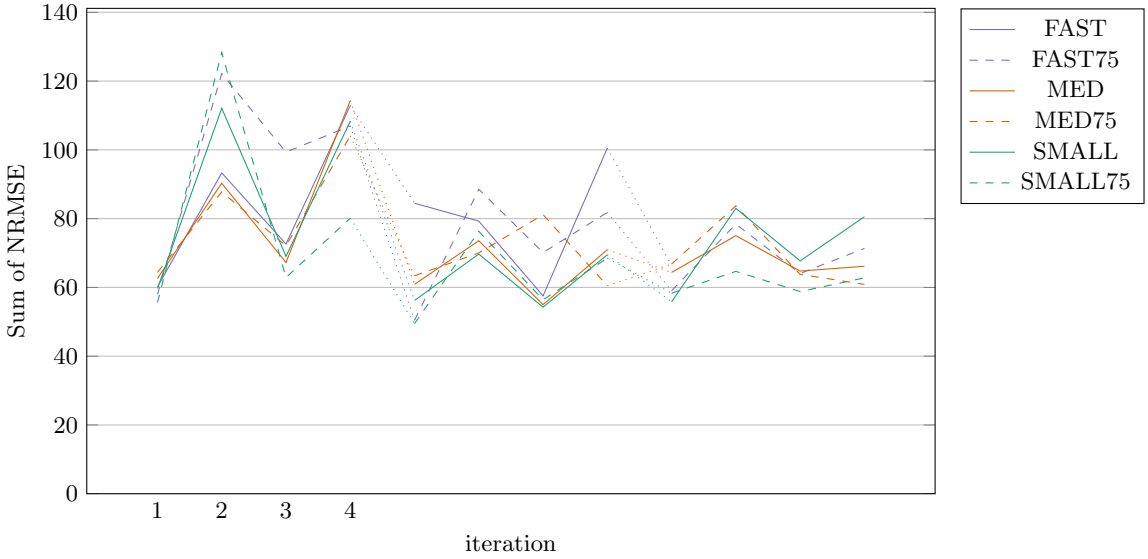

FIGURE 6.11: *The sum of the NRMSE all the vehicle counting stations when compared to the simulated flows of each of the configurations.*

6.5 Departures and arrivals

Figure 6.12 shows that the process that generates the departure times for the trips in the simulation is consistent. There are no significant differences between the departure times for each of the simulation configurations. The arrival distribution for all modes (see Figure 6.12) also does not show any significant differences between the different configurations.

6.6 TLD convergence

The sensitivity analysis has shown that changes to the fleet size and route decision criteria impact the trip distance table and, therefore, the trip distributions. This section evaluates how these changes affected the aggregate trip length distribution of the simulated, compared to the aggregate TLD obtained from the NHTS.

The arrival data for each iteration is compared to the observed TLD for each of the configurations and modes. Figure 6.14 plots the RMSE of each iteration for the mode *drive*. All the RMSE values that are stated hereafter are expressed in terms of 10^{-4} and rounded to the nearest decimal. The average RMSE for the first four iterations are 5.3, 3.8, 4.9, 4.5, 4.1, and 4.3 for the simulations FAST, FAST75, MED, MED75, SMALL and SMALL75. During the first four iterations a smaller fleet size produced a more accurate trip length distribution. Adjusting the route decision criteria from 1 to 0.75 improved the fit of the simulated trips to the observed distribution, except for simulation SMALL and SMALL75, where the adjustment increased the RMSE. This pattern persists through iterations 5 to 8 and 9 to 12. A smaller fleet size consistently leads to a lower RMSE values when $c = 1$ at the final iterations, 4, 8 and 12, before the next parameter calibration.

Figure 6.15 shows the RMSE of the TLD of the simulated traffic compared to the survey data for the mode *bus*. The average RMSE values for the first four iterations for the different parameter sets are, 3, 3.2, 3.2, 3.2, 3.1 and 3.1 and are not significantly different. The fleet size of simulations SMALL and SMALL75 produce higher RMSE values on average during iterations 5 to 8, than

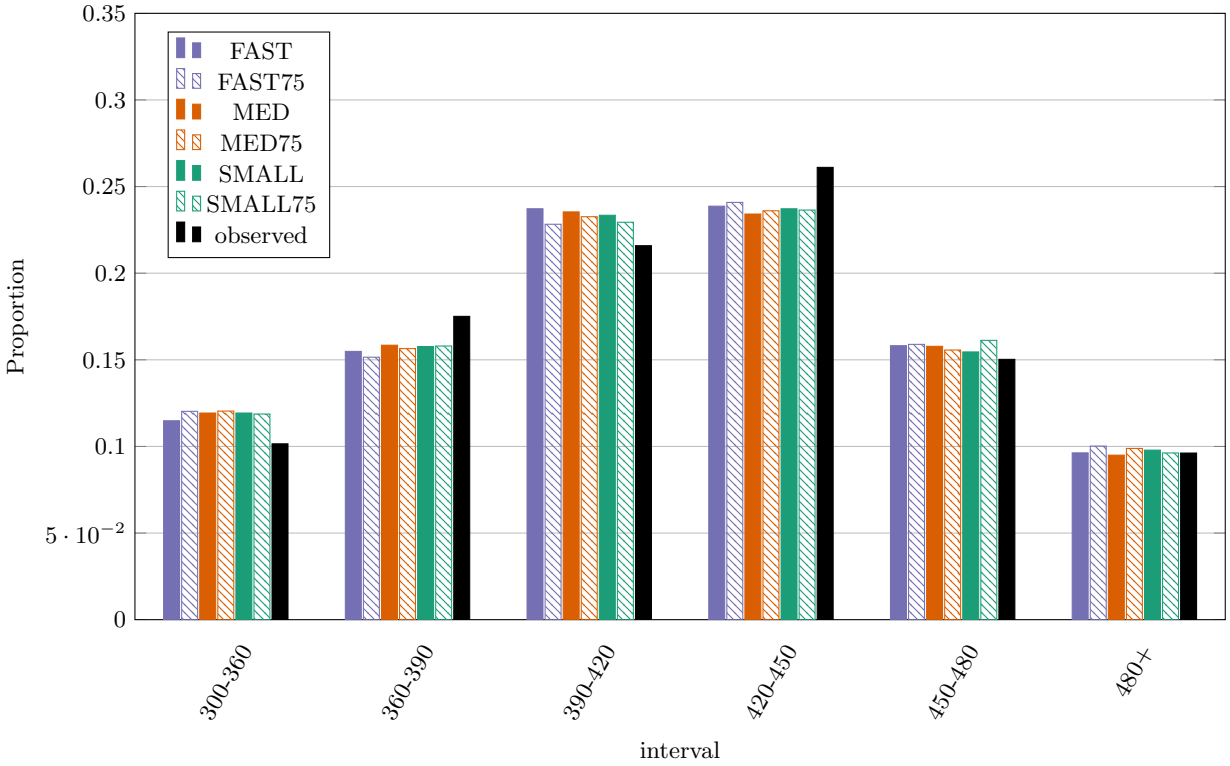

FIGURE 6.12: *A graph of the proportion of departure times for all modes and simulation configurations compared to the observed departure time proportions.*

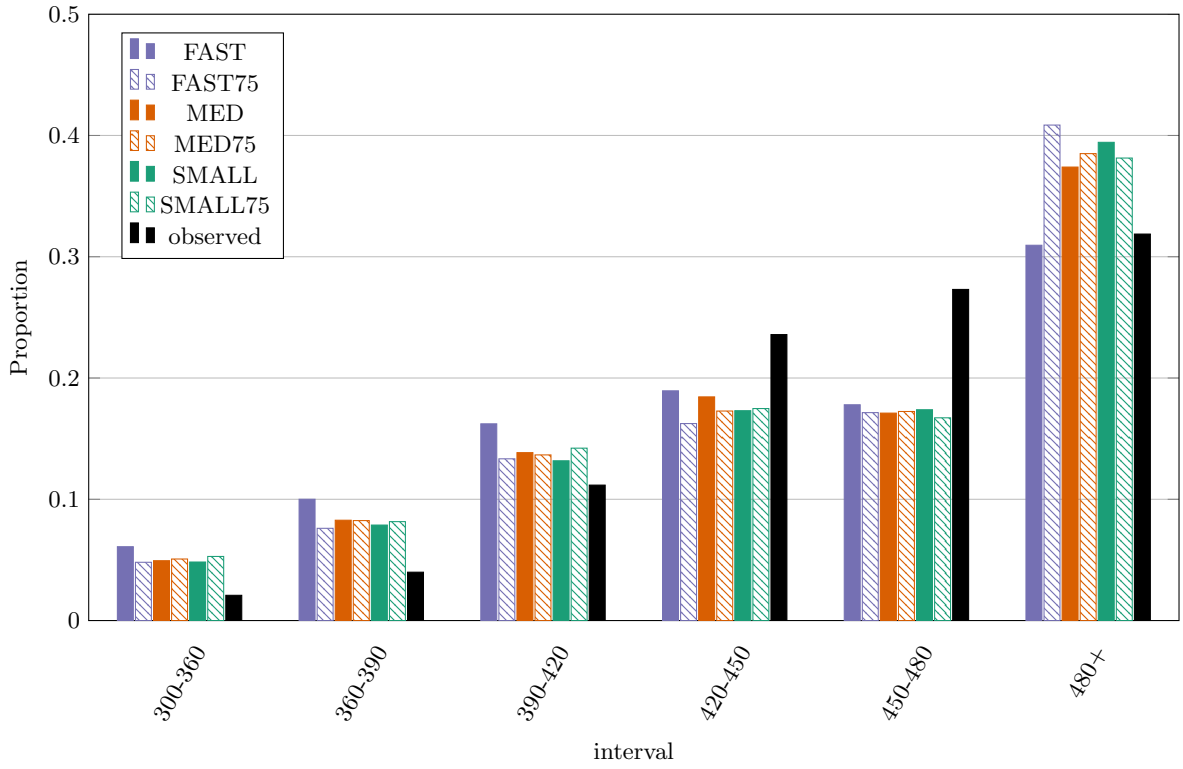

FIGURE 6.13: *A graph of the proportion of arrival times for all modes and simulation configurations compared to the observed arrival time proportions.*

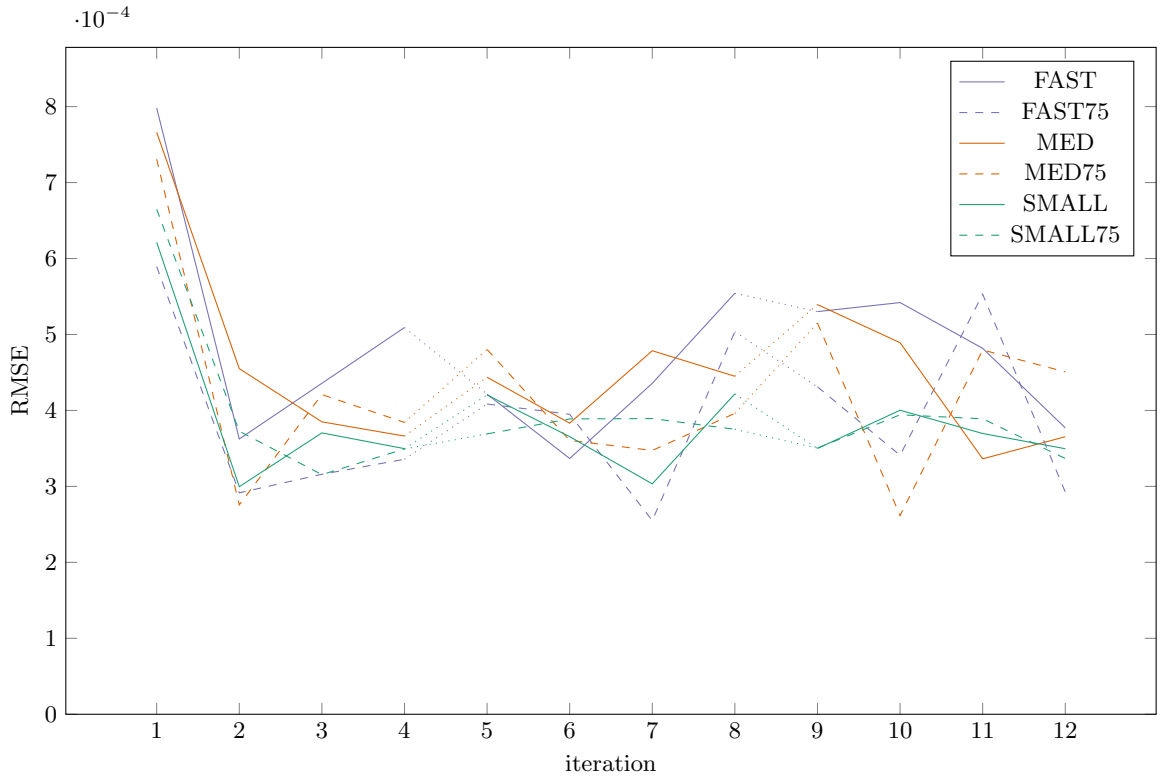

FIGURE 6.14: *A graph of the RMSE between OTLD and the TLD parsed from the arrival data of the traffic simulation data output for the mode* drive.

MED and MED75. The average RMSE for the mode *bus* is 1.7, 1.6, 1.4, 1.4, 1.5 and 1.4 for the simulations FAST, FAST75, MED, MED75, SMALL and SMALL75, respectively. The simulated TLD is not as sensitive to a change in fleet size or route selection criteria for the mode *bus* as *drive*. This is consistent with expectations because most of the trips for the mode *bus* are inter-TAZ trips.

The simulated TLD for the mode *taxi* is influenced by both the fleet size and route decision criteria. The average RMSE of the simulation configurations during iterations one to four are 3.3, 3.2, 3, 2.9, 2.9 and 2.7 for the simulations FAST, FAST75, MED, MED75, SMALL and SMALL75, respectively. A smaller fleet size translates to a more accurate simulated TLD. On average the RMSE during iterations 5 to 8 is 1.9, 2.1, 1.7, 1.8, 1.5 and 1.5. Fixing 25% of the routes to follow the shortest path in terms of edge length has a detrimental effect on the RMSE during this iteration period. After the third parameter calibration the average RMSE for each of the simulations are 1.8. 1.6, 1.5, 1.5, 1.3 and 1.1. This corresponds to the increase in α_t from 0.25 to 0.75 for SMALL and from 0.25 to 0.5 for SMALL75.

6.7 Simulation time scale

The line search procedure takes on average 35 minutes on a Intel i5-4690k (3.5 Ghz) with 8 GB of RAM when the work load of enumerating the parameter space is uniformly spread across its four cores. Solving the gravity model for the Western Cape takes on average 1.5 seconds on a single core. The time it takes the line search procedure will scale linearly with the number of cores available.

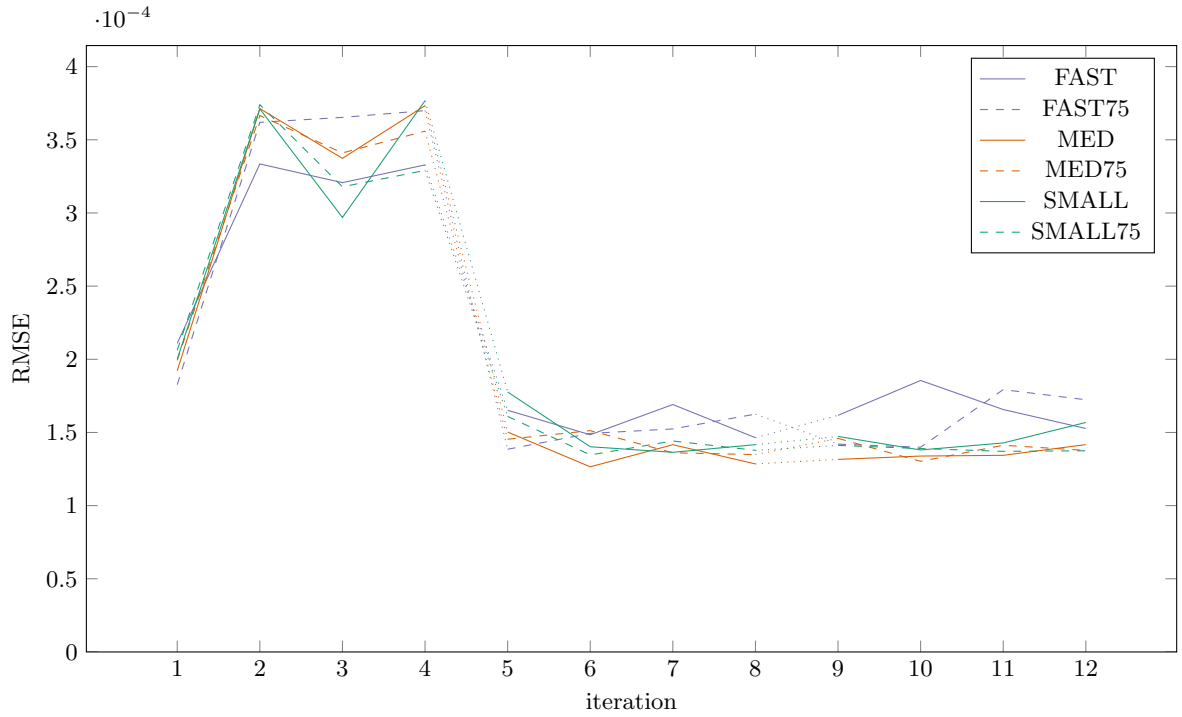

FIGURE 6.15: *A graph of the RMSE between OTLD and the TLD parsed from the arrival data of the traffic simulation data output for the mode* bus.

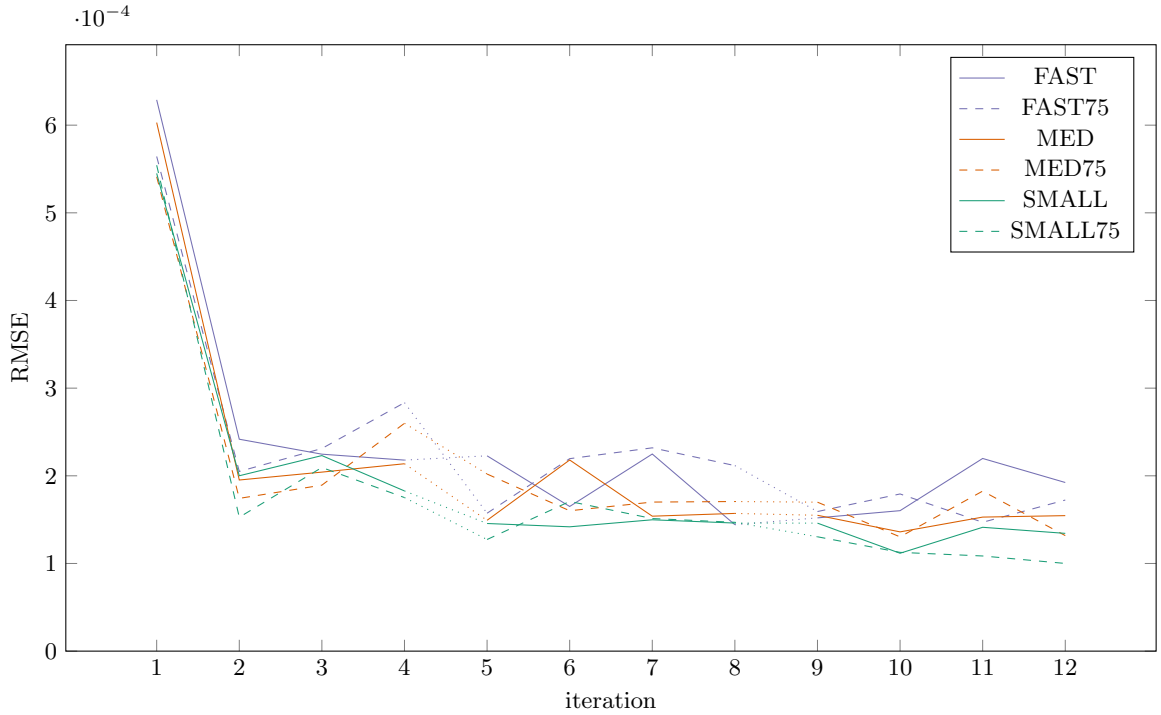

FIGURE 6.16: *A graph of the RMSE between OTLD and the TLD parsed from the arrival data of the traffic simulation data output for the mode* taxi.

Table 6.2 contains the run time and output of the traffic simulation for the different simulation parameter settings. As expected larger fleet sizes, produce less routes and therefore complete faster. The route selection criteria parameter c, has a small effect on simulation run time as well

as the outputs that it produces. The difference in run time between simulations FAST and MED is small due to the relatively small difference in the number of fleets. The simulation routes a tenth of the trips for a time period t before updating the network. The workload of finding the shortest routes through the network is spread over four cores. Once the shortest routes are determined, updating the network by flowing the trips is executed with a single thread.

The flowing dominates finding the shortest paths through the network for the fleet sizes in simulations FAST, FAST75, MED and MED75. As large fleets are split, it creates more fleets that have to be flowed. The time gained in finding the shortest route through the network is eventually lost when the large fleets are broken into smaller fleets. Therefore fleet large fleet sizes (FAST,FAST75) do not reduce the run time to justify the less representative average trip lengths.

Simulation name	Route output file size (MB)	Arrival data file size (MB)	Total average number of fleets	Average time per iteration (minutes)
FAST	113	14.3	22565	56
FAST75	107	14.1	22271	55
MED	142	18.0	28582	58
MED75	145	17.8	28476	62
SMALL	385	52.7	84370	106
SMALL75	398	52.5	84065	105

TABLE 6.2: *The parameter settings for the group sizes used in the the different simulations.*

Decreasing the fleet size to that of the simulation parameters for SMALL and SMALL75 do give marginally beneficial gains to the other metrics discussed in this chapter. However the run times almost double going from MED to SMALL. The average iteration time will increase hyperbolically, up to the upper bound of simulating each trip, as the total average number of fleets increase as fleet sizes are reduced.

6.8 Chapter conclusion

The trip length stability analysis showed that decreasing the fleet size leads to more stable trips. This is in line with expected simulation behaviour. Smaller simulated fleets produce more representative average travel times for both intra-TAZ and inter-TAZ trips. The stability can further be improved by decreasing the route selection parameter c from 1 to 0.75. When a fleet can be routed to the shortest distance path a quarter of the time, it also increases the trip length table stability. The mode *drive* is the most sensitive to a change in fleet size and route selection parameter because it makes up the bulk of PCEs in the network. The mode *taxi* is less sensitive to a change in the parameters than *drive*, but more sensitive than the mode *bus*.

Decreasing the route selection parameter c to 0.75 is only beneficial to trip table stability across all modes for the fleet sizes in configurations FAST and FAST75. The increase in trip length stability did not translate to an increase in trip table stability when the route selection parameter is increased. This is expected because routing a quarter of trips through the shortest distance-route irrespective of congestion, creates more congestion and skews average trip lengths.

The framework is partially sensitive to a change in c. It causes a marginal shift from intra-TAZ trips to inter-TAZ trips for the mode *drive*. The increased congestion caused by routing trips through the shortest distance route, ignoring congestion causes the trips distribution to destabilise. This does not translate to destabilising the split between the number of intra-TAZ and inter-TAZ routes or the route stability, it does however changes at what point the

equilibrium is approached.

Smaller fleet sizes does on average translate to a better match between simulated flows and observed vehicle counts. A decrease in c from 1 to 0.75 lead to more accurate simulated flows for the fleet sizes of FAST and SMALL. This could be an indication that drivers will ignore congestion if it is on the shortest distance route. More likely it could be that the increased levels of congestion produces more accurate traffic flows because it compensates for the absence of traffic from other trip purposes. It should be noted that the marginal accuracy gains of the smaller fleet sizes come at a great computational cost.

The TLD convergence analysis shows that the framework is marginally affected by changes in the fleet size as well as a decrease in c. This means that the framework when used in conjunction with the proposed gravity model is robust enough to find trip distributions such that it reproduces the OTLD for morning peak commuter traffic in the Western Cape. This could lead to less accurate trip distributions if only the TLD or average trip length is considered. It is therefore important that all aspects discussed in this chapter should be taken into consideration when and if the traffic simulation parameters are be calibrated or when traffic modelling is conducted.

This chapter illustrated to what extent the framework is sensitive to changes in route criteria and fleet size parameters. The results and visual output from the framework is discussed in the next chapter.

CHAPTER 7

Results

Contents

The previous chapter contained a sensitivity analysis of the traffic simulator parameters. This chapter contains a discussion of the outputs produced by the framework.

7.1 Visual output

The final simulation output from the Python simulation is inserted into a PostGIS enabled Postgres database. Once in Postgres, the output can be visualised with QGIS.

7.1.1 Routes

Zone 9020 is selected as an example because the trip length distributions, for each mode, as can be seen in Figures A.7, A.8 and A.9 is significantly different.

Figures 7.1,7.2 and 7.3 shows the routes of the trips originating from zone 9020, which is shaded in grey, produced by the traffic simulator, simulating the proposed model from simulation med. The width of the network edges in Figures 7.1(a), 7.2(a) and 7.3(a) are representative of the passenger car equivalents (PCE) for each of the modes. The width of the edges in Figures 7.1(b), 7.2(b) and 7.3(b) are representative of the number of trips. The graphical output highlights how inefficient driving to work alone is in terms of taking up space on the road compared to using public transportation based on the assumption that buses and taxis transport 33 and 15 people, respectively.

The thickness of the lines extend further for the mode *bus*, than for *drive* and *taxi* which is expected based on the fitted density functions in Appendix A. The fitted density function for the mode *bus* have more trips which are 100 minutes or longer. Figures 7.4,7.5 and 7.6 show the routes used by trips destined for zone 9020. From the graphical output it is evident that there

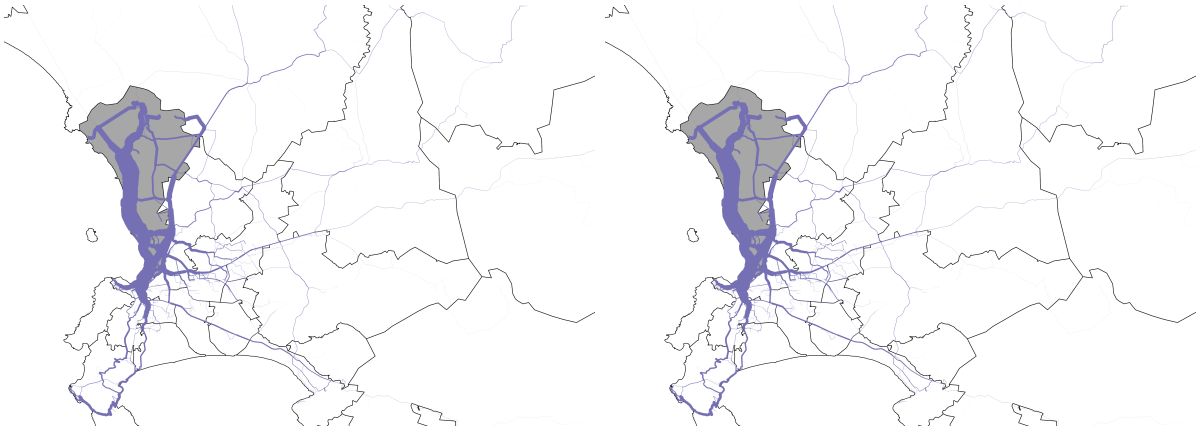

(a) *drive PCE* (b) *drive trips*

FIGURE 7.1: *Graphical output of routes taken from trips originating from zone 9020 mode drive.*

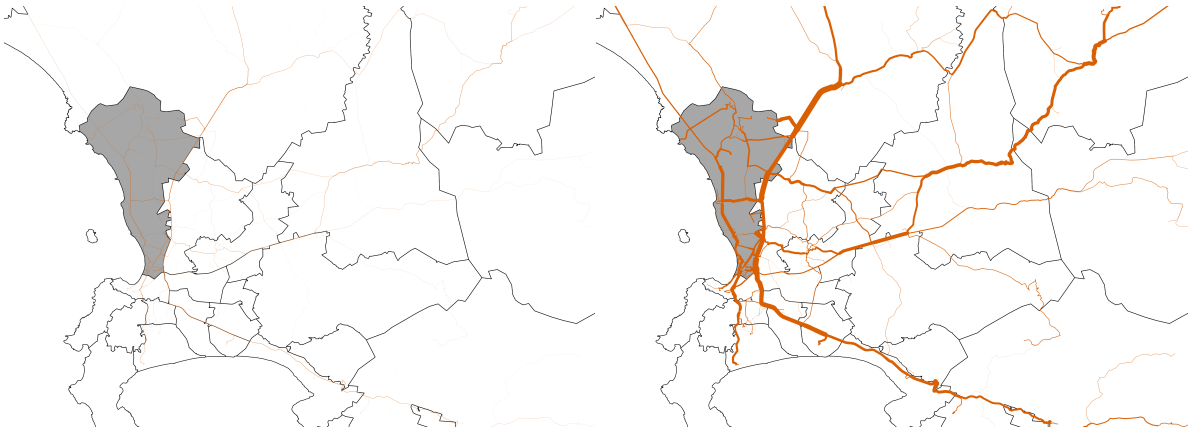

(a) *bus PCE* (b) *bus trips*

FIGURE 7.2: *Graphical output of routes taken from trips originating from zone 9020 mode bus.*

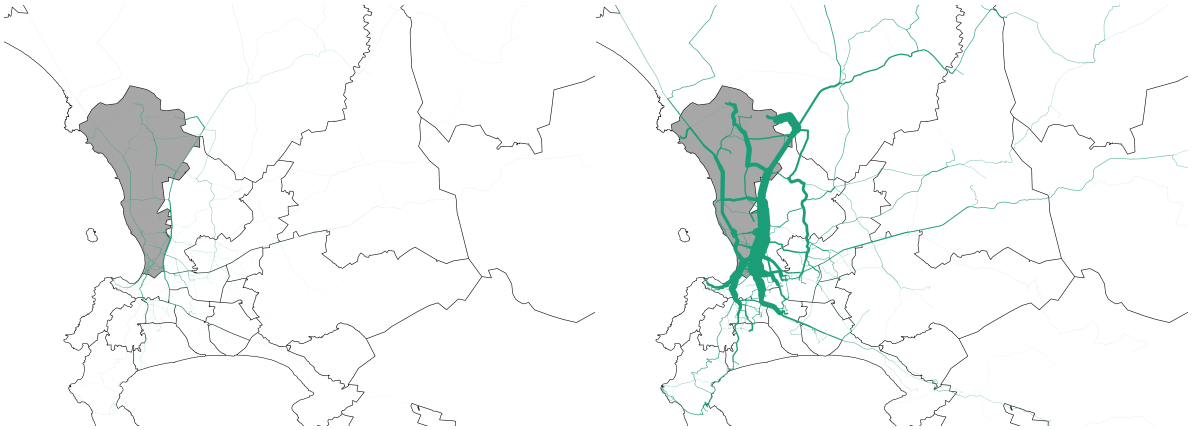

(a) *taxi PCE* (b) *taxi trips*

FIGURE 7.3: *Graphical output of routes taken from trips originating from zone 9020 mode drive.*

are many more trips destined for zone 9020, than leaving it. This is consistent with the input data, Table A.7, which shows that there are 152507 jobs in zone 9020 but only 95295 workers.

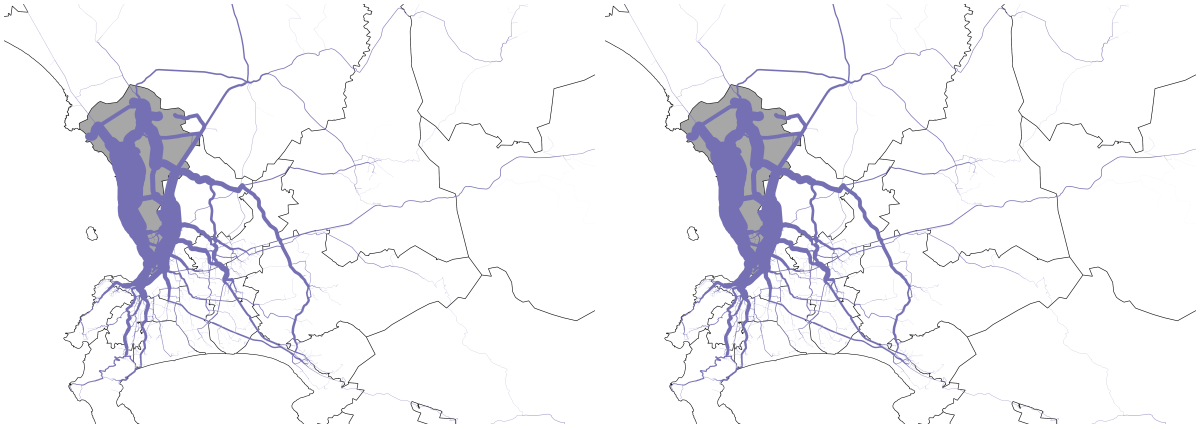

(a) *drive PCE* (b) *drive trips*

FIGURE 7.4: *Graphical output of routes taken from trips destined to zone 9020 for mode drive.*

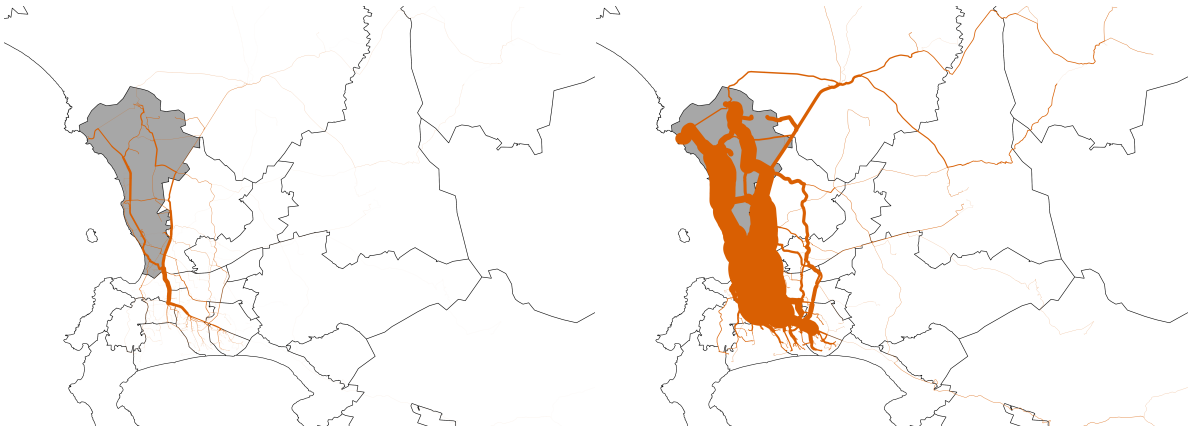

(a) *bus PCE* (b) *bus trips*

FIGURE 7.5: *Graphical output of routes taken from trips destined to zone 9020 for mode bus.*

7.1.2 Congestion

The congestion can be visualised as seen in Figure 7.7. The width of the lines is representative of the flow rate in terms of passenger car equivalents. The colours of the lines represent the level of congestion expressed in terms of the flow rate as a percentage of flow capacity.

Figure 7.8 shows a snapshot of where vehicles are present in the network at the end of an interval. The colours represent how full the edge is and the width indicates how many passenger car equivalents are present on the edge. This highlights the limitations of the traffic simulator which uses vertical queues to model congestion. The congestion would cause a ripple effect downstream causing more roads to be at their physical standing capacity.

The vertical queue sizes in Figure 7.9 represents the scale of congestion. Due to the limitation of the vertical queueing of the traffic simulator, congestion is not propagated back through the network, but queued everywhere when a vehicle arrives at a segment that does not have capacity.

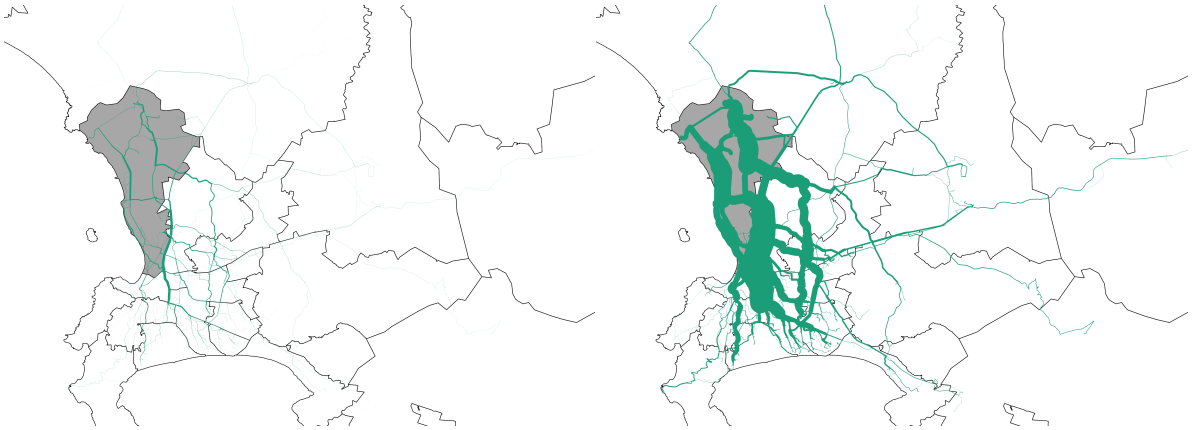

(a) *taxi PCE* (b) *taxi trips*

FIGURE 7.6: *Graphical output of routes taken from trips destined to zone 9020 for mode taxi.*

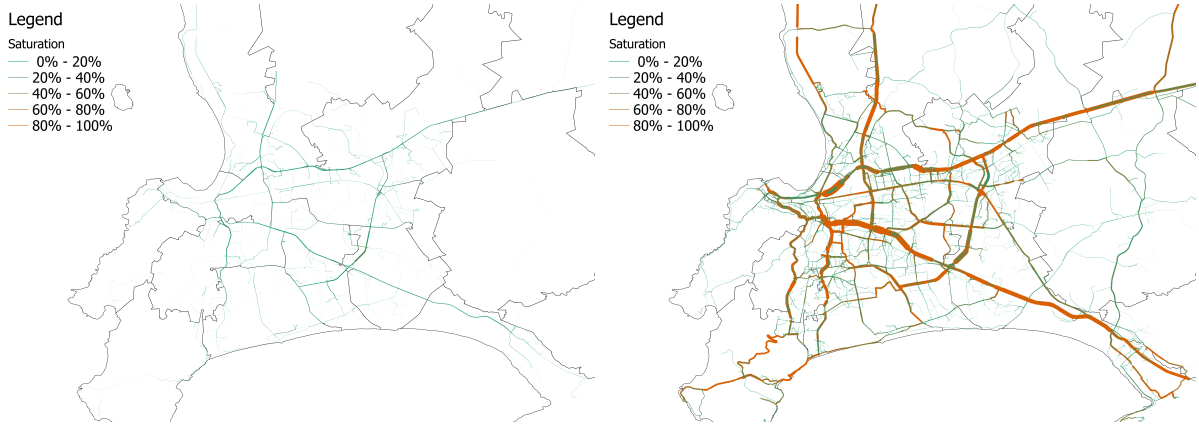

(a) *05:00 - 05:15* (b) *06:00 - 06:15*

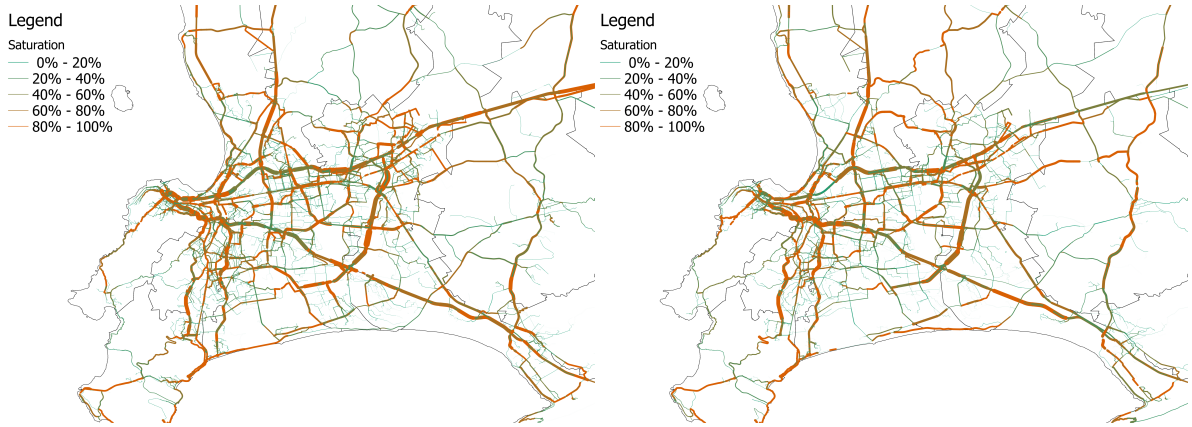

(c) *07:00 - 07:15* (d) *08:00 - 08:15*

FIGURE 7.7: *Traffic flow at 05:00–05:15, 06:00–06:15, 07:00–07:15 and 08:00–08:15.*

This means that vehicles travel through the network until they arrive at a segment that has been fully saturated and is then placed in a queue. These queues then build up over time due to the arrivals outpacing the segment capacity constraints.

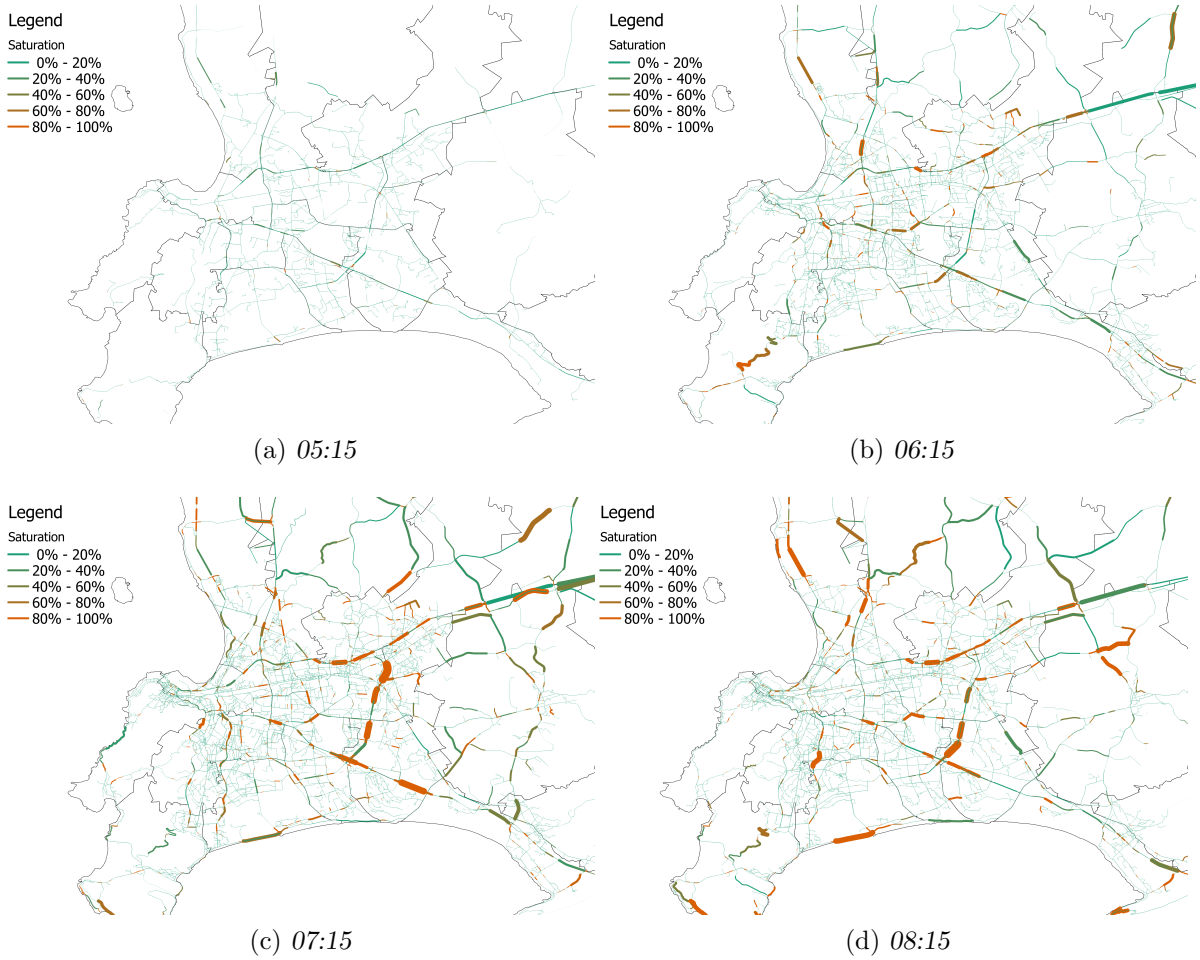

(a) *05:15* (b) *06:15*

(c) *07:15* (d) *08:15*

FIGURE 7.8: *PCE present at 05:00–05:15, 06:00–06:15, 07:00–07:15 and 08:00–08:15.*

7.2 Estimated congestion

The estimated congestion can be calculated by comparing each C_{ij} of the last iteration with the free flow times. The increase in travel time is expressed in terms of a 30 minute trip. For all trips destined for TAZ 9030, Central Cape Town, the estimated congestion can be found in Table 7.1. Trips leaving earlier have to travel further to get to Cape Town, but will eventually get stuck in traffic unless they depart before 05:30. The output of the traffic simulator estimates that trips leaving for ZONE 9030 at 06:30 suffer the effects of congestion the most with an average travel time increase of 72%. This corresponds to the 2015 estimated congestion figure from TomTom [48].

7.3 Chapter conclusion

The results contained in this chapter are an example of the outputs that the framework is capable of producing. It is based on a traffic network built out of assumptions of a very small segment sample size as well as only the input data of the morning commuter traffic, which does not include traffic from other purposes. Despite these shortcomings it accurately estimated the average level of congestion affecting trips destined for the central business district in Cape Town

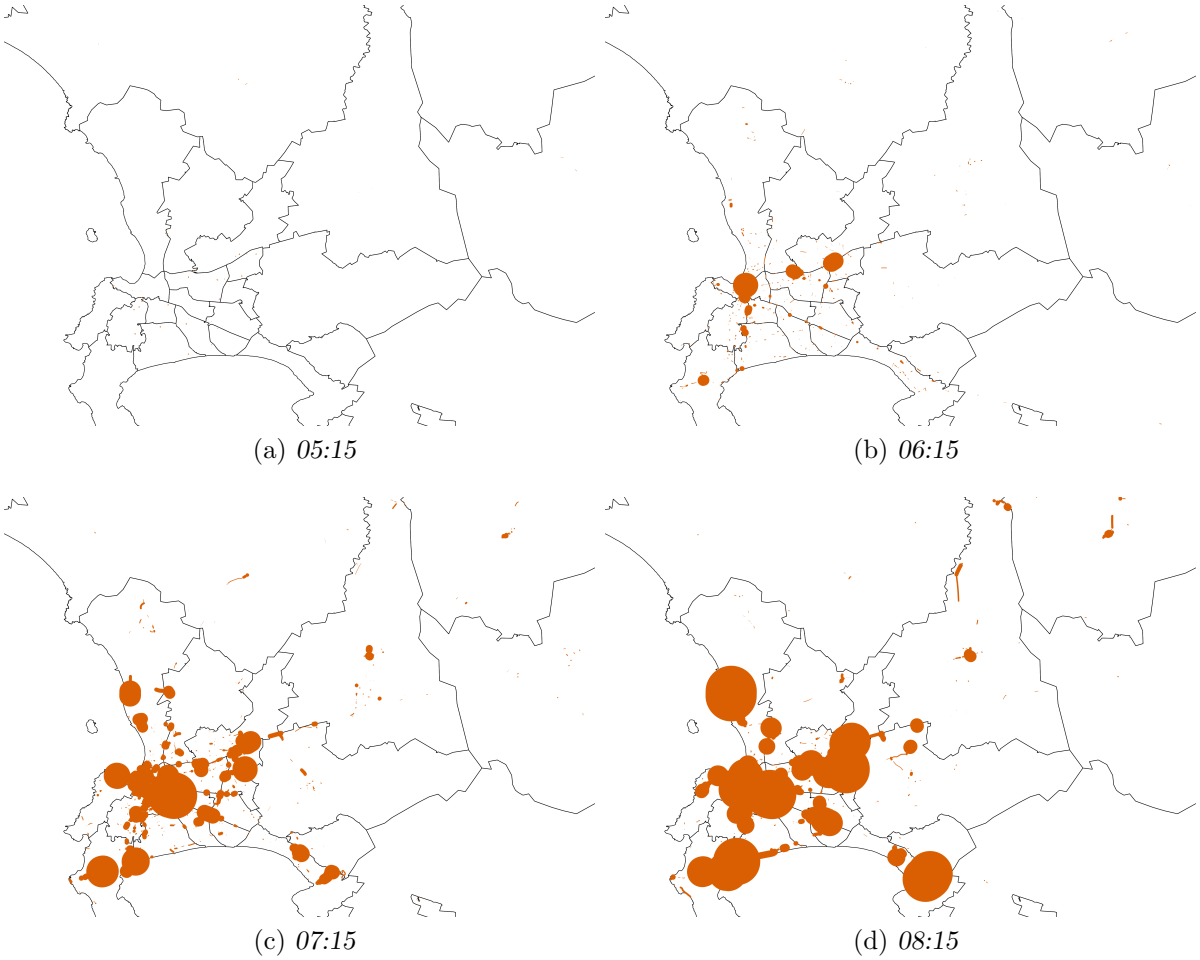

(a) *05:15* (b) *06:15*

(c) *07:15* (d) *08:15*

FIGURE 7.9: *PCE queues at 05:15, 06:15, 07:15 and 08:15.*

	Minutes			Percentage		
Departure time	*drive*	*bus*	*taxi*	*drive*	*bus*	*taxi*
05:30	8.56	8.99	13.55	29%	30%	45%
06:00	17.87	17.9	17.53	60%	60%	58%
06:30	21.66	22.55	22.13	72%	75%	74%
07:00	19.9	22.61	21.45	66%	75%	71%
07:30	19.91	20.45	20.57	66%	68%	69%
08:00	17.15	9.01	18.03	57%	30%	60%

TABLE 7.1: *Estimated average congestion on a 30 minute trip destined for TAZ 9030.*

(TAZ 9030). This can be attributed to the data preparation of the network which consisted of discerning the number of lanes on the national highways and provincial roads through Google Maps satellite imagery.

This chapter is used to show and discuss examples of the output that is produced by the framework. The next chapter serves as the conclusion to the thesis.

CHAPTER 8

Conclusion

Contents

The previous chapter contained a discussion of the outputs of the framework. This chapter summarises the findings of the thesis and serves as its conclusion.

The research conducted in this thesis investigated the feasibility of a scalable traffic modelling framework. It puts forth an extension to the doubly constrained gravity model, traditionally used in the FSM methodology, within a temporally dynamic iterative equilibrium estimation framework.

The thesis introduction in Chapter 1 contains a brief discussion on the concepts of traffic congestion and the nuances associated with transportation modelling. The problem statement in Section 1.3 highlights the importance of accurate transportation modelling: Infrastructure investment based on a misaligned view of congestion could lead to detrimental long term effects. This is the impetus for modelling transportation at a provincial level within the South African context. A more comprehensive framework with regards to the study size, should make it possible to more accurately quantify the up- and down stream of changes caused by a change to infrastructure or worker behaviour. The outputs of such a framework can be used to better inform policy decisions or infrastructure development plans. The following list of objectives served as a guide to construct the framework set forth within this thesis:

- Conduct a literature review on existing transportation modelling methodologies.
- Evaluate available data sources.
- Select and implement a traffic modelling framework.
- Validation of the framework.
- Sensitivity analysis of the framework.
- Conclusions and recommendations.

8.1 Key findings

The first objective is achieved in Chapter 2, which consists of an overview of different methods for modelling transportation. Most of the transportation methodologies do not scale well and one of the key findings of the literature review chapter is that the method for modelling transportation is very data dependent. The framework is therefore limited to be constructed around what data is available for the South African context.

The CSIR GAP, Open Street Map, 2011 National census and 2013 NHTS are identified as the available data sources for modelling South African transportation, and is discussed in Chapter 3. The available data is suitable to use in a disaggregate approach of transportation modelling. The discussion contained in Chapter 3 completes the second thesis objective.

A proposed gravity model is therefore developed by augmenting the doubly constrained gravity model typically used in literature. The augmentations aim to improve the temporal stability, which addresses a critique of the FSM methodology, and intra-TAZ trip attraction, to account for the incompleteness of the 2013 NHTS. The traditional FSM approach fits a impedance of travel function through a calibration process. In order to improve scalability to multiple TAZs, the proposed gravity model uses survey data to construct these impedance of travel function for each TAZ. This proposed model, defined in Chapter 4, is calibrated based on the intra-zonal and temporal parameter space, rather than fitting an impedance of travel function.

Both the traditional and proposed gravity models are implemented for trip distribution and modal split within a FSM framework. The framework uses an iterative, DTA method for route selection and is implemented within a mesoscopic traffic simulator.

The comparative analysis of the two gravity models contained in Chapter 5 also serves as the validation and verification of the framework implementation and completes the fourth thesis objective. The analysis shows that while both models converge, the proposed gravity model produces more accurate trip distributions than that of the traditional gravity model. The trip distributions of the proposed gravity model are also more sensitive to changes in the trip length tables.

The fifth thesis objective is achieved with the sensitivity analysis of the framework to changes in simulation parameters are evaluated in Chapter 6. The framework reacted within expectations of the changes to the fleet size and route selection criteria parameters. Assigning a proportion of routes based on the shortest travel distance increases trip length stability at the cost of destabilising the trip table convergence. The simulated traffic flows that routed a portion of trips through the shortest distance path, where trips are routed irrespective of congestion, were closer to observed traffic flows for a typical week day than the flows produced by simulations routing through the shortest travel time path. It is unclear whether this is a reflection of driver behaviour or an effect of only simulating the morning commuter traffic.

Smaller fleets, or simulating more trips, produce marginally more accurate trip distributions, that matches observed traffic flows better, at a linear cost to computational time and simulation output file size. The average trip lengths in the trip length tables become more representative as more fleets are simulated through the network which translate to more stable trip distributions.

The output obtained from the framework is visualised in a GIS environment in Chapter 7. The framework accurately predicts the level of congestion experienced by commuters destined to the central business district in Cape Town.

The framework constructed within this thesis establishes the precedence of large scale transportation modelling techniques. The recommendations that stem forth from its development are

aimed towards future researchers, current practitioners and transportation authorities. These recommendations fulfil the sixth and final thesis objective.

8.2 Conclusions and recommendations

As urban areas grow larger, it compounds the growing problem of traffic congestion. Changes in infrastructure have up- and down-stream effects, some of which cannot be fully accounted for, due to the limited scope of the traditional transportation modelling approaches. To avoid detrimental infrastructure investment or policy decisions, their impacts need to be assessed on a larger than previously necessary scale, due to the increase in urban population density.

The traditional gravity model is calibrated through finding an impedance of travel function which minimises the difference between the modelled and observed trip length distribution. This means that the same impedance of travel function, or underlying travel behaviour, is used to model the trip distribution for each TAZ. This approach does not scale well. A larger study area means there are more potential differences in travel behaviour from one TAZ to another.

The framework put forth in this thesis establishes a precedence for the viability of large scale transportation modelling. The proposed gravity model leverages the same survey data to produce temporally and spatially adjusted trip distributions that are more accurate than that of the traditional gravity model. The proposed gravity model requires an impedance of travel function to be fitted and fixed for each TAZ. It then calibrates the temporal adjustment and intra-zonal attraction parameters to find a parameterisation, that when the trip distributions for each TAZ is aggregated it, adds up to the observed aggregate travel behaviour. This is a fundamental paradigm shift wherein each TAZ's trip length distribution is preserved as opposed to each zone being assigned the same impedance of travel function that, when used to distribute trips, produces a similar aggregate TLD to that of the observed TLD. The proposed gravity model therefore improves upon the scalability of modelling methodologies based on a doubly constrained gravity model.

The use of large scale transportation modelling, based on a DTA approach, is recommended as an integral tool to assist practitioners. It provides a robust framework with which the potential up and down stream impacts of large infrastructure investments or to guide policy decisions regarding transportation can be evaluated. In addition, because transportation modelling is data dependent, it is recommended that:

- Researchers should further investigate and refine large scale transportation modelling techniques. Urban population density is forecast to increase, which will compound the up and down stream effects of changes to infrastructure or policy. Effective techniques should be available to evaluate these impacts.
- Practitioners should avoid an one size fits all or black box approach to transportation modelling. A fundamental understanding of the transportation modelling techniques, their limitations and data requirements should inform the selection of a suitable transportation modelling methodology.
- Transportation authorities should maintain a detailed spatial database of all transportation infrastructure. A central database containing the physical attributes of the transportation network and other related data will facilitate the implementation of more accurate transportation modelling.

8.3 Future work

The framework, as it is implemented in this thesis, is not sufficient to evaluate policy decisions or infrastructure investment, as it only incorporates people travelling to work during the morning peak. In order to measure the effect of increased public transportation, all instances of travel should be incorporated into the framework. This includes commercial vehicles (heavy and light), scholars/students travelling to school/academic institutions, as well as travel related to recreational purposes. Bus stops and taxi ranks should also be incorporated in to the TAZ connector selection.

8.3.1 Breadth-wise

Given that the road network data is accurate enough in terms of capacity and types of facilities, and that the traffic simulator is enhanced to incorporate horizontal queues spilling backwards, the framework developed in this thesis can be used to:

- estimate and forecast through traffic and the split between inter zonal travel per TAZ for more detailed single TAZ micro simulation models,
- determine specific routes between travel analysis zones that can be used for methods than have a proven equilibrium,
- measure congestion given that all reasons and modes for travelling are incorporated,
- estimate vehicular emissions,
- evaluate the effect of additional road capacity and
- investigate the effect of a shift from private to public transportation on congestion.

8.3.2 Depth-wise

The line search procedure used in this thesis to determine the gravity model parameters can be improved upon by means of an algorithm that dynamically searches the parameter space. A directed search method could be a more efficient than uniformly sampling the parameter space and could produce parameters that lead to more accurate trip distributions.

8.4 Chapter conclusion

The proposed gravity model put forth in this thesis aims to improve the scalability of disaggregate traffic demand modelling. It produces trip distributions that are more accurate than the traditionally used gravity model, within the framework presented in this thesis. Although it requires fitted kernel density functions from survey data to define unique impedance of travel functions for each TAZ, it improves the scalability of the doubly constrained gravity model.

References

[1] Abdel–Aal, M, 2014, *Calibrating a trip distribution gravity model straitified by the trip purposes for the city of Alexandria*, Alexandria Engineering Journal, **53(3)**, pp. 677–689.

[2] Akcelik, R, 2003, *Speed-Flow Models for Uninterrupted Traffic Facilities*, [online], [cited 2014-07-16], Available from `http://www.sidrasolutions.com/documents/AA_SpeedFlow Models_UninterruptedFacilities.pdf`.

[3] Alfa, AS, 1989, *Incremental stochastic model for the temporal distribution of peak traffic demand*, Mathematical and Computer Modelling, **12(8)**, pp. 1048.

[4] Arentze, TA and Timmermans, HJP, 2000, *ALBATROSS – A learning-based transportation oriented simulation system*, [online], [cited 2014-12-05], Available from `http://www.nctcog.org/trans/modeling/nextgeneration/Albatross.pdf`.

[5] Bellei, G, Gentile, G, and Papola, N, 2005, *A within-day dynamic traffic assignment model for urban road networks*, Transportation Research Part B, **39(1)**, pp. 1–29.

[6] Botha, H and Mikros Traffic Monitoring (Pty) Ltd, 2012, *SANRAL Traffic Count Information Mega Yearbook 2011*, Enquiries to: Mr G Ackermann, 012-844 8000.

[7] Braess, D, 2005, *On a Paradox of Traffic Planning*, INFORMS, **39(4)**, pp. 446–450.

[8] Britton, H, 1994, *The Real Issues Concerning Lee's Requiem*, Journal of the American Planning Association, **60(1)**, pp. 31–34.

[9] Celik, HM, 2010, *Sample size needed for calibrating trip distribution and behaviour of the gravity model*, Journal of Transport Geography, **18(1)**, pp. 183–190.

[10] Centre for Economics and Business Research, 2014, *The future economic and environmental costs of gridlock in 2030*, [online], [cited 2014-12-04], Available from `http://www.cebr.com/wp-content/uploads/2014/10/INRIX_costs-of-congestion_Cebr-report_v5_FINAL.pdf`.

[11] Chiu, Y, Bottom, J, Mahut, M, Paz, A, Balakrishna, R, Waller, T, and Hicks, J, 2011, *Dynamic Traffic Assignment: A primer*, [online], [cited 2014-03-07], Available from `http://onlinepubs.trb.org/onlinepubs/circulars/ec153.pdf`.

[12] Depolo, V and Jovic, J, 2011, *The role of trip generation models in sustainable transportation planning in South-East Europe*, Transport, **26(1)**, pp. 88–95.

[13] Dijkstra, EW, 1959, *A Note on Two Problems in Connexion with Graphs*, Numerische Matimatik, **1(1)**, pp. 269–271.

[14] Douglass, LB, 1973, *Requiem for Large-Scale Models*, Journal of the American Institute of Planners, **39(3)**, pp. 163–178.

[15] Duranton, G and Turner, MA, 2011, *The Fundamental Law of Road Congestion: Evidence from US Cities*, American Economic Review, **101(6)**, pp. 2616–52.

[16] Ettema, D, Borgers, A, and Timmermans, H, 1994, *Simulation Model of Activity Scheduling Behaviour*, [online], [cited 2014-12-05], Available from `http://alexandria.tue.nl/repository/freearticles/589547.pdf`.

[17] Evans, AW, 1970, *Some properties of trip distribution methods*, Transportation Research, **4(1)**, pp. 19–36.

[18] Evans, AW, 1970, *The calibration of trip distribution models with exponential or similar cost functions*, Transportation Research, **5(1)**, pp. 15–38.

[19] Evans, SP and Kirby, HR, 1974, *A Three-dimensional furness procedure for calibrating gravity models*, Transportation Research, **8(2)**, pp. 105–122.

[20] Faghri, A, Aneja, S, and Vaziri, M, 1999, *Estimation of percentage of pass–by trips generated by a shopping center using artificial neural networks*, Transportation Planning and Technology, **22(4)**, pp. 271–286.

[21] Foundation, PS, 2014, *Python Language Reference, version 3.4*, URL: `http://www.python.org`.

[22] Freeman, LC, 1977, *A Set of Measures of Centrality Based on Betweenness*, Sociometry, **40(1)**, pp. 35–41.

[23] Friesz, TL, Bernstein, D, Smith, TE, Tobin, RL, and and, BWW, 1993, *A variational inequality formulation of the dynamic network user equilibrium problem*, Operations Research, **41(1)**, pp. 179–191.

[24] Friesz, TL, Luque, FJ, Tobin, RL, and and, BWW, 1989, *Dynamic network traffic assignment considered as a continuous time optimal control problem*, Operations Research, **37(1)**, pp. 893–901.

[25] Gardner, B and TRANSIMS, 2014, *Transportation Analysis and Simulation*, [online], [cited 2014-12-05], Available from `http://sourceforge.net/projects/transims/`.

[26] Garling, T, Kwan, M, and Golledge, RG, 1994, *Computational-process modelling of houshold activity scheduling*, Transportation Research Part B, **28(5)**, pp. 355–364.

[27] Garling, T, Kwan, M, and Golledge, RG, 1991, *Computational-Process Modelling of Travel Decisions: Review and Conceptual Analysis*, [online], [cited 2013-03-15], Available from `http://www.uctc.net/research/papers/209.pdf`.

[28] Gentile, G, Velona, P, and Cantarella, GE, 2014, *Uniqueness of stochastic user equilibrium with asymmetric colume-delay functions for mergin and diversion*, EURO Journal on Transport and Logistics, **3(4)**, pp. 309–331.

[29] GmbH, G, 2013, *GeoFabrik OSM Extract*, [online], [cited 2013-08-07], Available from `http://http://www.geofabrik.de//`.

[30] Golob, TF and McNally, MG, 1997, *A model of activity participation and travel interactions between household heads*, Transportation Research Part B, **31(3)**, pp. 177–194.

[31] Hagerstrand, T, 1970, *What about people in Regional Science?*, Regional Science Association Papers, **24(1)**, pp. 7–21.

[32] HJ, S, 1995, *South African Trip Generation Rates, Report PR92/228*, 2nd Edition, Department of Transport, Chief Directorate.

[33] Huntsinger, L, Rouphail, N, and Bloomfield, P, 2013, *Trip Generation Models Using Cumulative Logistic Regression*, Journal of Urban Planning and Development, **139(3)**, pp. 176–184.

[34] Institute of Transportation Engineers, 2008, *Trip Generation: an ITE international report*, Edition, Institute of Transportation Engineers, Washington (DC).

[35] Krygsman, S, de Jong, T, and Nel, J, 2009, *Functional transport regions in South Africa: An examination of national commuter data*, Proceedings of the 28th Southern African Transport Conference, pp. 144–154.

[36] Lo, HK and Tung, YK, 2003, *Network with degradable links: capacity analysis and design*, Transportation Research Part B, **37(4)**, pp. 345–363.

[37] Martin, BV, Memmott, FW, and Bone, AJ, 1965, *Principles and techniques of predicting future demand for urban area transportation*, M.I.T. Press, Cambridge (Mass).

[38] McNally, MG and Rindt, CR, 2007, *The Activity-Based Approach*, [online], [cited 2014-12-03], Available from `http://www.its.uci.edu/its/publications/papers/CASA/UCI-ITS-AS-WP-07-1.pdf`.

[39] Naude, A, Badenhorst, W, Zietsman, L, Huyssteen, EV, and Maritz, J, 2007, *Geospatial Analysis Platform – Version 2: Technical overview of the mesoframe methodology and South African Geospatial Analysis Platform. CSIR Report number: CSIR/BE/PSS/IR/2007/0104/B.*

[40] Ortuzar, JDD and Willumsen, LG, 2011, *Modelling Transport*, Edition, Wiley, Chichester West Sussex United Kingdom.

[41] Plummer, AV, 2012, *The Chicago area transportation study: Creating the First Plan*, [online], [cited 2013-12-03], Available from `http://www.surveyarchive.org/Chicago/cats%5C_1954-62.pdf`.

[42] Recker, WW, McNally, MG, and Root, GS, 1986, *A model of complex travel behaviour: Part I – Theoretical development*, Transportation Research Part A, **20(4)**, pp. 307–318.

[43] Recker, W, 1994, *The Household Activity Pattern Problem: General formulation and solution*, Transportation Research Part B, **29(1)**, pp. 61–77.

[44] StatsSA, 2013, *2011 National Census*, [online], [cited 2014-08-10], Available from `http://interactive.statssa.gov.za/superweb/login.do`.

[45] StatsSA, 2013, *National Household Travel Survey 2013*, Available on CD-ROM, requestable from info@statssa.gov.za.

[46] Sumalee, A and Xu, W, 2011, *First-best marginal cost toll for a traffic network with stochastic demand*, Transportation Research Part B, **45(1)**, pp. 41–59.

[47] Texas Transportation Institute, 1997, *Activity-Based Travel Forecasting Conference, New Orleans, Louisiana, June 2-5, 1996. Summary, recommendations, and compendium of papers*, [online], [cited 2013-04-06], Available from `http://ntl.bts.gov/lib/11000/11400/11469/006848.pdf`.

[48] TomTom, 2015, *TomTom Traffic Index*, [online], [cited 2015-06-03], Available from `http://www.tomtom.com/en_za/trafficindex/`.

[49] United Nations, 2015, *World Urbanization Prospects The 2014 Revision*, ST/ESA/SER.A/366, URL: `http://esa.un.org/unpd/wup/Publications/Files/WUP2014-Report.pdf`.

[50] (US), NRC, 2010, *HCM 2010: Highway Capacity Manual*, [online], [cited 2013-02-16], Available from `http://www.hcm2010.org/`.

[51] USDOT, 2014, *TRANSIMS – background*, [online], [cited 2014-12-05], Available from `https://www.fhwa.dot.gov/planning/tmip/resources/transims/`.

[52] Vaingast, S, 2014, *im2graph*, [online], [cited 2014-07-15], Available from `http://im2graph.co.il/`.

[53] Vrtic, M, Frohlich, P, Schussler, N, Axhausen, KW, Lohse, D, Schiller, C, and Teichert, H, 2007, *Two-dimensionally constrained disaggregate trip generation, distribution and mode choice model: Theory and application for Swiss national model*, Transportation Research Part A, **41(1)**, pp. 857–873.

[54] Wardrop, JG, 1952, *Some theoretical aspects of road traffic research*, Proceedings of the ICE - Civil Engineering: Engineering Divisions, Part II, pp. 325–362.

[55] Watling, D, 2002, *A second order stochastic network equilibrium model, I: theoretical foundation*, Transportation Science, **36(2)**, pp. 149–166.

[56] Weiner, E, 1992, *Urban Transportation Planning in the United States: An Historical Overview*, 2nd Edition, US Department of Transportation, Washington (DC).

[57] Williams, I, 1976, *A Comparison of some calibration techniques for double constrained models with an exponential cost function*, Transportation Research, **10(2)**, pp. 91–104.

[58] Zhang, C, Chen, X, and Sumalee, A, 2011, *Robust Wardrop's user equilibrium assignment under stochastic demand and supply: Expected residual minimization approach*, Transportation Research Part B, **45(3)**, pp. 543–552.

[59] Zhang, K and Mahmassani, H, 2008, *A Probit-based time-dependent stochastic user equilibrium traffic assignment mode*, [online], [cited 2013-03-10], Available from `http://www.transportation.northwestern.edu/docs/2008/2008.01.31.Zhang.Paper.pdf`.

[60] Zhou, Z and Chen, A, 2008, *Comparitive analysis of three user equilibrium models under stochastic demand*, Journal of Advanced Transportation, **42(3)**, pp. 239–263.

[61] Zhou, Z and Chen, A, 2010, *The alpha-reliable mean-excess traffic equilibirum model with stochastic travel times*, Transportation Research Part B, **44(4)**, pp. 493–513.

Appendices

APPENDIX A

Auxiliary formulas figures and graphs

Given the parameters in Table A.1,

Symbol	Definition
T_F	Length of simulation time frame
v_f	Free-flow speed
Q	Capacity
k_n	Density at capacity
v_n	Speed at capacity
t_f	Free-flow travel time
t_n	Travel time at capacity
d_n	Traffic delay at capacity
h_n	Average headway at capacity
L_n	Average spacing at capacity
q_o	Flow limit for free-flow speed
x_o	Saturation below which speed equals free-flow speed
q_a	Number of traffic arrivals

TABLE A.1: *Parameter definitions for calculating the flow speed in a network segment.*

the flow speed, v can be expressed as

$$v = \begin{cases} \frac{v_f}{(1+0.25 v_f T_f \left(z+\sqrt{z^2+8k_d \frac{x'-x_o}{QT_f}+\frac{16k_d N}{(QT_f)^2}}\right)} & \text{for } N>0 \\ \frac{v_f}{(1+0.25 v_f T_f \left(x-1+\sqrt{(x-1)^2+8k_d \frac{x-x_o}{QT_f}}\right)} & \text{for } N=0 \\ v_f \quad \text{for } q_a < q_o. \end{cases}, \tag{A.1}$$

The parameters x, x_o, k_d and z are defined as

$$x = \frac{q_a}{Q} \tag{A.2}$$

$$x_0 = \frac{q_o}{Q} \tag{A.3}$$

$$k_d = \frac{2Q(\frac{v_f}{v_n}-1)^2}{v_f^2 T_f (1-x_o)}, \tag{A.4}$$

$$z = x - 1 + \frac{2N}{QT_f} \tag{A.5}$$

Enumeration Area type
Collective living quarters
Commercial
Farms
Formal residential
Industrial
Informal residential
Parks and recreation
Small holdings
Traditional residential
Vacant

TABLE A.2: *Census Enumeration Area types*

Enumeration Area gtype
Farms
Traditional
Urban

TABLE A.3: *Census Enumeration Area gtypes*

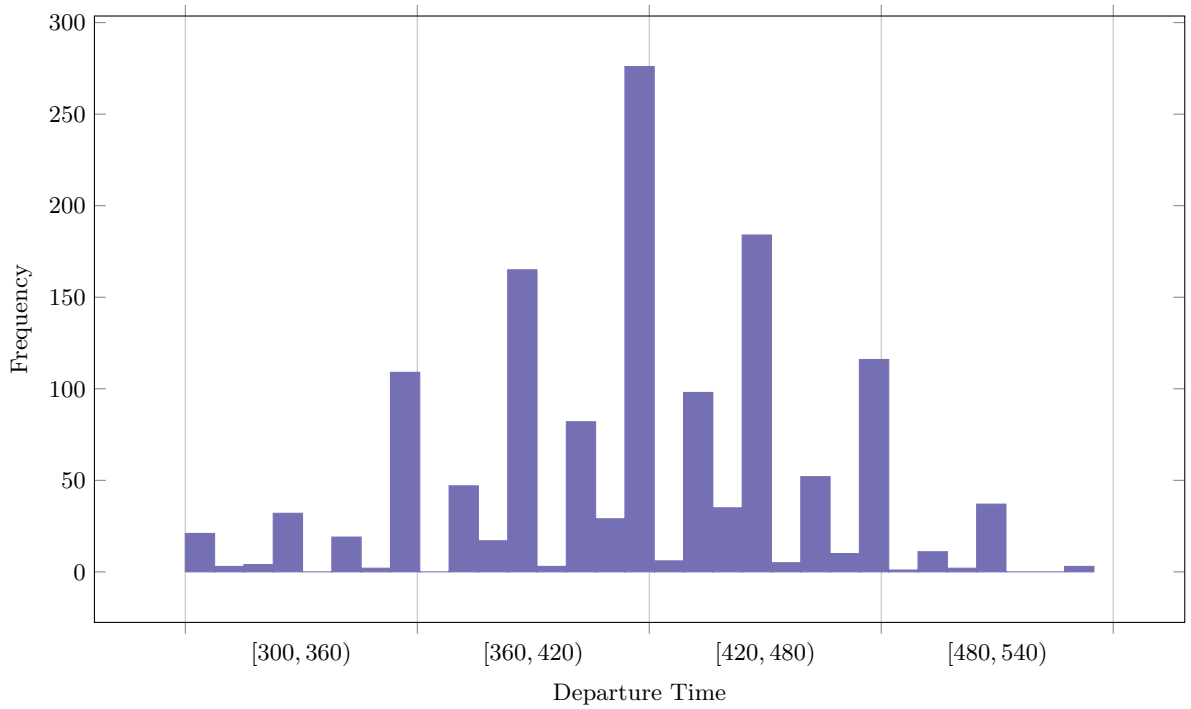

FIGURE A.1: *Binned surveyed departure times from the 2013 NHTS for respondents who drove all the way to work in the Western-Cape.*

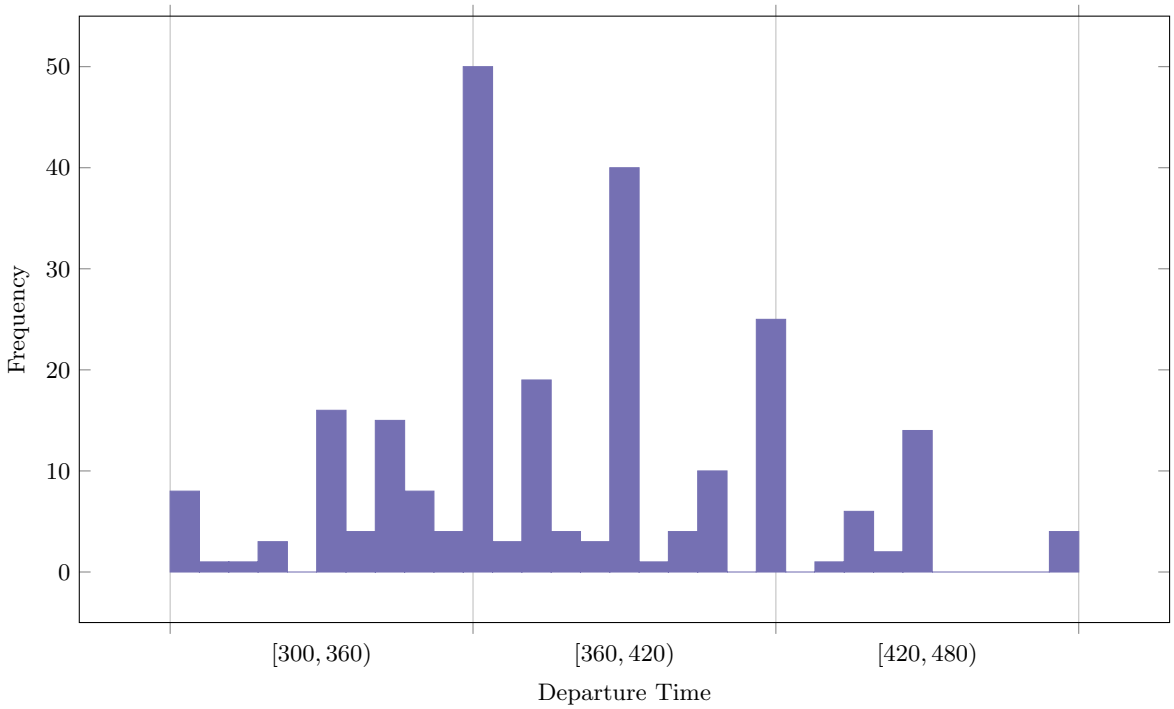

FIGURE A.2: *Binned surveyed departure times from the 2013 NHTS for respondents who took a bus all the way to work in the Western-Cape.*

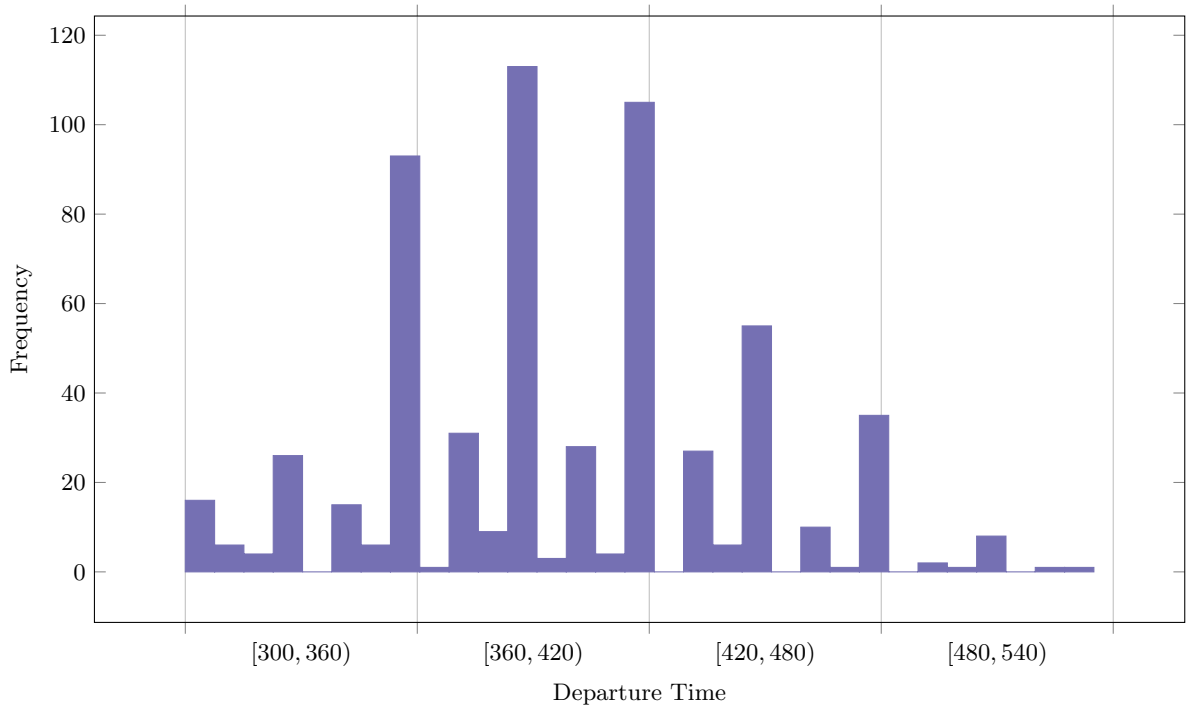

FIGURE A.3: *Binned surveyed departure times from the 2013 National Household Travel Survey for respondents who took a taxi all the way to work in the Western-Cape.*

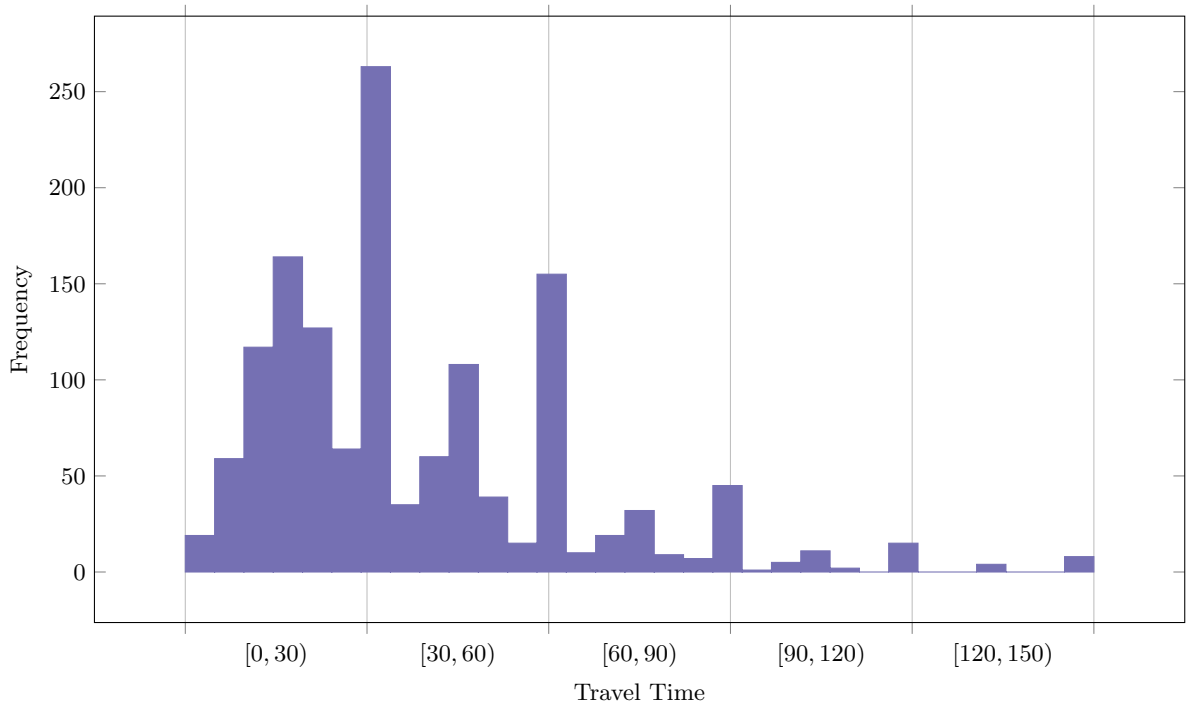

FIGURE A.4: *Binned surveyed travel times from the 2013 National Household Travel Survey for respondents who drove all the way to work in the Western-Cape.*

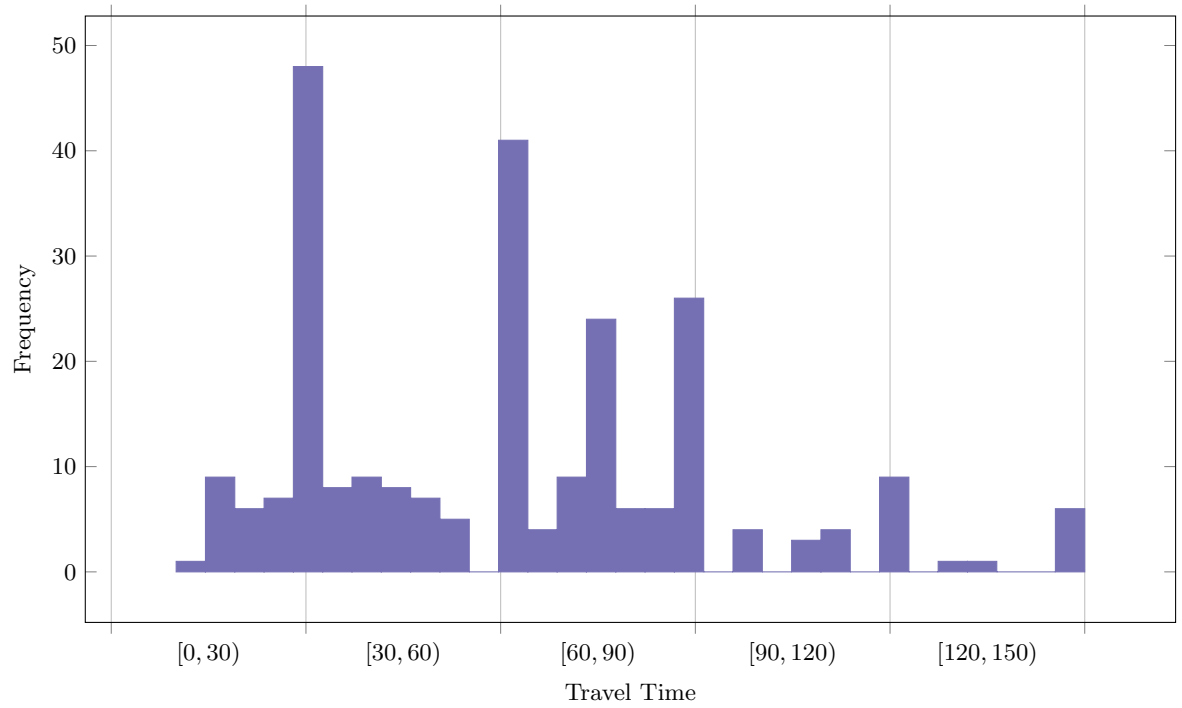

FIGURE A.5: *Binned surveyed travel times from the 2013 National Household Travel Survey for respondents who took a bus all the way to work in the Western-Cape.*

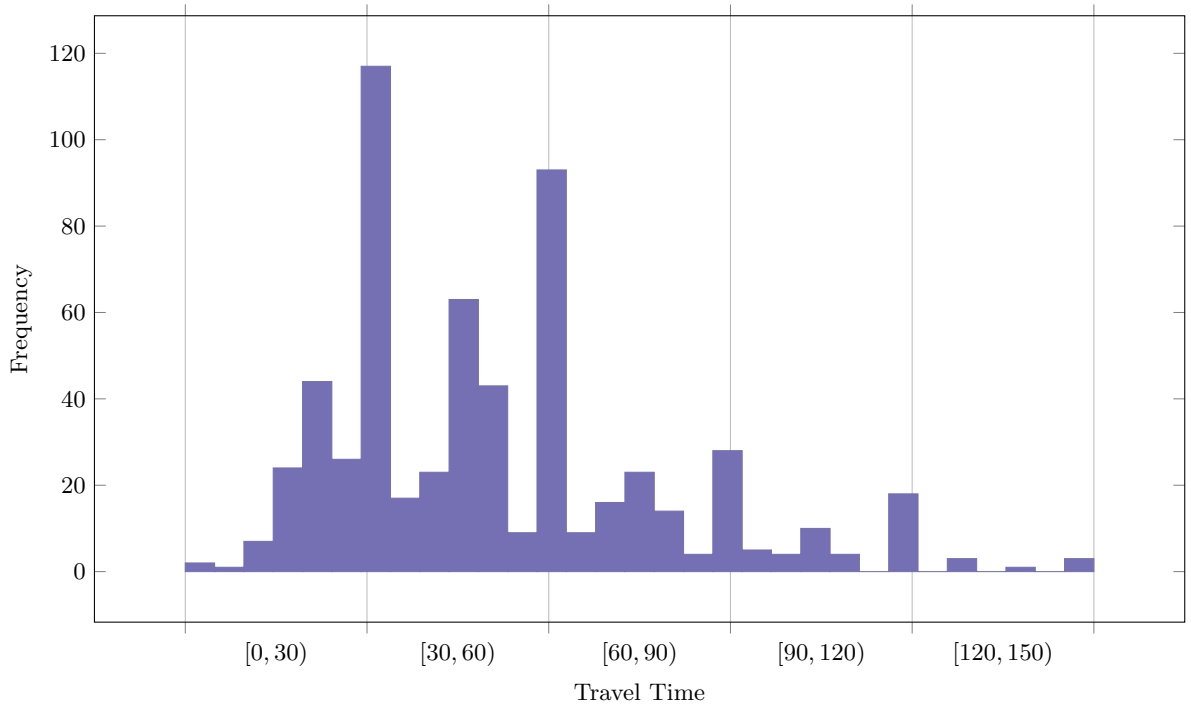

FIGURE A.6: *Binned surveyed travel times from the 2013 National Household Travel Survey for respondents who took a taxi all the way to work in the Western-Cape.*

Road Type	
access	2
motorway	2
motorway_junction	2
motorway_link	1
primary	2
primary_link	1
residential	2
residential_link	2
road	2
secondary	2
secondary_link	1
service	2
services	2
tertiary	2
tertiary_link	1
trunk	2
trunk_link	1
turning_circle	2

TABLE A.4: *Lane Assumptions for network development*

Free-flow speed (km/h)	Capacity Q (pce/h/lane)
120	2400
110	2350
100	2300
90	2250
80	1850
70	1800
60	1800
<60	1800

TABLE A.5: *Table of capacity in terms of passenger car equivalent per lane per for different free-flow speeds.*

lanes	Adjustment Factor
1	1
2	0.838
3	0.872
4	0.776
5	0.74
6	0.698
7	0.585
8	0.438

TABLE A.6: *Table of flow capacity factors derived from vehicle counting station data.*

TAZ name	TAZ id	workers	jobs
Matzikama	9001	13208	17358
Cederberg	9002	8130	10377
Bergrivier	9003	12698	18270
Saldanha Bay	9004	33039	30443
Swartland	9005	27722	32951
Witzenberg	9006	21590	29736
Drakenstein	9007	69974	80542
Stellenbosch	9008	40295	55872
Langeberg	9009	37885	49554
Langeberg	9010	20263	24801
Theewaterskloof	9011	25220	31101
Overstrand	9012	24709	25976
Mossel Bay	9015	24897	25254
Oudtshoorn	9016	18296	19857
George	9017	52126	56290
George Rural/Knysna/Bitou	9018	1963	1846
Central Karoo	9019	1728	1979
Northern Corridor	9020	95295	152507
Kraaifontein	9021	64353	32059
Parow/Bellville	9023	104736	174904
Blue Downs	9024	87596	18654
Belgravia	9025	61675	42842
Grassy Park	9026	96702	67234
Mitchells Plain/Gugulethu	9027	170203	99574
Khayelitsha	9028	119027	19153
Somerset West	9029	9601	26627
Central Cape Town	9030	52523	290323
Kuilsrivier	9031	33689	37615
Durbanville	9032	37640	9430
Oostenberg	9033	59395	86061
Langa/Bishop Lavis	9035	62779	67439
Strand	9036	72933	48769
Simonstown	9037	47863	40251
Wynberg	9038	56498	116447
Sea Point	9040	54201	28778
Cape Agulhas/Swellendam	9041	9989	10598
Cape Agulhas/Swellendam	9042	7904	10205
Hessequa	9043	12142	13859
Hessequa	9044	3907	3865
George Rural/Knysna/Bitou	9045	14261	15667
George Rural/Knysna/Bitou	9046	20256	20546
Central Karoo	9047	7829	9450
Central Karoo	9048	2286	2535

TABLE A.7: *Table of the number of workers and jobs within a TAZ.*

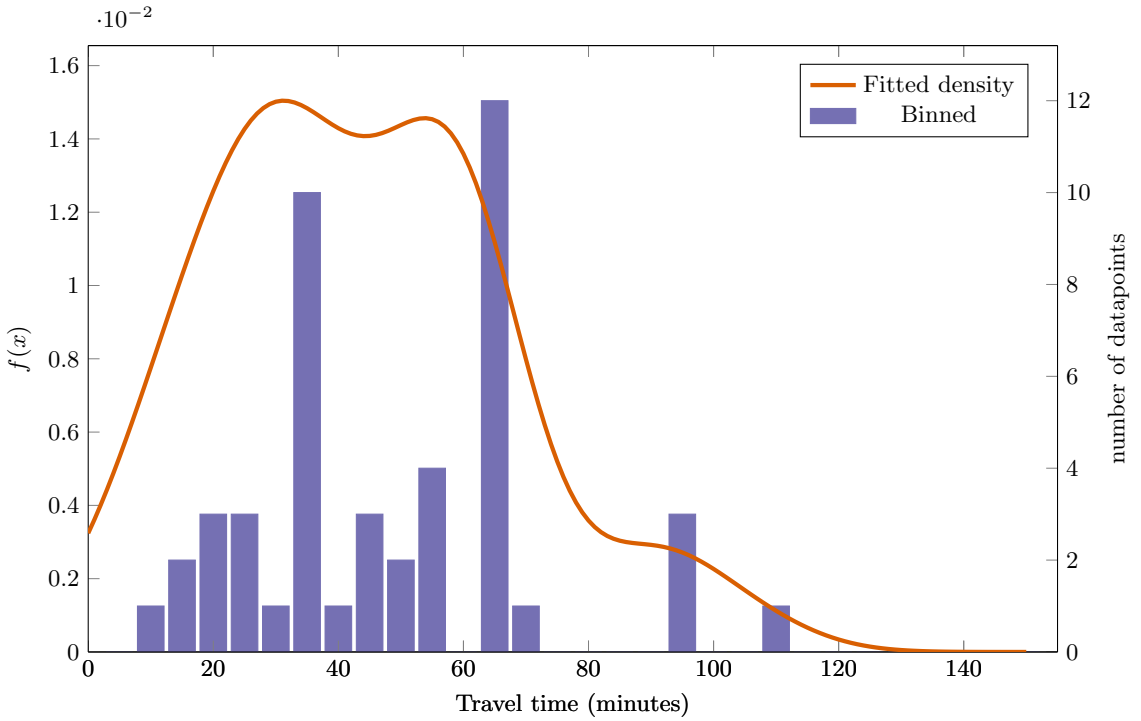

FIGURE A.7: *Fitted kernel density functions with binned data histogram for TAZ 9020 for modes* drive

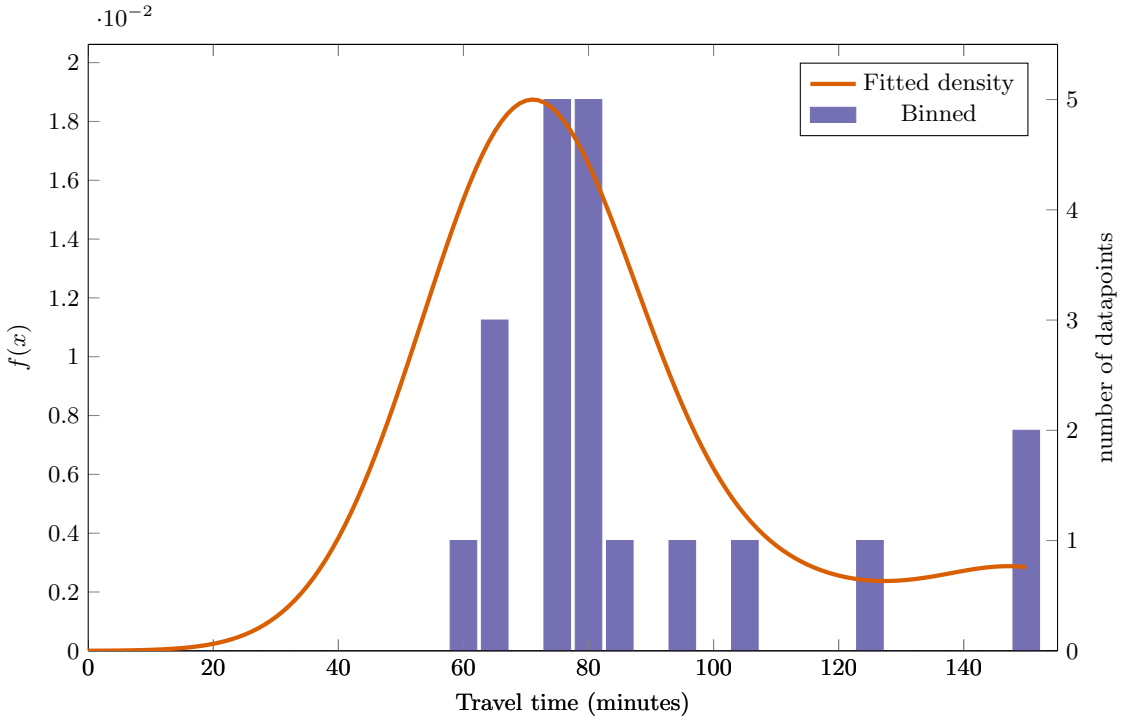

FIGURE A.8: *Fitted kernel density functions with binned data histogram for TAZ 9020 for modes* bus

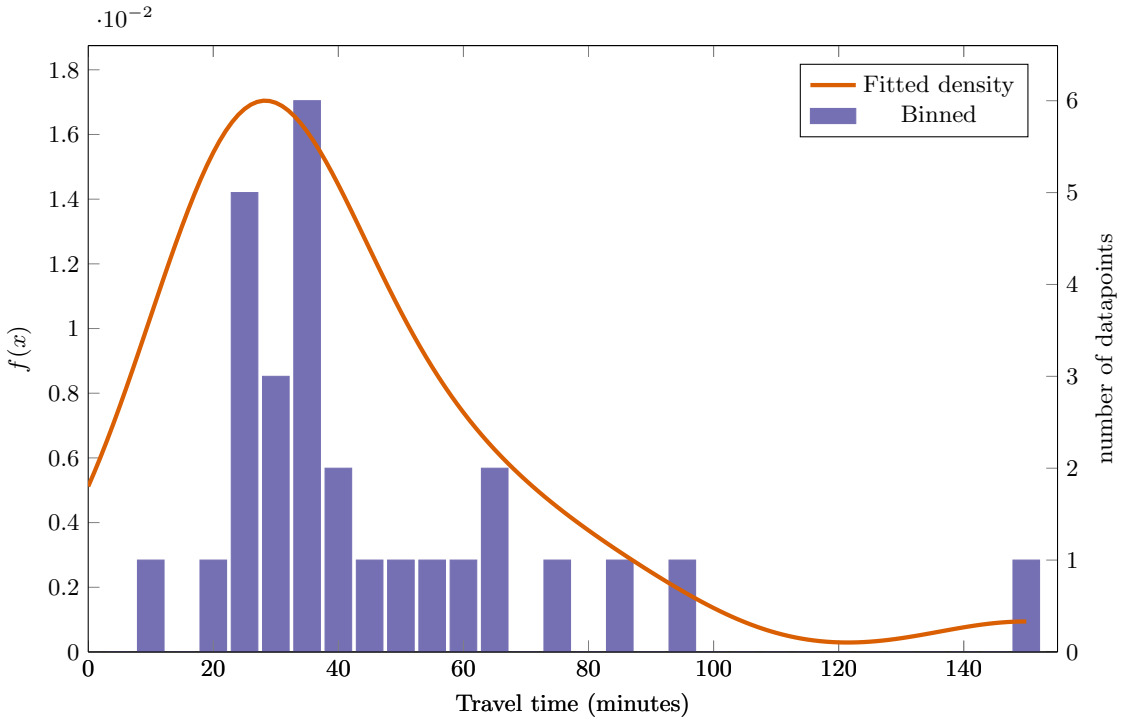

FIGURE A.9: *Fitted kernel density functions with binned data histogram for TAZ 9020 for modes* taxi

Station Code	Station Code
035	5012
085	5016
1040	5017
1114	5019
1132	5021
1203	5022
1229	5023
1243	5025
1275	5026
1328	5027
1330	5028
1331	5029
1336	5050
1337	5060
1366	5061
1397	5062
1398	610
1399	612
2324	706
2325	708
2400	710
2402	712
2403	720
279	880
5005	881
5006	917
5008	970
5011	

TABLE A.8: *Vehicle counting station codes.*

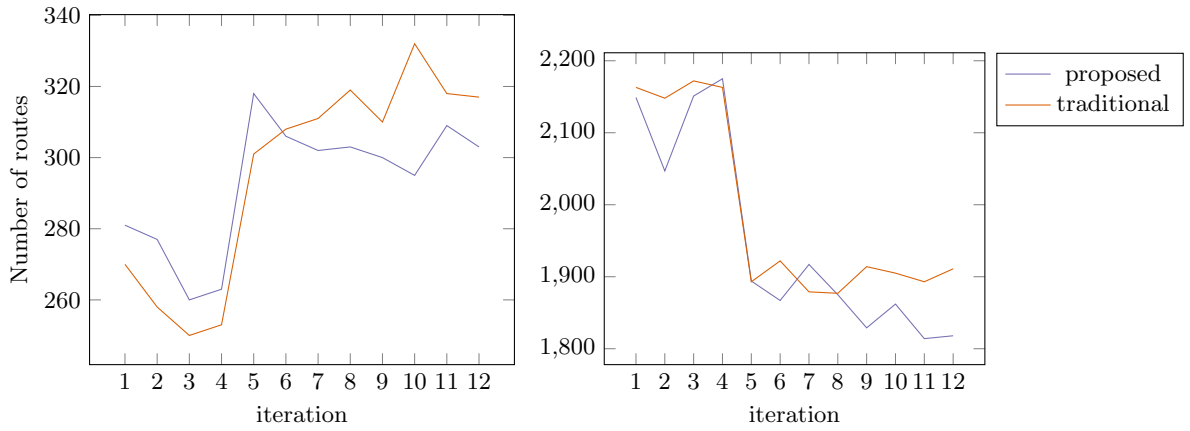

(a) *intra* (b) *inter*

FIGURE A.10: *Total number of intra- and inter-zonal routes, given a 10% overlap for the mode* drive.

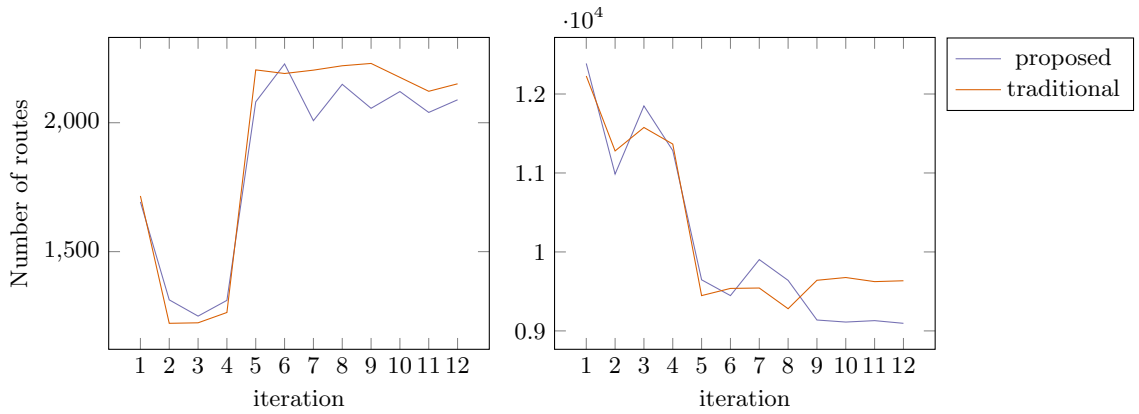

(a) *intra* (b) *inter*

FIGURE A.11: *Total number of intra- and inter-zonal routes, given a 90% overlap for the mode* drive.

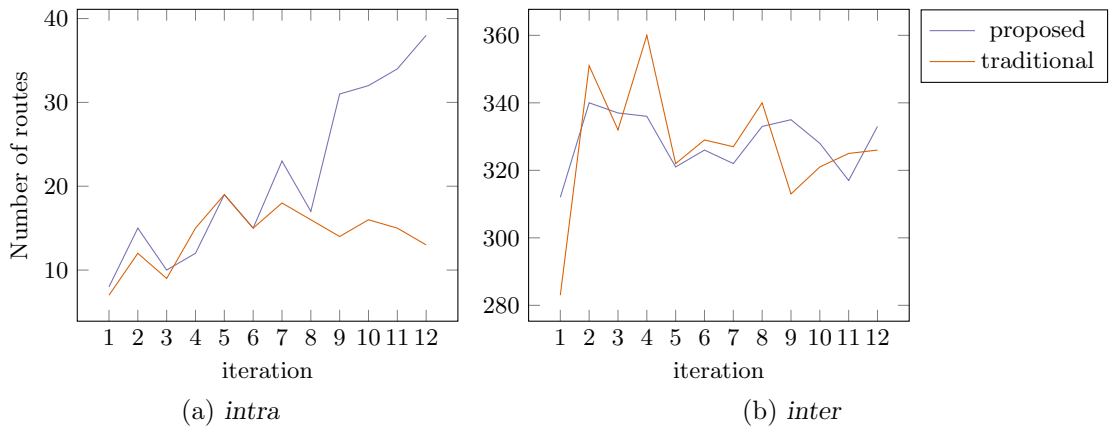

(a) *intra* (b) *inter*

FIGURE A.12: *Total number of intra- and inter-zonal routes, given a 10% overlap for the mode* bus.

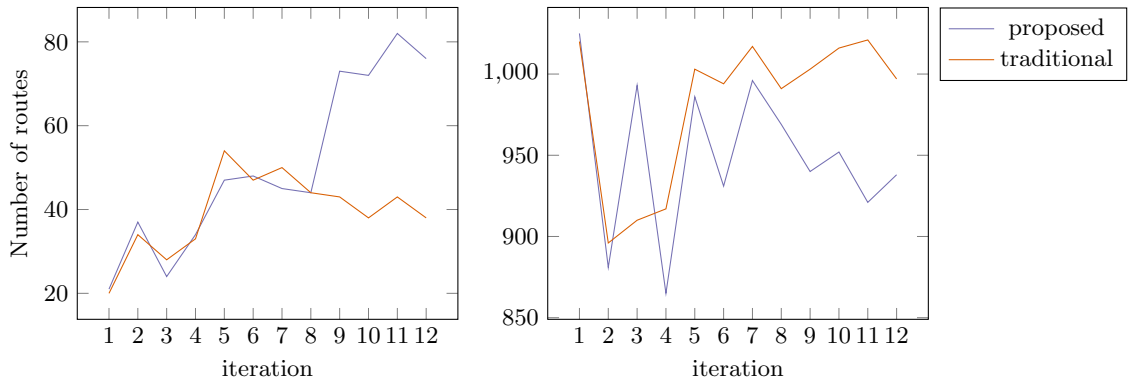

(a) *intra* (b) *inter*

FIGURE A.13: *Total number of intra- and inter-zonal routes, given a 90% overlap for the mode* bus.

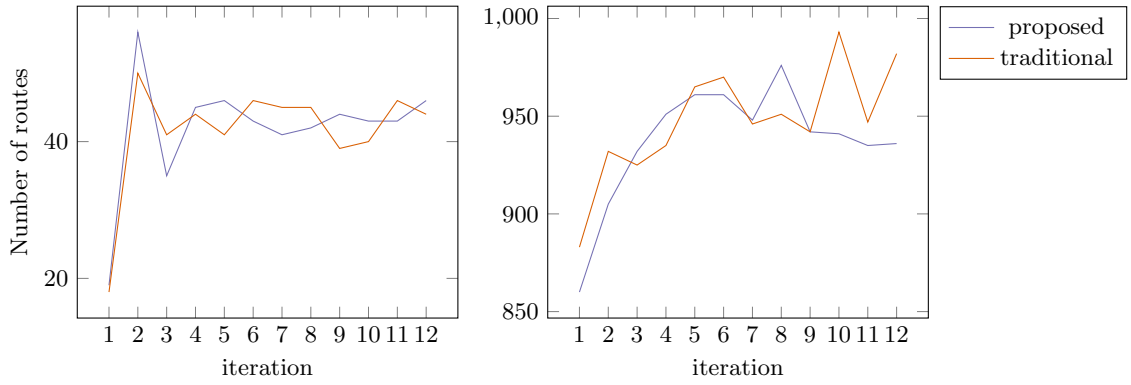

(a) *intra* (b) *inter*

FIGURE A.14: *Total number of intra- and inter-zonal routes, given a 10% overlap for the mode* taxi.

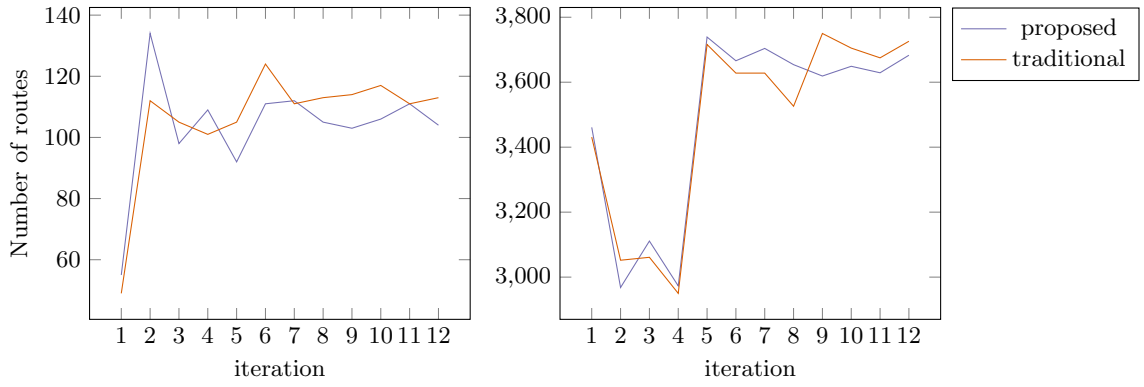

(a) *intra* (b) *inter*

FIGURE A.15: *Total number of intra- and inter-zonal routes, given a 90% overlap for the mode* taxi.

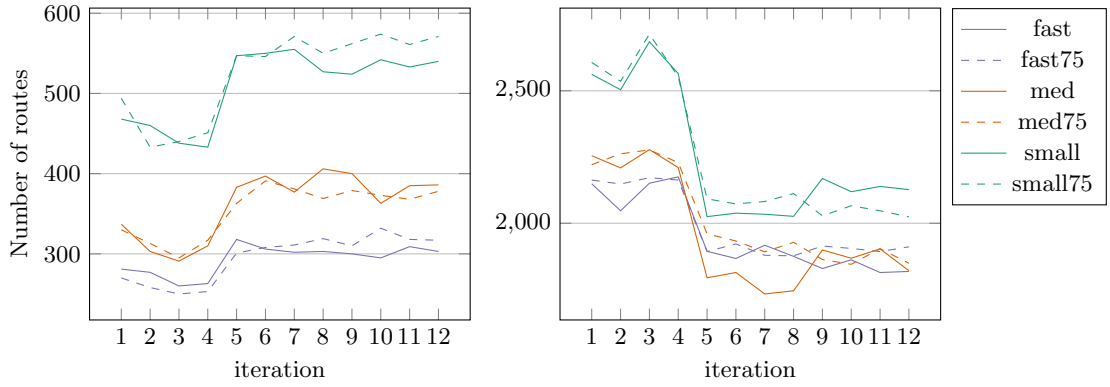

(a) *intra* (b) *inter*

FIGURE A.16: *Total number of intra- and inter-zonal routes, given a 10% overlap for the mode* drive.

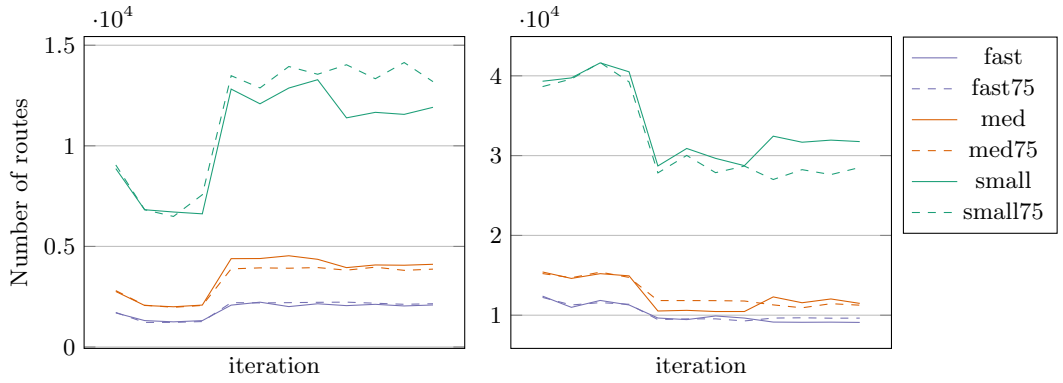

(a) *intra* (b) *inter*

FIGURE A.17: *Total number of intra- and inter-zonal routes, given a 90% overlap for the mode* drive.

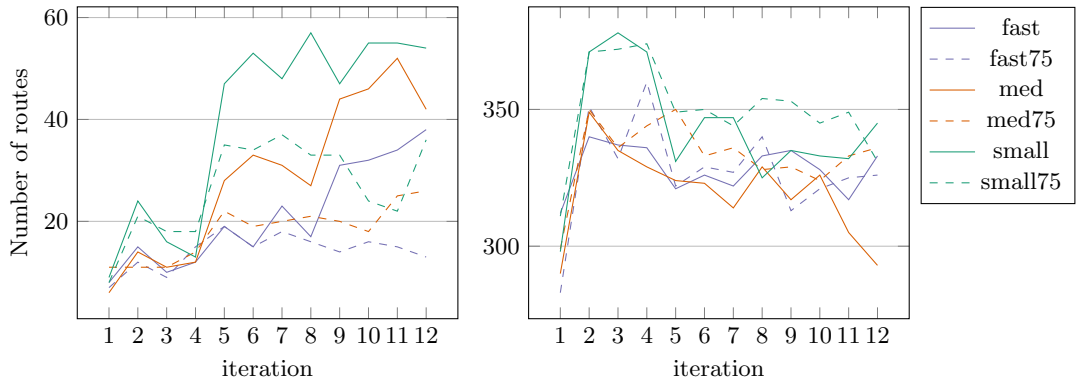

(a) *intra* (b) *inter*

FIGURE A.18: *Total number of intra- and inter-zonal routes, given a 10% overlap for the mode* bus.

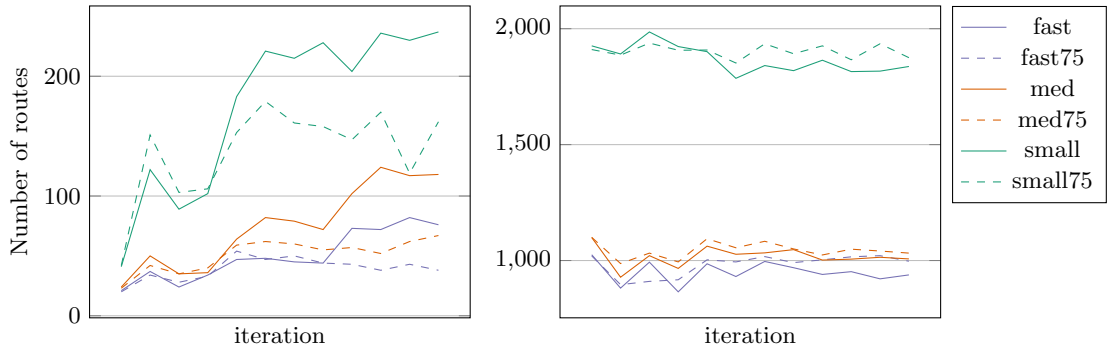

(a) *intra* (b) *inter*

FIGURE A.19: *Total number of intra- and inter-zonal routes, given a 90% overlap for the mode* bus.

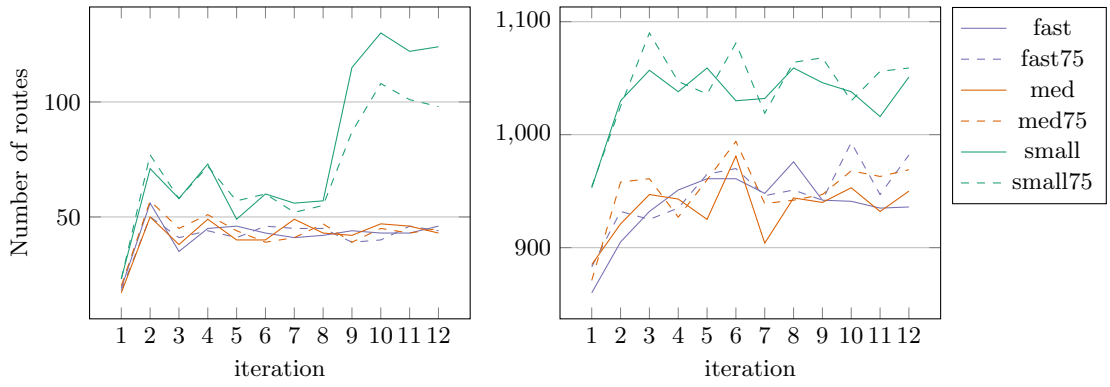

(a) *intra* (b) *inter*

FIGURE A.20: *Total number of intra- and inter-zonal routes, given a 10% overlap for the mode* taxi.

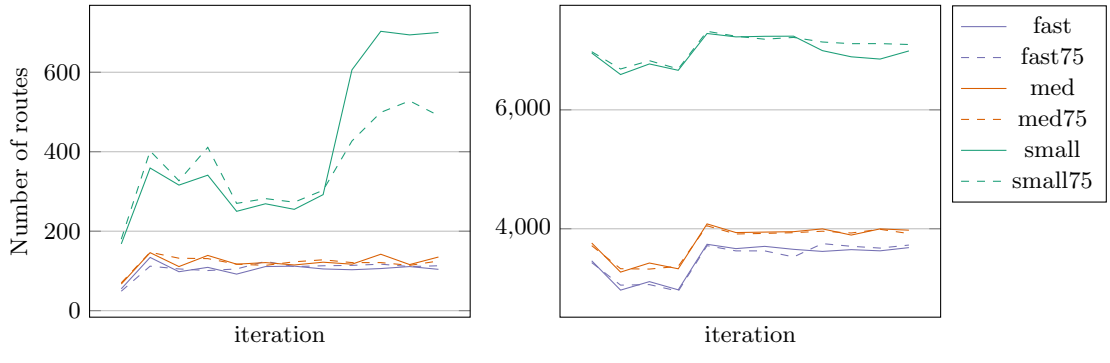

(a) *intra* (b) *inter*

FIGURE A.21: *Total number of intra- and inter-zonal routes, given a 90% overlap for the mode* taxi.